Justus-Liebig-University Giessen
Faculty 08 (Biology and Chemistry)
Institute for Animal Physiology
Animal Physiology and Molecular Biomedicine

JUSTUS-LIEBIG-UNIVERSITÄT GIESSEN

Structural development and functional reconstitution in the olfactory system of the clawed frog *Xenopus laevis*

Dissertation

for the award of the degree
“Doctor rerum naturalium”
(Dr. rer. nat.)

Submitted by

Melina Kahl

07 August 2025

Dean: Prof. Dr. Holger Zorn

1st Reviewer: Prof. Dr. Ivan Manzini

2nd Reviewer: Prof. Dr. Martin Diener

„Das Geheimnis des Erfolgs liegt darin,
sein Ziel zu kennen und niemals aufzugeben.“
Benjamin Franklin

Table of contents

Table of contents

1 Abstract

The transition of tetrapods to terrestrial habitats is concomitant with the adaptation of the olfactory system (OS) to the environment. This is reflected at the anatomical and functional levels with the formation of different subsystems, including cell subpopulations that exhibit distinct protein expression at the molecular level. The expression patterns of specific proteins vary between different species, although the olfactory systems show general anatomical similarities. For instance, in fish the calcium-binding protein S100Z is expressed in different cell types in their olfactory epithelium, while in mammals it is associated with cells within the vomeronasal organ (VNO). In the course of my thesis, I analyzed the expression pattern of S100Z in the OS of the anuran *Xenopus laevis.* Using immunohistochemistry in whole mount and slice preparations I identified a subgroup of S100Z expressing olfactory receptor neurons (ORNs) in the larval main OS and in the middle cavity of adult *Xenopus laevis.* In larval animals, these ORNs showed a lateral distribution bias in the olfactory epithelium and exclusively projected into the intermediate and lateral glomerular cluster. In conclusion, S100Z expression in the OS of *Xenopus laevis* is exclusively associated with the main OS and not with the VNO.

Maintaining regenerative capacity is essential for the OS because of its exposed position to toxic substances or physical trauma. This capacity is attributed to the presence of two main cell types. Firstly, the basal cells of the olfactory epithelium, which are neuronal stem cells and support constant renewal by developing new supporting cells and ORNs. Secondly, the olfactory ensheathing cells (OECs), which enwrap the axons of ORNs until they project into the olfactory bulb (OB) in the forebrain. To date, the existence and role of OECs in the OS of *Xenopus laevis* have not been investigated in detail. I found vimentin expressing OECs enwrapping ORN axon bundles from the epithelium until the OB in larval *Xenopus* using immunohistochemistry. The presence of fibroblasts and macrophages in the olfactory nerve (ON) was determined through the utilization of immunohistochemistry and transgenic *Xenopus* lines. Unilateral ON transection induced a temporary transient and dynamic phosphorylation of the ribosomal protein S6 in these non-neuronal cells. In summary, I identified various cell types within the ON which protein expression is influenced by ON injury. The exact function of phosphorylated ribosomal protein S6 in the OS of *Xenopus* is still unknown.

2 Zusammenfassung

Der Übergang der Tetrapoden zu terrestrischen Lebensräumen geht einher mit der Anpassung des Geruchssystems an die Umwelt. Dies spiegelt sich auf anatomischer und funktioneller Ebene in der Bildung verschiedener Subsysteme wider, einschließlich Zellsubpopulationen, die eine unterschiedliche Proteinexpression auf molekularer Ebene aufweisen. Die Expressionsmuster spezifischer Proteine variieren zwischen den verschiedenen Arten, obwohl die Geruchssysteme allgemeine anatomische Ähnlichkeiten aufweisen. So wird beispielsweise das Kalzium-bindende Protein S100Z bei Fischen in verschiedenen Zelltypen des Riechepithels exprimiert, während es bei Säugetieren mit Zellen im Vomeronasalorgan (VNO) assoziiert ist. Im Rahmen meiner Dissertation habe ich das Expressionsmuster von S100Z im olfaktorischen System des Anuren *Xenopus laevis* untersucht. Mittels Immunhistochemie, in intakten- und geschnittenen Präparaten, identifizierte ich eine Untergruppe von S100Z exprimierenden olfaktorischen Rezeptorneuronen (ORNs) im larvalen olfaktorischen Hauptriechsystem und in der mittleren Kavität des erwachsenen *Xenopus laevis*. In larvalen Tieren, zeigten diese ORNs eine laterale Verteilung im Riechepithel und projizierten ausschließlich in den intermediären und lateralen glomerulären *cluster*. Zusammenfassend lässt sich sagen, dass die Expression von S100Z im Geruchssystem von *Xenopus laevis* ausschließlich mit dem Hauptgeruchssystem und nicht mit dem VNO assoziiert ist.

Die Aufrechterhaltung der Regenerationsfähigkeit hat für das olfaktorische System eine essentielle Bedeutung, da es aufgrund der exponierten Lage toxischen Substanzen oder physischen Traumata ausgesetzt ist. Die Regenerationsfähigkeit wird auf das Vorhandensein von zwei Hauptzelltypen zurückgeführt. Zum einen, den Basalzellen des olfaktorischen Epithels, bei welchen es sich um neuronale Stammzellen handelt, die für eine konstante Erneuerung von Zellen sorgen, indem sie neue Stützzellen und ORNs bilden. Zum anderen, den olfaktorischen Hüllzellen, die die Axone der ORNs umhüllen, bis diese den *Bulbus olfactorius* (OB) im Vorderhirn erreichen. Bisher wurden die Existenz und die Rolle der OECs im Riechsystem von *Xenopus laevis* noch nicht im Detail untersucht. Mittels Immunohistochemie fand ich Vimentin exprimierende OECs, die ORN-Axon Bündel vom Epithel bis zum OB in larvalen *Xenopus* umhüllen. Das Vorhandensein von Fibroblasten und Makrophagen im olfaktorischen Nerv (ON) wurde mittels Verwendung von Immunohistochemie und transgenen *Xenopus*-Linien nachgewiesen. Unilaterale Nervdurchtrennung führte zu einer vorübergehenden und dynamischen Phosphorylierung des ribosomalen Proteins S6 in diesen nicht-neuronalen Zellen. Zusammenfassend habe ich verschiedene Zelltypen innerhalb des ON identifiziert, deren Proteinexpression durch eine ON-Verletzung beeinflusst wird. Die genaue Funktion des phosphorylierten ribosomalen Proteins S6 im olfaktorischen System von *Xenopus* ist noch unbekannt.

3 Publication information

My results of this thesis are already published as shown in chapter 5 in the following journals:

Kahl, M., Offner, T., Trendel, A., Weiss, L., Manzini, I., & Hassenklöver, T. (2024). S100Z is expressed in a lateral subpopulation of olfactory receptor neurons in the main olfactory system of *Xenopus laevis*. *Developmental Neurobiology*, *84*(2), 59–73. https://doi.org/10.1002/dneu.22935
First published: 04 March 2024

Kahl, M., Weiss, L., Walter, J., Hassenklöver, T., & Manzini, I. (2025). Olfactory nerve transection transiently activates olfactory ensheathing cells in *Xenopus laevis* larvae. *European Journal of Neuroscience*, 62, 1-16. http://dx.doi.org/10.1111/ejn.70211
First published 04 August 2025

The references of my two publications are included in chapter 5. Supplementary figures of my 2nd publication are attached as accepted to chapter 11.

4 Scientific background

4.1 The sense of smell

The olfactory system (OS) is a central sensory organ in animals, enabling the perception and discrimination of odorant stimuli (Eisthen & Polese, 2007; Zarzo, 2007; Korsching, 2016). It influences essential behaviors, including foraging, prey acquisition, reproduction, social interactions, and danger avoidance (Ache & Young, 2005; Eisthen & Polese, 2007; Zarzo, 2007; Weiss, Manzini, *et al.*, 2021; Manzini *et al.*, 2022). Despite phylogenetic diversity, the OS remains structurally and functionally similar across species (Eisthen, 2002; Ache & Young, 2005; Eisthen & Polese, 2007; Weiss, Manzini, *et al.*, 2021; Manzini *et al.*, 2022; Hawkins *et al.*, 2024).During the course of evolution, it has adapted to diverse environments and is present in aquatic and terrestrial vertebrates, as well as invertebrates (Ache & Young, 2005; Eisthen & Polese, 2007; Weiss, Manzini, *et al.*, 2021). The adaptability has facilitated the colonialization of various ecological niches. At the cellular, molecular, and anatomical levels, the OS consists of several specialized subsystems (Manzini *et al.*, 2022). These subsystems differ in olfactory receptor protein expression, sensory neuron positioning in the nasal cavity, signaling mechanisms for odor transduction, and axonal projections to specific regions of the olfactory forebrain (Breer *et al.*, 2006; Eisthen & Polese, 2007; Munger *et al.*, 2009).

4.2 Odorants and vertebrate olfactory receptor proteins

Olfaction in vertebrates begins when odorant molecules (odorants) interact with olfactory receptor proteins. To process these signals, the OS performs a dual function of detecting odorants and analyzing the chemical composition of the environment (Ache & Young, 2005; Manzini *et al.*, 2014; Manzini *et al.*, 2022; Wyatt, 2015).

Odorants are chemical molecules that differ in size, shape, charge, and functional groups (Ache & Young, 2005; *Malnic et al.*, 1999; Manzini *et al*., 2022). The OS is typically exposed to complex odorant mixtures rather than single compounds (Manzini *et al.*, 2022). These include airborne and waterborne compounds from diverse chemical classes (Hoover, 2010; Keller & Vosshall, 2016). Airborne odorants must be volatile, such as alcohols, aldehydes, amines, hydrocarbons, organic acids, esters, and ethers (Johnson & Leon, 2007; Nara *et al.*, 2011). Waterborne odorants have to be water-soluble, such as amino acids, bile acids, nucleotides, steroids and prostaglandins (Hara, 1994; Hoover, 2010).

Odorants may travel from few centimeters to kilometers, undergoing physical and chemical transformations that influence their detectability before binding to olfactory receptor proteins (Eisthen & Polese, 2007; Manzini *et al.*, 2022). Olfactory receptor proteins are located on the membrane of the apical appendages (cilia or microvilli) of olfactory receptor neurons (ORNs), which are embedded in the olfactory epithelium (Bear *et al.*, 2016; Glezer & Malnic, 2019). To process the vast diversity of environmental chemicals, organisms employ receptor repertoires,

signaling pathways, and anatomically segregated subsystems (Kaupp, 2010). However, biophysical constraints limit olfactory receptor proteins to interacting with subsets of chemical molecules enabling odor discrimination (Bear *et al.*, 2016). The dimensionality of chemical space and the diversity of encountered stimuli have driven the evolution of multiple olfactory receptor gene families. These families encode an extensive repertoire of transmembrane receptor proteins, serving as chemosensors across animal evolution (Bear *et al.*, 2016; Manzini *et al.*, 2022; Niimura & Nei, 2007). Since my work focuses on the vertebrate OS, I will introduce the vertebrate olfactory receptor families relevant for fish, amphibians, and rodents.

The majority of vertebrate olfactory metabotropic receptors belong to the G protein-coupled receptors (GPCR) characterized by seven-transmembrane domains (Spehr & Munger, 2009; Kaupp, 2010). In vertebrates, most ORNs express a single olfactory receptor gene from one of four main GPCR multigene families: Odorant receptors (OR-type), Trace Amine Associated Receptors (TAARs), Vomeronasal Type 1 Receptors (V1Rs), and Vomeronasal Type 2 Receptors (V2Rs) (Figure 1). Additionally, other receptor types contribute to olfaction in rodents, including Formyl Peptide Receptors (FPRs), and membrane spanning four-pass proteins (MS4A) (Figure 1; Bear *et al.*, 2016; Dalton & Lomvardas, 2015; Manzini *et al.*, 2022).

4.2.1 Odorant receptors

The first discovered rhodopsin-type GPCR multigene family was named "odorant receptors" (OR-type; Figure 1; Buck & Axel, 1991; Niimura, 2009). OR-type receptors form the largest olfactory receptor family and are present in all vertebrates, though the number of functional genes varies across species (Zhang & Firestein, 2002; Niimura, 2009). The vertebrate OR-type genes are subdivided into type 1 and type 2, each with several subfamilies (Niimura & Nei, 2007; Niimura, 2009). A distinct nomenclature is employed for mammalian OR-type receptors: class I (subfamily α and β) ORs and class II (γ) ORs (Niimura, 2009).

About 1000 distinct OR-types have been identified in mammals (Krautwurst *et al.*, 1998; Malnic, 2007; Malnic *et al*., 1999; Nara *et al.*, 2011; Saito *et al.*, 2009). They primarily bind small volatile molecules such as alcohols, ketones, esters, and aldehydes (Nara *et al.*, 2011; Saito *et al.*, 2009) and operate via a combinatorial coding system, where each odorant is recognized by multiple OR-types. (Malnic *et al.*, 1999). This mechanism enables the discrimination of millions of odorants (Malnic *et al.*, 1999; Malnic, 2007). A comprehensive study of Saito *et al.* (2009) analyzed the ligand specificity of OR-type genes. They demonstrated that mammalian class I OR-types typically detect more hydrophilic, water-soluble, compounds than class II OR-types.

During the transition to a terrestrial lifestyle, the number of OR-type genes changed based on environmental needs (Niimura, 2009). In mammals, birds, and reptiles, class I OR-type genes, which detect water-soluble odorants, were reduced, while class II OR-type genes expanded.

Amphibians, adapted to both aquatic and terrestrial environments, continue to possess OR-type genes for both airborne and water-soluble odorants (Niimura, 2009).

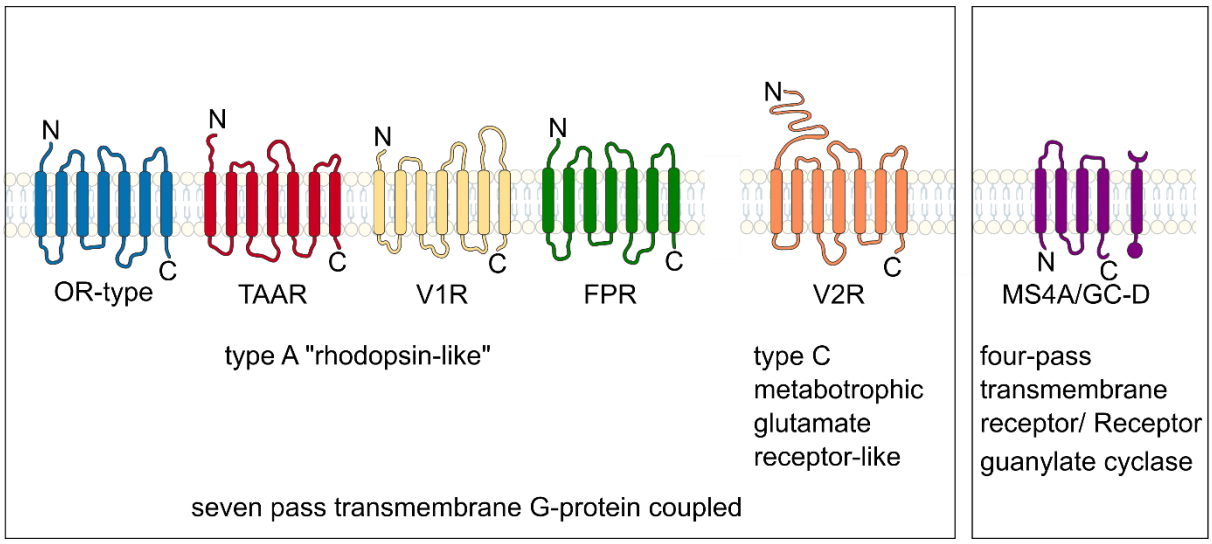

Figure 1: Olfactory receptors in vertebrates. Most vertebrate olfactory receptor proteins are G-protein coupled receptors (GPCRs) with seven transmembrane domains, which either belong to type A or type C. The exception is the four-pass transmembrane-spanning 4A receptor (MS4A), which often colocalizes with guanylyl cyclase D (GC-D). FPR formyl peptide receptor; MS4A/GC-D four-pass transmembrane-spanning receptor with guanylyl cyclase D; OR-type odorant receptor; TAAR trace amine-associated receptor; V1R vomeronasal type 1 receptor; V2R vomeronasal type 2 receptor.

4.2.2 Trace amine-associated receptors

Trace amine-associated receptors (TAARs) form a second olfactory receptor subfamily within the rhodopsin-like class A GPCRs (Figure 1; Borowsky *et al.*, 2001; Hashiguchi & Nishida, 2007; Liberles & Buck, 2006; Lindemann & Hoener, 2005). TAARs are present in the olfactory epithelia of mammals, amphibians, birds, and fish (Borowsky *et al.*, 2001; Gloriam *et al.*, 2005; Liberles & Buck, 2006; Hashiguchi & Nishida, 2007; Dieris *et al.*, 2021), though their evolutionary origin remains debated (Dieris *et al.*, 2021). TAAR genes are found in cartilaginous jawed fishes, with ray-finned fishes possessing a particularly large repertoire (Gloriam *et al.*, 2005; Hashiguchi & Nishida, 2007; Sharma *et al.*, 2019; Syed *et al.*, 2023). Zebrafish (*Danio rerio*) have 112 taar genes, while later-diverging vertebrates retain fewer, including 15 in mice, six in *Xenopus tropicalis*, six in humans, and three in chickens (Gloriam *et al.*, 2005; Lindemann *et al.*, 2005; Liberles & Buck, 2006; Hashiguchi & Nishida, 2007; Hussain *et al.*, 2013). The extensive TAAR diversity in teleost fish suggests an essential role in aquatic olfaction (Hashiguchi & Nishida, 2007; Dieris *et al.*, 2021).

In vertebrates, olfactory TAARs can recognize volatile or water-soluble trace amines (Borowsky *et al.*, 2001; Lindemann & Hoener, 2005; Lindemann *et al.*, 2005; Xu & Li, 2020), which are structurally similar to biogenic amines but occur at much lower concentrations (Berry, 2004; Xu & Li, 2020). A common process that produces volatile trace amines is the decarboxylation of amino acids. Some TAAR agonists are present in animal body fluids or decaying foods and can mediate specific animal behaviors, including sexual attraction,

predator avoidance, and aversive response, which are critical for animal survival and reproduction (Xu & Li, 2020). TAARs also play a significant role in pheromone-mediated behaviors across species, although vomeronasal receptors were initially considered the primary pheromone detectors.

4.2.3 Vomeronasal type 1 receptors

The type 1 vomeronasal receptor (V1R) multigene family was first identified in the vomeronasal organ (VNO) of mice (Dulac & Axel, 1995). The VNO, present in most terrestrial tetrapods, is a distinct olfactory organ with unclear evolutionary origins and functions (Eisthen, 1997; Munger *et al.*, 2009). V1Rs belong to the class A rhodopsin-like GPCRs (Figure 1; Spehr & Munger, 2009) and are found in species from teleost fish to humans (Pfister & Rodriguez, 2005; Saraiva & Korsching, 2007; Shi & Zhang, 2007). In fish, this receptor family is termed olfactory receptor class A-related GPCRs (ORA) because these receptors were already involved in olfaction before the VNO evolved in tetrapods. Unlike tetrapods, fish possess a single olfactory organ per side of the head, composed of lamellae lined with olfactory epithelium, without a distinct VNO (see chapter 4.3.1; Pfister & Rodriguez, 2005; Saraiva & Korsching, 2007).

Systematic analysis revealed that mice's V1Rs function as highly sensitive pheromone detectors, identifying small organic pheromones important for social and sexual communication (Leinders-Zufall *et al.*, 2000). Pheromones, defined as substances secreted by one individual and perceived by another of the same species, influence behavior and physiology, particularly in mating, sexual recognition, and neuroendocrine responses (Karlson & Lüscher, 1959; Silva & Antunes, 2017).

4.2.4 Vomeronasal type 2 receptors

Shortly after the identification of V1Rs, a second vomeronasal receptor family, the vomeronasal type 2 receptors (V2Rs), was discovered in a distinct subset of neurons within the rodent VNO (Herrada & Dulac, 1997; Matsunami & Buck, 1997; Ryba & Tirindelli, 1997). Unlike previously mentioned receptor families, V2Rs belong to class C GPCRs, which are more closely related to metabotropic glutamate receptors and possess a larger extracellular NH_2-terminus (Figure 1; Dulac & Torello, 2003; Manzini *et al.*, 2022; Mombaerts, 2004; Tirindelli *et al.*, 1998). V2Rs bind water-soluble peptides and pheromones (Leinders-Zufall *et al.*, 2000; Shi & Zhang, 2007; Munger *et al.*, 2009), enabling the detection of molecules dispersed in aquatic environments (Silva & Antunes, 2017).

The V2R gene repertoire varies across species, likely influencing specific behaviors (Shi & Zhang, 2007). Since fish lack a VNO, V2R homologous in fish are termed olfactory class C GPCRs (OlfC; Manzini & Korsching, 2011). These receptors were first identified in cartilaginous fish (Manzini & Korsching, 2011). In cartilaginous fish, nearly all olfactory receptor

genes belong to the V2R/OlfC family, suggesting their primary role in olfaction (Sharma *et al.*, 2019; Syed *et al.*, 2023). In teleost fish, the OlfC gene family exhibits substantial variation in size (Bjarnadóttir *et al.*, 2005; Cao *et al.*, 1998; Johnstone *et al.*, 2009; Yang *et al.*, 2019). Within amphibians, the V2R family expanded considerably, reaching its largest known size in *Xenopus tropicalis,* which possesses 270 intact genes and over 400 pseudogenes (Shi & Zhang, 2007; Nei *et al.*, 2008; Silva & Antunes, 2017). Studies in *Xenopus laevis* suggest that amino acids may serve as V2R ligands (Syed *et al.*, 2013, 2017).

Reptiles maintain a relatively large V2R repertoire, whereas some mammalian lineages lack functional V2Rs (Shi & Zhang, 2007; Silva & Antunes, 2017). In rodents, V2Rs are implicated in pheromone-induced male aggression and the detection of water-soluble pheromones in urine (Leinders-Zufall *et al.*, 2004; Kimoto *et al.*, 2005; Brennan & Zufall, 2006; Haga *et al.*, 2010; Chamero *et al.*, 2012). Overall, the V2R gene family exhibits high variability in later diverging vertebrates (Shi & Zhang, 2007).

4.2.5 Other olfactory receptors

In recent years, additional olfactory receptor types have been identified. In 2009 formyl peptide receptors (FPRs) were discovered as olfactory receptors in rodents (Liberles *et al.*, 2009; Rivière *et al.*, 2009). These class A, rhodopsin-like GPCRs are expressed in microvillous receptor neurons of the VNO and bind structurally diverse peptides or proteins linked to inflammation and disease, enabling the detection of pathogens or diseased conspecifics (Figure 1; Kaupp, 2010; Liberles *et al.*, 2009; Mohrhardt *et al.*, 2018; Munger *et al.*, 2009; Rivière *et al.*, 2009; Spehr & Munger, 2009).

Another olfactory receptor family, the membrane-spanning four-pass proteins (MS4A), is co-expressed with guanylyl cyclase (GC-D) in a subset of rodent receptor neurons (Figure 1; Bloom *et al.*, 2020; Greer *et al.*, 2016; Juilfs *et al.*, 1997; Leinders-Zufall *et al.*, 2007). Receptors encoded by this gene family are four-pass transmembrane proteins with both, the COOH- and NH2-termini located intracellularly (Greer *et al.*, 2016) and detect conspecific and predator-derived chemosignals, gases, pheromones, and food-related odorants, triggering behavioral responses (Munger *et al.*, 2010; Greer *et al.*, 2016; Mohrhardt *et al.*, 2018; Bloom *et al.*, 2020; Zimmerman & Munger, 2021).

Since FPRs and MS4As appear to be rodent-specific and have not been detected in other vertebrate olfactory systems, their cellular signaling mechanisms will not be discussed further in this work.

4.3 Components of the vertebrate OS and transduction mechanisms

In vertebrates, odor molecules bind to olfactory receptor proteins, initiating the sense of smell (Bear *et al.*, 2016; Glezer & Malnic, 2019). These receptors are located on the cilia or microvilli of ORNs within the nasal olfactory epithelium (Munger *et al.*, 2009; Bear *et al.*, 2016). In order to study the cellular composition of the OS, it is of fundamental importance to know how the system is structured and how its anatomy and morphology changes during development and regeneration.

4.3.1 Organization of the vertebrate OS

The OS of vertebrates consists of the peripheral olfactory epithelium (OE) in the nose, the olfactory nerve (ON), the olfactory bulb (OB) and higher olfactory brain centers in the cortex (Bear *et al.*, 2016; Manzini *et al.*, 2022). Early diverging vertebrates, like fish, have a single olfactory OE and OB on each side of the head (Hamdani & Døving, 2007). During evolution, many vertebrates have developed distinct subsystems within the OS. Reptiles and amphibians have evolved a dual OS, comprising a main and an accessory OS which differ in anatomical, cellular and molecular characteristics (Manzini *et al.*, 2022; Taniguchi *et al.*, 2007; Taniguchi & Taniguchi, 2014; Weiss *et al.*, 2021). The main OE (MOE) and the main OB (MOB) build the main system, while the accessory system consists of the accessory OB (AOB) and the VNO epithelium (Breer *et al.*, 2006; Munger *et al.*, 2009; Bear *et al.*, 2016; Mohrhardt *et al.*, 2018). In rodents, the OS is even more subdivided, incorporating additional specialized structures such as the Grueneberg ganglion, the septal organ of Masera, and the guanylate cyclase-D necklace system (Munger *et al.*, 2009; Fleischer, 2021; Zimmerman & Munger, 2021). Despite the functional differences across vertebrates, such as the response to different odorant molecules, the expression of different olfactory receptors, the use of distinct signaling cascades, and the connection to different higher brain centers, the overall organization of the OS remains highly conserved (Manzini *et al.*, 2022; Munger *et al.*, 2009).

The OE has a pseudostratified organization that is divided into three characteristic cell layers and cell types (Figure 2; Morrison & Costanzo, 1992). The basal cell layer is made up of a number of round and polyhedral basal cells (BCs) that are found close to the basal lamina. BCs serve as stem and progenitor cells, generating new ORNs and supporting cells for tissue maintenance and regeneration (Figure 2; Astic & Saucier, 2001; Beites *et al.*, 2005; Schwob, 2002). Morphologically, BCs include two subtypes: horizontal BCs, which directly contact the basal lamina, and globose BCs, located above them (Calof & Chikaraishi, 1989; Calof *et al.*, 2002). Globose BCs are the primary stem cell population, generating all differentiated cell types in the OE. Horizontal BCs function as reserve stem cells, remaining quiescent until activated for instance by injury (Schnittke *et al.*, 2015).

The supporting cell layer is made up of the somata of non-neuronal column-shaped sustentacular supporting cells (SCs) that are arranged in columns at the apical border of the OE. SCs terminate on the basal lamina, with their so called “endfeet”, and extend thin prolongations through the entire width of the epithelium (Figure 2; Hassenklöver *et al.*, 2008; Rafols & Getchell, 1983). SCs share features with glial cells, providing structural and chemical support by insulating ORNs (Okano & Takagi, 1974; Voigt *et al.*, 1993; Suzuki *et al.*, 1996; Hansen *et al.*, 1998). They also contribute to signal transduction and regulate extracellular ion concentrations (Hegg & Lucero, 2006; Hassenklöver *et al.*, 2008).

The ORN layer consists of bipolar ORN somata, primarily located in the middle of the OE, each extending a single dendrite to the apical surface (Figure 2). Every dendrite terminates in a knob-like structure with cilia or microvilli bearing olfactory receptors (Eisthen, 1992; Hansen *et al.*, 1998; Schild & Restrepo, 1998; Spehr & Munger, 2009). Additional ORN types , such as crypt cells in fish (Hansen & Finger, 2000), and kappe and pear-shaped neurons in zebrafish (Ahuja *et al.*, 2014; Wakisaka *et al.*, 2017) have been identified. Hybrid ORNs with both cilia and microvilli occur in some birds and reptiles (Graziadei & Bannister, 1967; Hansen, 2007; Wakabayashi & Ichikawa, 2008). Typically, each ORN expresses a single olfactory receptor gene (monogenic expression) from one allele (monoallelic expression; Malnic *et al., 1999;* Manzini *et al.*, 2022; Mombaerts, 2004).

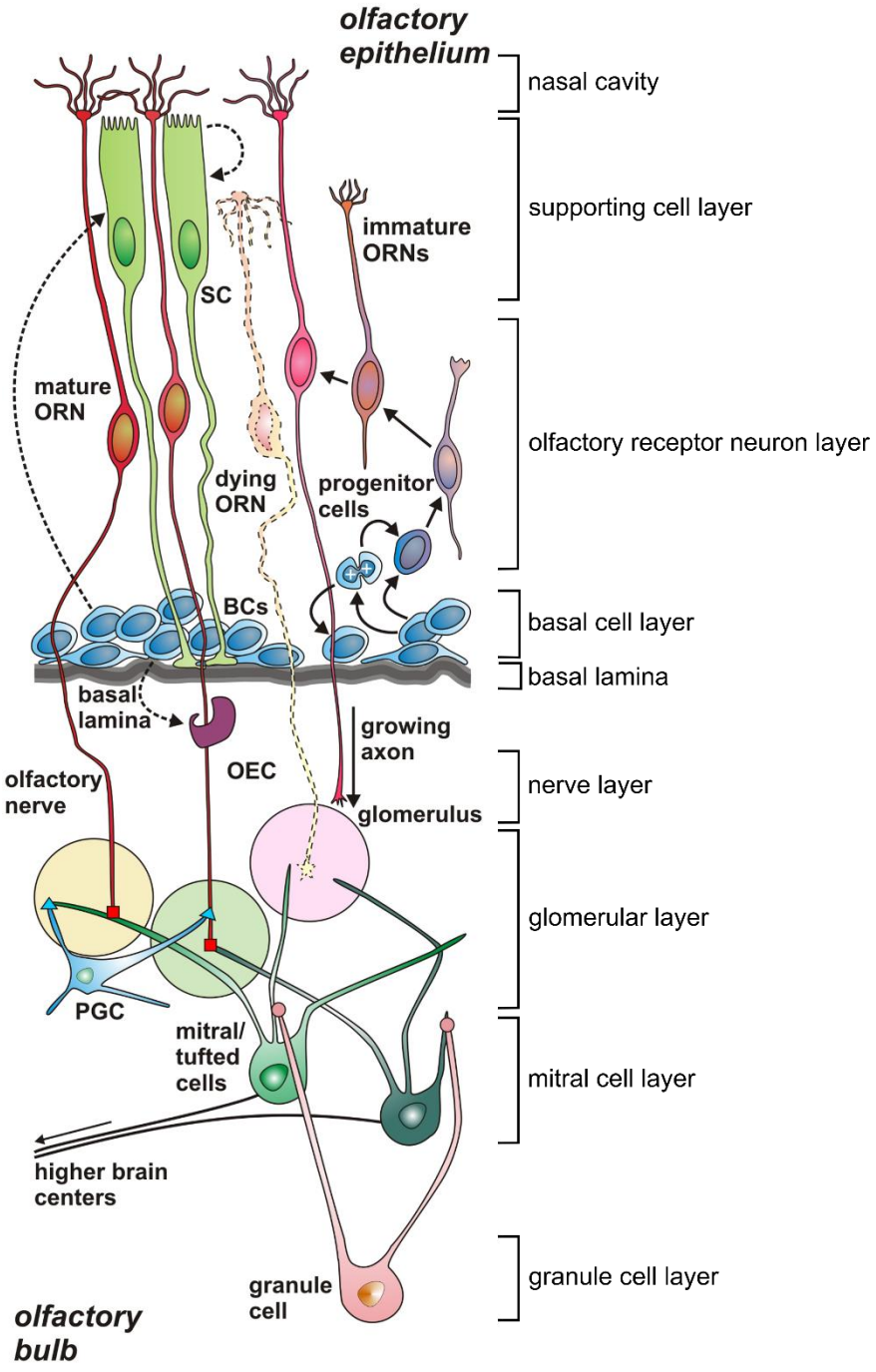

Figure 2: Schematic overview of the cellular organization and layers in the olfactory system of vertebrates. The olfactory epithelium contains three main cellular components: the olfactory receptor neurons (ORNs), non-neuronal supporting cells (SC) and olfactory stem cells, the basal cells (BC). BCs are precursors of ORNs and SCs and possess the ability of neurogenesis throughout life. The cell bodies of SCs are located in the apical layer of the OE, the cell bodies of the bipolar ORNs are located in the olfactory receptor neuron layer in the middle of the epithelium, and the BCs are located basal in the epithelium in the basal cell layer close to the basal lamina. Axons of the ORNs are enwrapped by olfactory ensheathing cells (OEC), grow through the basal lamina of the OE and enter the olfactory bulb (OB). The axons of ORNs converge into olfactory glomeruli in the glomerular layer of the OB. There they form synapses with dendrites of second order neurons called mitral/tufted cells (MTCs), which cell bodies are localized in the mitral cell layer of the OB, which project their axons to higher brain centers. In addition, axons of the ORNs form synapses with interneurons like periglomerular cells (PGC) Dendrites of granule cells form modulatory synapses with dendrites of MTCs and are the most common type of interneurons. The cell bodies of granule cells are localized in the granule cell layer of the OB. Adapted and modified from (Manzini, 2015).

Despite the vast diversity of receptors that are currently understood, the intracellular signaling pathways are highly conserved throughout vertebrates (Manzini & Korsching, 2011; Schild & Restrepo, 1998). Two well-studied mechanisms include a cyclic adenosine monophosphate (cAMP)-dependent transduction pathway linked to OR- and TAAR-type receptors in ciliated ORNs, and a cAMP-independent transduction pathway associated with V1R/ORA- and V2R/OlfC-type receptors in microvillous ORNs (Figure 3 and 4; Firestein *et al.*, 1991; Manzini & Korsching, 2011; Nakamura & Gold, 1987).

4.3.1.1 cAMP-dependent signaling pathway in ciliated ORNs

$G_{\alpha olf}$, the α-subunit of a heterotrimeric G-protein, has been identified as a key component of the signal transduction cascade in mouse ciliated ORNs (Jones & Reed, 1989). Binding of an extracellular ligand to the GPCRs triggers the exchange from guanosine diphosphate (GDP) to guanosine-5'-triphosphate (GTP) in the binding domain of $G_{\alpha olf}$ (Figure 3).This leads to the dissociation of the βγ-dimer and the activation of membrane-bound adenylate-cyclase III (ACIII) (Figure 3; Bakalyar & Reed, 1990; Pace *et al.*, 1985). Adenosine-5`-triphosphate (ATP) is transformed by ACIII into cAMP, a second messenger. Cyclic nucleotide gated (CNG) ion channels are opened by intracellular cAMP, allowing an influx of cations like Na^+ and Ca^{2+} from the external mucus (Nakamura & Gold, 1987). A receptor potential is created by the cation influx and the Ca^{2+} influx leads to a Cl^- efflux through calcium-activated anoctamin (ANO)-2 chloride channels (Figure 3; Billig *et al.*, 2011; Kleene & Gesteland, 1991; Kurahashi & Yau, 1993). This leads to the depolarization of the cell and triggers action potential generation, which enables the transmission of odorant-related information to the cells of the OB.

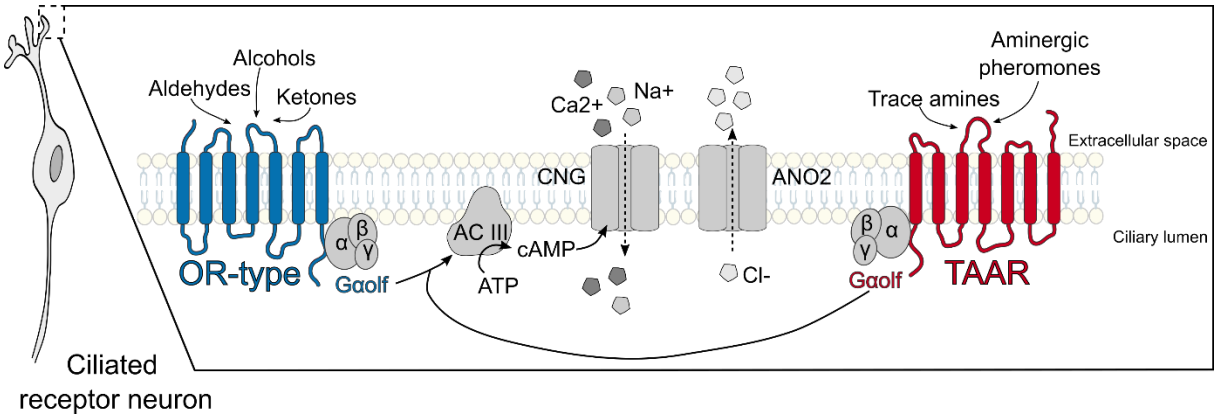

Figure 3: Schematic of the cAMP-dependent signaling pathway in ciliated ORNs. OR-type and TAARs are generally expressed by ciliated ORNs in the main olfactory epithelium of rodents. These receptor types are associated with an intracellular signaling pathway that depends on $G_{\alpha olf}$, which triggers the activation of adenylate cyclase III (ACIII), thereby producing cAMP. Consequently, increases in intracellular cAMP promote the influx of cations and the efflux of anions. The ligands displayed for each type of receptor are generalized to all vertebrates. ACIII adenylate cyclase III; ANO2 anoctamin-2 chloride channel; ATP Adenosine-5`-triphosphate; cAMP cyclic adenosine monophosphate; CNG Cyclic nucleotide gated; OR-type odorant receptor; ORNs olfactory receptor neurons; TAAR trace amine associated receptor.

4.3.1.2 cAMP-independent signaling pathway in microvillous ORNs

Inositol-1,4,5-trisphosphate (IP3), diacylglycerol (DAG), and the transient receptor cation channel type 2 (TRPC2) are the primary constituents of cAMP-independent transduction mechanisms (Figure 4). Extracellular odorant ligands bind to the GPCRs, GTP-bound $G_{\alpha o/i2}$ dissociates and the βγ-dimer activates the membrane-bound phospholipase C (PLC). PLC catalyzes the production of DAG and IP3 (Rünnenburger *et al.*, 2002). Two pathways are used by the second messengers, DAG and IP3, to initiate the Ca^{2+}-influx: DAG triggers the transient receptor cation TRPC2-dependent calcium and sodium influx (Lucas *et al.*, 2003), whereas IP3 mediates the intracellular calcium influx (Figure 4; Yang & Delay, 2010). As a result, increased intracellular calcium levels amplify the receptor potential by opening chloride channels and causing enough membrane depolarization to trigger action potential generation (Yang & Delay, 2010).

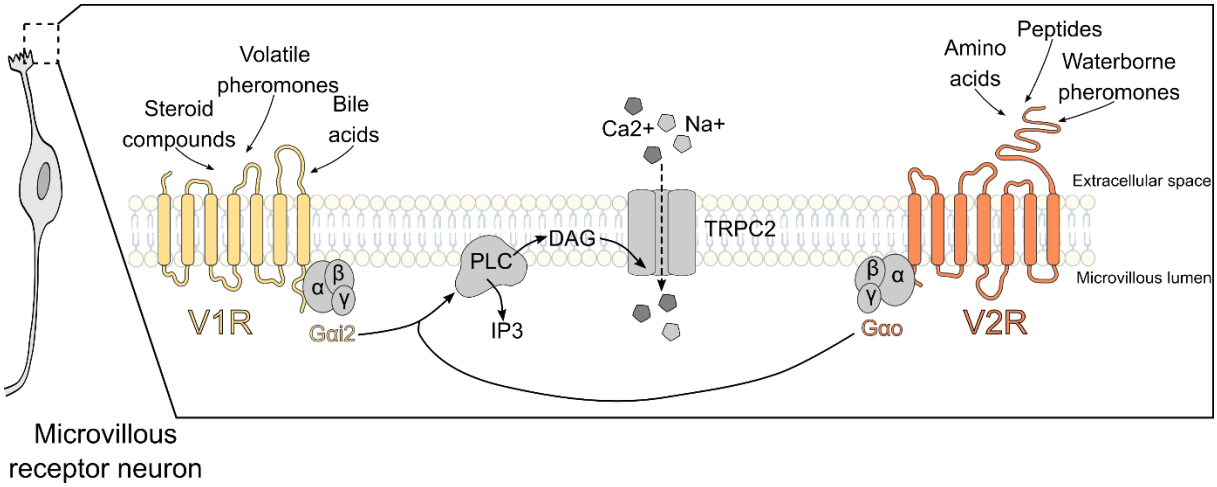

Figure 4: Schematic of the cAMP-independent signaling pathway in microvillous ORNs. Rodents' VNO contains microvillous ORNs that express V1Rs associated with $G_{\alpha i2}$ or V2Rs associated with $G_{\alpha o}$. The cAMP-independent signaling pathway uses a membrane bound phospholipase C (PLC) and a TRPC2 dependent influx of cations. The ligands displayed for each type of receptor are generalized to all vertebrates. DAG diacylglycerol; IP3 inostitol-1-4-5-triphosphate; ORNs olfactory receptor neurons; PLC phospholipase C; TRPC2 receptor cation channel C2; V1R vomeronasal type 1 receptor; V2R vomeronasal type 2 receptor.

In summary, olfactory receptors detect odorants and activate intracellular G proteins, triggering second messenger cascades that open ion channels and depolarize the sensory cell (Ache & Young, 2005; Kaupp, 2010; Manzini *et al.*, 2022; Spehr & Munger, 2009). This process converts a chemical stimulus into an electrochemical signal transmitted by neurons (Bear *et al.*, 2016).

The unmyelinated axons of ORNs converge into fascicles, forming the ON. In rodents, ON fibroblasts surround these axonal bundles, creating a perineurium-like structure, with a small number of ON macrophages positioned externally (Li *et al.*, 1998; Wright *et al.*, 2020). Olfactory glia, also known as olfactory ensheathing cells (OECs), encircle bundles of ten to hundred

ORN axons from the basal lamina of the OE to the glomerular layer of the OB (Figure 2; Doucette, 1993; Higginson & Barnett, 2011; Pellitteri *et al.*, 2010; Sonigra *et al.*, 1999).

The ON connects the OE with the OB in the anterior telencephalon. Axons of ORNs expressing the same olfactory receptor allele converge on a small number of common target structures in the OB known as glomeruli (Ressler *et al.*, 1994; Feinstein & Mombaerts, 2004; Munger *et al.*, 2009). A glomerulus is a dense neuropil network and consists of the terminal branches of ORNs and dendrites of interneurons and projection neurons, which axons project to higher brain centres (Figure 2; Bear *et al.*, 2016; Nagayama *et al.*, 2014). The number of innervated glomeruli and their connectivity patterns vary by species, developmental stage, and olfactory subsystem (Eisthen & Polese, 2007; Weiss, Jungblut, Pozzi, Zielinski, *et al.*, 2020; Weiss, Manzini, *et al.*, 2021; Offner *et al.*, 2023).

4.4 Functional and molecular segregation of olfactory input and projections

Three decades after the discovery of olfactory receptor genes, studies have shown that ORNs expressing the same receptor are distributed in a mosaic-like pattern within the OE, mixed with different ORN populations (Ressler *et al.*, 1994; Vassar *et al.*, 1994; Mombaerts *et al.*, 1996; Syed *et al.*, 2023). While these distributions vary among receptor genes, they broadly overlap (Syed *et al.*, 2023). This "half-random" organization has been observed in fish, frogs, rats, and mice (Kowatschew & Korsching, 2022; Miyamichi *et al.*, 2005; Syed et al., 2013, 2023; Weth *et al.*, 1996; Zapiec & Mombaerts, 2020).

In fish, OR-type receptors, TAARs, V1Rs, and V2Rs are expressed by different ORN-types within the single OE (Hamdani & Døving, 2007; Olivares & Schmachtenberg, 2019; Manzini *et al.*, 2022). Amphibians exhibit the first segregation of receptor gene families between the MOE and VNO (Eisthen, 1992; Manzini & Schild, 2010; Weiss, Manzini, *et al.*, 2021). In *Xenopus laevis*, OR-type receptors, TAARs, V1Rs, and ancestral V2Rs are found in the main OE, while later-diverging V2Rs are restricted to the VNO (see Figure 5; Date-Ito *et al.*, 2008; Freitag *et al.*, 1995; Gliem *et al.*, 2013; Hagino-Yamagishi *et al.*, 2004; Manzini *et al.*, 2022; Syed *et al.*, 2013; Weiss *et al.*, 2021). Thus, vomeronasal receptors are not entirely restricted to the VNO, resulting in an incomplete separation of the main and accessory pathways (Date-Ito *et al.*, 2008; Eisthen, 1992; Syed *et al.*, 2013, 2017; Weiss, Manzini, *et al.*, 2021). In mammals, olfactory receptor gene expression is typically segregated: OR-type receptors, TAARs, and MS4As are found in ORNs of the MOE, while V1Rs, V2Rs, and FPRs are restricted to receptor neurons in the VNO (Breer *et al.*, 2006; Fleischer, 2021; Greer *et al.*, 2016; Liberles *et al.*, 2009; Liberles & Buck, 2006; Manzini *et al.*, 2022; Mombaerts, 2004; Munger *et al.*, 2009). Additionally, the Grueneberg ganglion and septal organ express subsets of TAARs, V1Rs, and OR-type receptors (Breer *et al.*, 2006; Fleischer, 2021; Manzini *et al.*, 2022; Munger *et al.*, 2009).

Axons of ORNs expressing the same olfactory receptor allele converge on specific glomeruli in the OB through molecular sorting and axonal guidance (Ressler *et al.*, 1994; Vassar *et al.*, 1994; Feinstein & Mombaerts, 2004; Mombaerts, 2006). The distribution of ORNs expressing the same receptor and their axonal projections in the OB vary by species and olfactory subsystem.

4.4.1 Olfactory adaptations in amphibians

Amphibians are particularly interesting for studying adaptations required for both terrestrial and aquatic olfaction. Most species have an aquatic larval stage followed by an adult that lives more or less independently from the water (Weiss, Manzini, *et al.*, 2021; Woodley, 2015). Their olfactory receptor repertoire must be capable of detecting both waterborne and airborne odorants, reflecting their developmental stage and lifestyle (Shi & Zhang, 2007; Silva & Antunes, 2017). The secondary aquatic frog *Xenopus laevis* has adapted to live an almost exclusive aquatic lifestyle, but occasionally moves across land in search of water bodies or food (Du Plessis, 1966; Measey, 2016). Adult animals have both an air-nose and a water-nose. Both, their aquatic lifestyle and their evolutionary intermediate position between fish and terrestrial vertebrates, are reflected in their olfactory receptor repertoire (Dittrich *et al.*, 2016; Hansen *et al.*, 1998; Reiss & Eisthen, 2008; Weiss *et al.*, 2021).

4.4.2 Structural and functional reorganization of the OS during metamorphosis

Larval and adult *Xenopus laevis* differ in nasal cavity morphology and olfactory receptor expression. The nasal cavity of tadpoles consists of a half-moon shaped main OE, also known as principal cavity (PC), and a spatial separated more oval-shaped VNO (Figure 5). During metamorphosis, the larval main OE is functionally reorganized in the PC and a new OE forms the middle cavity (MC), while the VNO is retained (Figure 5, Altner, 1962; Dittrich *et al.*, 2016; Hansen *et al.*, 1998; Weiss, Manzini, *et al.*, 2021). In adults, the VNO, the PC, and the MC are interconnected (Woodley, 2014). A valve directs air to the PC (also known as an air-nose) and water to the MC (also known as a water-nose). Throughout life, the VNO remains water-filled (Altner, 1962; Weiss *et al.*, 2021; Woodley, 2014).

The larval MOE harbors both, ciliated and microvillous ORNs, while the VNO of tadpoles and adults exclusively contains microvillous ORNs (Figure 5). In adults, the PC harbors only ciliated ORNs, whereas the MC is lined with both ciliated and microvillous ORNs (Figure 5; Weiss *et al.*, 2021; Hansen *et al.*, 1998; Woodley, 2014).

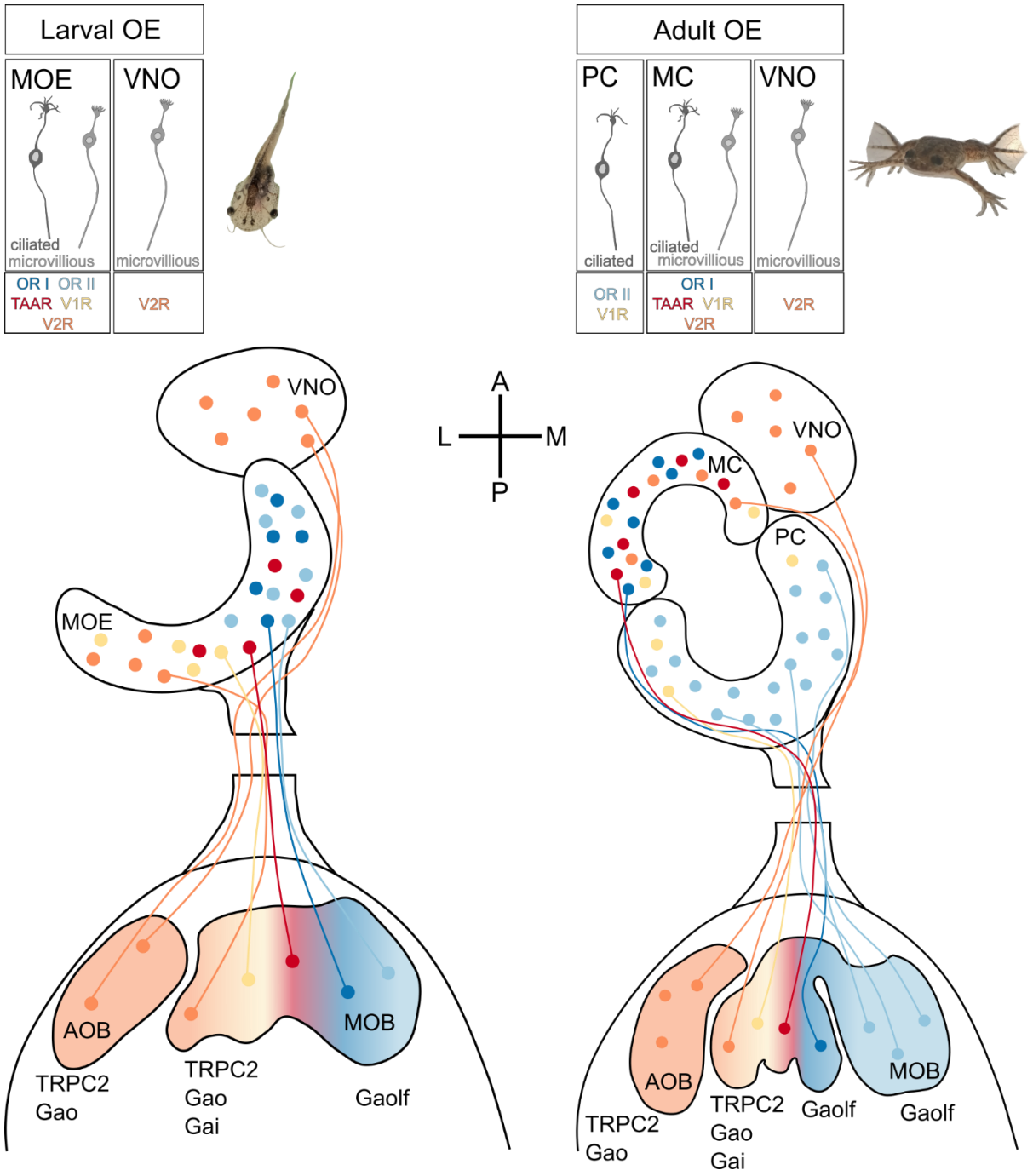

Figure 5: Subsystem segregation in the larval and adult olfactory system of *Xenopus laevis*. The schematic summarizes a simplified overview of the olfactory subsystems in both larval and adult *Xenopus laevis*. The morphological types of ORNs and their receptors expressed in different olfactory organs are represented by the boxes on top. Only the left side of the system is shown. The clawed frog has a clearly segregated VNO-AOB pathway. The adult frog's main OE (MOE) is separated into two areas: the principal cavity (PC) and the middle cavity (MC), which innervate different zones of the main OB (MOB) and are linked to aquatic and aerial olfaction, respectively. The depicted schemes are mainly based on the following publications and reviews: (Gliem et al., 2013; Manzini & Schild, 2010; Syed et al., 2013, 2017; Weiss, et al., 2021; Weiss, Manzini, et al., 2021) and the scheme is adapted and modified from (Weiss, Manzini, *et al.*, 2021). A anterior; AOB accessory olfactory bulb; D dorsal; L lateral; M medial; MC middle cavity; MOB main olfactory bulb; MOE main olfactory epithelium; OE olfactory epithelium; OB olfactory bulb; ON olfactory nerve; OR I odorant receptor-type I; OR II, mammalian class II/γ subfamily of odorant receptor; P posterior; PC principal cavity; TAAR trace amine associated receptor; V ventral; V1R vomeronasal type 1 receptor; V2R vomeronasal type 2 receptor; VNO vomeronasal organ.

4.4.3 Distribution pattern of olfactory receptors in the larval and adult *Xenopus* epithelia

The microvillar ORNs in the larval and adult VNO of *Xenopus laevis* express V2Rs and rely on $G_{\alpha o}$ and TRPC2 for signal transduction (Gliem *et al.*, 2013; Hagino-Yamagishi *et al.*, 2004; Sansone *et al.*, 2014; Syed *et al.*, 2013). Although the VNO and MOE are anatomically distinct, vomeronasal receptor expression is not strictly confined to the VNO (Woodley, 2014). In *Xenopus*, V1Rs are exclusively expressed in the larval MOE and the adult MC and PC, but not in the VNO (Date-Ito *et al.*, 2008; Gliem *et al.*, 2013). Additionally, more ancestral V2Rs are expressed by ORNs whose somata are located in more basal layers in the larval MOE and the adult MC, whereas later diverging V2Rs are restricted to the VNO (Date-Ito *et al.*, 2008; Hagino-Yamagishi *et al.*, 2004; Sansone *et al.*, 2014; Syed *et al.*, 2013, 2017). The classification of the PC as the adult "air-nose" is further supported by the preferential expression of OR-type receptors from the OR II subfamily, which expanded in terrestrial vertebrates, in both the larval MOE and the adult PC (Freitag *et al.*, 1995). Moreover, TAARs are expressed in the larval MOE as well as in the PC and MC of adults (Gliem *et al.*, 2009). TAARs and ORs are typically expressed by ciliated ORNs (Firestein *et al.*, 1991; Manzini & Korsching, 2011; Nakamura & Gold, 1987).

4.4.4 Axonal projection patterns in the olfactory bulb of olfactory receptor neurons expressing the same receptor are quite similar in larval and adult *Xenopus*

In amphibians, the ORNs of the MOE project their axons to the MOB, and the sensory neurons of the VNO project their axons to the AOB (Woodley 2014). In *Xenopus laevis*, distinct regions of the olfactory epithelia project to distinct areas of the main OB (see Figure 5). In adults, ORNs from the PC project their axons to the dorsal MOB, while ORNs from the MC project their axons to the ventral MOB (Saito & Taniguchi, 2000). The axonal projections of larval and adult *Xenopus laevis* can be divided into two functional streams: the lateral cluster of glomeruli is primarily amino acid sensitive, cAMP-independent, and most likely mediated by microvillous ORNs that express V1Rs or V2Rs and use the $G_{\alpha o}$ protein for signaling. (Figure 5; Gliem *et al.*, 2013; Hawkins *et al.*, 2024; Manzini *et al.*, 2007; Nakamuta *et al.*, 2011; Syed *et al.*, 2017). In contrast, the medial cluster of glomeruli is sensitive to alcohols, ketones, bile acids, amines, and aldehydes, cAMP-dependent, uses $G_{\alpha olf}$ for signaling, and form part of putatively ciliated, primarily OR-type (or possibly TAARs) expressing, ORNs *(*Figure 5; Gliem *et al.*, 2013; Manzini *et al.*, 2007; Nakamuta *et al.*, 2011). The expression of olfactory receptors in both the dendrites and the axons of receptor neurons is crucial for the creation of a glomerular map via axonal projections to the OB (Mombaerts, 2006; Offner *et al.*, 2023; Weiss *et al.*, 2021; Weiss *et al.*, 2020). Despite significant progress, key molecular markers are still needed to clearly differentiate olfactory receptor families and neuronal subtypes in the OS of *Xenopus laevis*.

4.5 Neurogenesis and regenerative capacity of vertebrates

Neurogenesis continues throughout development and adult life in specific areas of the vertebrate central nervous system (Altman, 1962; Brann & Firestein, 2014; Fairless & Barnett, 2005; Graziadei & Graziadei, 1979 a,b; Mackay-Sim & Kittel, 1991). These areas include the subgranular zone, which generates granule cells for the hippocampus; the subventricular zone, which produces interneurons for the OB; and the olfactory epithelia, the OE and VNO, where BCs, the neural stem cells, generate new excitatory ORNs and SCs throughout life (Altman, 1962; Brann & Firestein, 2010; 2014; Kaplan & Hinds, 1977; Liao *et al.*, 2024; Graziadei & Graziadei, 1979b; Schwob, 2002). Due to the ORNs' exposed position in the OE, this is necessary, because they are easily damaged by exposure to harmful chemicals, infections, pollutants, or injuries (Manzini, 2015; Schwob, 2002). The ability of ORNs for continual axon growth and successful targeting into the corresponding glomerular regions in the OB is facilitated, by OECs, the glial cells of the OS (Barton *et al.*, 2017; Doucette, 1990; Ekberg *et al.*, 2012; Ekberg & St John, 2014; Key & St John, 2002; Mackay-Sim & Kittel, 1991; Raisman, 1985)

4.5.1 Influence and characteristics of olfactory ensheathing cells during regeneration

OECs are a special type of glia cells, which can migrate from the peripheral into the central nervous system (Doucette, 1990; Ekberg *et al.*, 2012; Raisman, 1985). They can survive and renew throughout life (Chehrehasa *et al.*, 2010; Ekberg *et al.*, 2012; Liao *et al.*, 2024). OECs encircle and guide ORN axon bundles, support their growth with a diverse neurotrophic profile, and assist in axon sorting for projection into the corresponding glomerular regions of the OB (Boruch *et al.*, 2001; Chehrehasa *et al.*, 2010; Windus *et al.*, 2011; Ekberg *et al.*, 2012; Liao *et al.*, 2024). They also serve as innate immune cells in the OS, phagocytosing ON fragments and apoptotic ORNs (Nazareth, Lineburg, *et al.*, 2015; Su *et al.*, 2013). *In vitro* studies have shown that OECs secrete neurotrophic factors and express distinct markers depending on their location along the ORN axons (Boruch *et al.*, 2001; Woodhall *et al.*, 2001; Chehrehasa *et al.*, 2010; Ekberg *et al.*, 2012). These characteristics make OECs promising candidates for nerve injury treatments (Ekberg *et al.*, 2012; Barton *et al.*, 2017; Murtaza *et al.*, 2022; Huang *et al.*, 2024; Liao *et al.*, 2024). However, their exact mechanisms remain poorly understood, and the majority of data come from mammalian models (Pellitteri *et al.*, 2010; Ekberg *et al.*, 2012; Bettini *et al.*, 2019; Murtaza *et al.*, 2022; Huang *et al.*, 2024; Liao *et al.*, 2024). The absence of OEC-specific markers further complicates research (Reshamwala *et al.*, 2020). But nevertheless, early branching vertebrates, like amphibians demonstrate enormous ability for brain and OS regeneration (Alesci *et al.*, 2022). Comparative neurobiology of the olfactory systems, particularly OECs across species, could advance our understanding of neuronal degeneration and regeneration.

4.5.2 Regenerative capacity and OECs in *Xenopus laevis*

The principles governing cell turnover in the OS and the characteristics of the neural stem cells in the OE are conserved across vertebrates (Manzini *et al.*, 2022; Schwob *et al.*, 2017; Sokpor *et al.*, 2018). Stem cell proliferation and cell death take place during the process of natural turn-over and following OS injury (Brann & Firestein, 2014; Graziadei & Metcalf, 1971; Graziadei & Graziadei, 1979b; Schwob, 2002; Schwob *et al.*, 2017). Amphibians, with their high OS regenerative capacity, provide an opportunity to study the evolution of olfaction in air and water environments (Schwob, 2002; Cheung *et al.*, 2014; Weiss, Manzini, *et al.*, 2021; Alesci *et al.*, 2022). In *Xenopus laevis*, the OS is fully functional during the larval stage (Alesci *et al.*, 2022). Many data about the cellular structure, neuronal circuity, and function of the anuran sense of smell have been acquired from research of the African clawed frog *Xenopus laevis* (Weiss, Manzini, *et al.*, 2021). The transparency of its tissues, peripheral location, and organized cellular composition make it an ideal model for studying stem cell, axon, and synaptic differentiation (Alesci *et al.*, 2022; Manzini, 2015).

In *Xenopus laevis*, ORN axons reach the OB in developing stages 37/38 (Nieuwkoop & Faber, 1994; Byrd & Burd, 1991), where they form glomerular synapses, which are well developed by stage 40 (Byrd & Burd, 1991; Hansen *et al.*, 1998). During metamorphosis, the OS gradually reorganizes without losing its ability to process olfactory information. The system undergoes a substantial rewiring and the majority of ORNs are replaced (Dittrich *et al.*, 2016; Manzini, 2015). Like all adult vertebrates, *Xenopus* maintains constant ORN turnover after metamorphosis (Hansen *et al.*, 1998; Dittrich *et al.*, 2016). In addition, the OS of larval *Xenopus laevis* regenerates with high accuracy after ON lesion (Cervino *et al.*, 2017; Hawkins *et al.*, 2017, 2024; Manzini, 2015; Terni *et al.*, 2017). However, little is known about the role and function of OECs during regeneration in *Xenopus*. Putative OECs exhibit phagocytic activity in the ON at all developmental stages (Burd, 1991), though a specific marker for *Xenopus* OECs remains unidentified. Research in non-mammalian species could provide crucial insights into OEC function and their potential for treating nerve injuries.

4.6 Aims of the thesis

During tetrapod evolution, the olfactory system has increasingly diverged into functionally and morphologically distinct subsystems. While teleost fish possess a single peripheral olfactory surface, tetrapods exhibit separate primary and accessory olfactory organs: the main olfactory epithelium (MOE) and the vomeronasal organ (VNO). This segregation extends to the brain, where olfactory projections target the main and accessory olfactory bulbs. In amphibians, as in other tetrapods, the VNO is distinct but not fully separated at the molecular level, as olfactory receptor neurons with different identities remain interspersed in the MOE. S100 calcium-binding protein Z (S100Z), a less characterized member of the S100 protein family, is associated with the VNO in mammals and a specific subpopulation of cells in the olfactory placode of zebrafish. This thesis investigates S100Z expression in *Xenopus laevis*, an amphibian model.

Aims of this part are:

1. Identification of cell types in the olfactory epithelium that express S100Z and subsequent analysis of their distribution within the epithelium
2. Investigation of the axonal projection of S100Z expressing ORNs in the OB
3. Comparison of the larval and adult expression pattern of S100Z in the OS

The second part of this thesis examines the regenerative capacity of the olfactory system in *Xenopus laevis* larvae, which relies on basal cells in the epithelium and olfactory ensheathing cells (OECs) in the olfactory nerve (ON). While basal cells function in this organism is relatively well studied, the properties of non-neuronal OECs remain largely unexplored. This thesis examines non-neuronal cell populations in the olfactory nerve of *Xenopus laevis* larvae, their morphological diversity, and the activity-dependent phosphorylation of ribosomal proteins following nerve transection.

Aims of this part are:

1. Identification of different cell types in the ON
2. Analysis of different morphologies of putative OECs labelled by single-cell electroporation
3. Investigation and analysis of the dynamic and activity dependent phosphorylation of ribosomal protein S6 in non-neuronal cells in the ON after lesion in larval *Xenopus*

5 Publications

5.1 1st publication: S100Z is expressed in a lateral subpopulation of olfactory receptor neurons in the main olfactory system of *Xenopus laevis*

Received: 20 December 2023 | Revised: 7 February 2024 | Accepted: 15 February 2024

DOI: 10.1002/dneu.22935

RESEARCH ARTICLE

WILEY

S100Z is expressed in a lateral subpopulation of olfactory receptor neurons in the main olfactory system of *Xenopus laevis*

Melina Kahl | **Thomas Offner** | **Alena Trendel** | **Lukas Weiss** | **Ivan Manzini** | **Thomas Hassenklöver**

Institute of Animal Physiology, Department of Animal Physiology and Molecular Biomedicine, Justus-Liebig-University Giessen, Giessen, Germany

Correspondence
Thomas Hassenklöver, Institute of Animal Physiology, Department of Animal Physiology and Molecular Biomedicine, Justus-Liebig-University Giessen, 35392, Giessen, Germany.
Email: thomas.hassenkloever@physzool.bio.uni-giessen.de

Present addresses
Thomas Offner, Zebrafish Neurobiology, European Neuroscience Institute, Göttingen, Germany.
Lukas Weiss, Department of Ecology and Evolutionary Biology, Princeton University, Princeton, NJ, USA.

Funding information
Deutsche Forschungsgemeinschaft, Grant/Award Number: 4113/4-1

Abstract

In contrast to other S100 protein members, the function of S100 calcium-binding protein Z (S100Z) remains largely uncharacterized. It is expressed in the olfactory epithelium of fish, and it is closely associated with the vomeronasal organ (VNO) in mammals. In this study, we analyzed the expression pattern of S100Z in the olfactory system of the anuran amphibian *Xenopus laevis*. Using immunohistochemistry in whole mount and slice preparations of the larval olfactory system, we found exclusive S100Z expression in a subpopulation of olfactory receptor neurons (ORNs) of the main olfactory epithelium (MOE). S100Z expression was not co-localized with TP63 and cytokeratin type II, ruling out basal cell and supporting cell identity. The distribution of S100Z-expressing ORNs was laterally biased, and their average number was significantly increased in the lateral half of the olfactory epithelium. The axons of S100Z-positive neurons projected exclusively into the lateral and intermediate glomerular clusters of the main olfactory bulb (OB). Even after metamorphic restructuring of the olfactory system, S100Z expression was restricted to a neuronal subpopulation of the MOE, which was then located in the newly formed middle cavity. An axonal projection into the ventro-lateral OB persisted also in postmetamorphic frogs. In summary, S100Z is exclusively associated with the main olfactory system in the amphibian *Xenopus* and not with the VNO as in mammals, despite the presence of a separate accessory olfactory system in both classes.

KEYWORDS
amphibian, calcium-binding protein, frog, larval, olfaction, tadpole, vomeronasal organ

1 | INTRODUCTION

Calcium (Ca^{2+}) is a ubiquitous intracellular messenger, which influences and regulates a variety of cellular processes in multifaceted ways (Berridge et al., 2003; Carafoli et al., 2001). Ca^{2+} signaling fundamentally depends on intracellular Ca^{2+} concentration changes in complex spatio-temporal patterns (Berridge et al., 2000). These signals are detected, modulated, and transduced by a diverse set of molecular elements, including Ca^{2+}-binding proteins, to regulate cell physiology (Elíes et al., 2019; Yáñez et al., 2012). The superfamily of Ca^{2+}-binding proteins with EF-hand motif plays a key role in

this process by buffering cytosolic Ca^{2+}, fine-tuning the spatial and temporal properties of Ca^{2+} signals and mediating functional changes (Schwaller, 2020).

The S100 protein family is a distinct class of EF-hand Ca^{2+}-binding proteins and has only been identified in vertebrates (Gonzalez et al., 2020). It consists of more than 20 known members that exhibit cell type-specific expression (Gonzalez et al., 2020). A shared feature of S100 proteins is a characteristic dimeric architecture, where each monomer contains two EF-hand motifs connected by a flexible linker region (Santamaria-Kisiel et al., 2006). Binding of Ca^{2+} leads to conformational changes in these regions that ultimately facilitate the interaction with target proteins to regulate their activity (Santamaria-Kisiel et al., 2006). S100 proteins are involved in cell differentiation and proliferation, cell motility, apoptosis, regulation of enzymes, immune homeostasis, and modulation of membrane-cytoskeletal interactions, among others (Gonzalez et al., 2020). It has been well-established in both humans and rodents that S100 dysregulation can be the cause of various diseases such as cancer, inflammatory/autoimmune conditions, diabetes, and neurodegenerative diseases (Gonzalez et al., 2020; Singh & Ali, 2022). S100 proteins play an important role also in neurons, where they directly modulate ion channels shaping neuronal activity (Hermann et al., 2012). Notably, S100 proteins not only act as intracellular regulators but some members are secreted into extracellular space to exert effects on distant cells (Donato, 2003).

S100 calcium-binding protein Z (*s100z*) is a less well-characterized member of the S100 protein family. The function of S100Z is still largely unknown, but the studies available suggest an important role in the olfactory system. In larval zebrafish, *s100z* expression is exclusively found in the olfactory placode and is restricted to a subpopulation of cells, presumably neurons (Kraemer et al., 2008). In the olfactory organ of adult zebrafish, the regions comprising olfactory receptor neurons (ORNs) express *s100z* (Dieris et al., 2021). In mammals, *s100z* is associated with the accessory olfactory system, specifically the vomeronasal organ (VNO; Hecker et al., 2019). Notably, the evolutionary reduction/loss of the VNO in aquatic mammals, several bats, and primates coincides with an inactivation of the *s100z* gene (Hecker et al., 2019).

During tetrapod evolution, the olfactory system shows a trend toward functional and morphological segregation into distinct subsystems (Bear et al., 2016). While teleost fish have a peripheral olfactory organ with a single sensory surface, tetrapods have distinct main and accessory olfactory organs: the main olfactory epithelium (MOE) and the VNO (Bear et al., 2016; Mohrhardt et al., 2018; Weiss et al., 2021). The different subsystems are also separated at the level of the brain, where the olfactory projections target a main and an accessory olfactory bulb (AOB; Bear et al., 2016; Mohrhardt et al., 2018; Weiss et al., 2021). Olfactory sensory neurons associated with these subsystems differ in their morphology and molecular properties, like olfactory receptor gene family expression and transduction machinery (Bear et al., 2016; Mohrhardt et al., 2018; Weiss et al., 2021). Although amphibians present a distinct VNO, as other tetrapods, the organizational division is incomplete and ORNs with different molecular identities are intermingled in the MOE (Date-Ito et al., 2008; Gliem et al., 2013; Sansone, Hassenklöver, et al., 2014; Sansone, Syed, et al., 2014; Syed et al., 2013; Weiss et al., 2021).

Since *s100z* has been linked to the VNO in mammals, this raises the question of how it is distributed in basal tetrapods, the amphibians. Here, we examined whether the expression of *s100z* is always strictly associated with the VNO in an anuran amphibian. We applied immunohistochemistry to investigate the expression pattern of S100Z in the pre- and postmetamorphic olfactory system of *Xenopus laevis*.

2 | MATERIALS AND METHODS

2.1 | Animals

Wildtype albino *X. laevis* (both sexes) and transgenic albino paired box 6 (*pax6*)-green fluorescent protein (GFP) [Xla.Tg (*pax6*: GFP; *cmv*: DsRED)^{Papal} (xenopusresource.org) bred into an albino background in our lab] *X. laevis* were used. They were kept and bred at the animal husbandry facility of the Institute of Animal Physiology of the Justus-Liebig-University Giessen. Tanks with volumes of 1.8−7.5 L and constant water circulation at 19−22°C were used. Tadpoles were fed with a mixture of *Spirulina* and *Chlorella* algae (MS-Tierbedarf) and frogs with ESF 10 Krallenfrosch Extrudat (Granovit AG). Tadpoles of stages 48−52 were used as a representative of the premetamorphic developmental phase, and froglets of stage 66 were used as a representative of the post-metamorphic developmental phase (Nieuwkoop & Faber, 1994). All animal procedures were performed in accordance with the guidelines of Laboratory animal research of the Institutional Care and Use Committee of the University of Giessen (649_M).

Before experimental procedures, animals were anesthetized using 0.02% MS-222 (ethyl 3-aminobenzoate methanesulfonate, TCI Tokio Chemicals) in tap water. Anesthetized animals were killed by severing the transition between the brainstem and spinal cord. Tissue blocks containing the noses and the rostral part of the telencephalon were excised.

2.2 | General labeling of ORNs

In some samples, we labeled sensory neurons by using a biocytin backfill. Within the tissue blocks, we transected both

ONs with fine scissors without damaging surrounding tissue and placed Biocytin (ε-biotinoyl-L-lysine, Molecular Probes, ThermoFisher Scientific) crystals into the lesioned ONs. With this approach, all ORNs of the olfactory organ that have an axon at the transection site were labeled. The lesion was closed with tissue adhesive (Histoacryl L; Braun) and tissue blocks were incubated for 1 h at room temperature in frog Ringer solution (98 mM NaCl, 2 mM KCl, 1 mM $CaCl_2$, 2 mM $MgCl_2$, 5 mM Na-pyruvate, 5 mM glucose, 10 mM HEPES, pH 7.8, osmolarity of 230 mOsmol/l).

2.3 | Fixation

All samples were fixed in 4% formaldehyde for 1 h at room temperature and washed three times, each 10 min, with phosphate-buffered saline (PBS: 137 mM NaCl, 2.7 mM KCl, 8 mM Na_2HPO_4, 1.4 mM KH_2PO_4, dissolved in purified water, pH 7.4).

2.4 | Whole mount and tissue slice preparation

We either used whole mount preparations or tissue slices for labeling. In whole mounts, we investigated the whole olfactory system by cutting the olfactory nerves (ONs) close to the noses and extracting the entire brain from the tissue block. The complete olfactory epithelium was preserved and processed independently. We did not use any embedding medium for the tissue blocks. For the preparation of tissue slices of the olfactory system, we glued tissue blocks directly onto the stage of a half-automatic vibratome (VT1200S; Leica Biosystems). Tissue blocks containing the olfactory epithelium were sliced horizontally at 200−250 μm thickness, whereas OB slices were sliced at 330 μm thickness.

2.5 | Immunohistochemistry

All tissues were permeabilized using phosphate-buffered saline containing 0.2% Triton-X100 (PBST; Carl Roth) three times, each 10 min, and non-specific binding was blocked with 2% normal goat serum (NGS; MP Biomedicals) for 1 h at room temperature. The samples were incubated with primary antibodies (1:100) in PBST and 2% NGS at 4°C for 68 to 72 h with one or two of the following antibodies: anti-*Homo sapiens* S100Z (MBS2033797, polyclonal, derived from rabbit; BioTrend); anti-*X. laevis* cytokeratin type II (Cytok II; 1h5, RRID:AB_528323, monoclonal, derived from mouse; deposited to the Developmental Studies Hybridoma Bank by Klymkowsky, M.); anti-calretinin (6B3, RRID:AB_10000320 monoclonal, derived from mouse, Swant); anti-neural cell adhesion molecule 1 (NCAM1; 4d, RRID:AB_528389, monoclonal, derived from mouse, deposited to the Developmental Studies Hybridoma Bank by Rutishauser, U.); anti-beta tubulin (TUBB; E7, RRID:AB_528499, monoclonal, derived from mouse, deposited to the Developmental Studies Hybridoma Bank by Klymkowsky, M.); anti-TP63 (ab735, RRID:AB_305870, monoclonal, derived from mouse, Abcam). The human S100Z protein (NCBI Reference Sequence: XP_054207898.1) shows an amino acid identity similarity of ~75% and ~87% positives, compared to the translated mRNA sequence of the *X. laevis* L/S homeologs (NM_001097818.2, XM_041580516.1; tblastn). Green fluorescent protein signals were enhanced with anti-GFP (ab1218, RRID:AB_298911, monoclonal, derived from mouse; Abcam). The primary antibodies were washed off with PBS three times, each 10 min.

The samples with biocytin-backfilled ORNs were additionally incubated in Alexa 488-conjugated streptavidin (Molecular Probes, Thermo Fisher Scientific) at a final concentration of 5 μg/mL in PBST for 5 h and repeatedly rinsed in PBS. They were incubated with the secondary antibodies Alexa Fluor 594 goat anti-rabbit (Invitrogen, Thermo Fisher Scientific; 1:250) in PBS with 2% NGS at 4°C for 68 to 72 h.

All other samples were incubated with the secondary antibodies Alexa Fluor 488 goat-anti mouse or/and Alexa Fluor 488 or 594 goat-anti rabbit (Invitrogen, Thermo Fisher Scientific; 1:250) in PBS with 2% NGS at 4°C for 68 to 72 h. The secondary antibodies were washed off with PBS three times, each 10 min.

In samples with only one primary antibody application, cell nuclei were labeled with 10 μg/mL propidium iodide (Molecular Probes, Thermo Fisher Scientific) for 15 min and subsequently washed three times with PBS, each 10 min. It was standard procedure to perform negative antibody controls.

2.6 | Image acquisition and processing

Samples were transferred into a recording chamber in PBS and stabilized with a platinum frame stringed with nylon threads. The OBs were imaged with the ventral surface up and the olfactory epithelia were imaged with the dorsal surface up.

The image stacks were acquired using multiphoton microscopy (A1R MP; Nikon) at an excitation wavelength of 780 nm. Axial resolution of OB and MOE samples was 3 and 2 μm, respectively. Fluorescence emission was detected with three different detectors (blue 400−492 nm, green 500−550 nm, red 601−657 nm). The brightness and contrast of the image stacks were adjusted using the image processing software ImageJ (Schindelin et al., 2012) and median filtering was applied to reduce image noise when

necessary. Pigmentation-derived autofluorescence was mathematically removed by subtracting the blue channel from the other channels using the image calculator function in ImageJ. Images showing the whole olfactory system of adult animals were combined from multiple image stacks using a stitching algorithm (Preibisch et al., 2009).

2.7 | Data analysis

S100Z-positive cells of the MOE were manually counted using ImageJ. The MOE was divided into smaller z-stacks (six to ten substacks) from dorsal to ventral. In all image planes, the basal and apical boundaries of the OE were traced with the freehand tool. These reference outlines were used for the distribution analysis of S100Z-positive cells. Each cell soma showing fluorescence signal was manually outlined using the region of interest (ROI) manager of ImageJ. The absolute position of each cell was defined as the centroid of cell soma outline. The relative position within the MOE was defined as the angle from the center of the fluid-filled nasal cavity. A vector through the average coordinates of the basal and apical boundary regions was identified as a good proxy for the middle of the MOE. We connected the position of each identified cell to the apical boundary central point and calculated the angle to the central vector (see also Figure 3a). An angle of 0° was defined at a position directly in the middle of the lateral to medial axis of the MOE. Negative and positive angles indicated lateral and medial positions, respectively. The distribution pattern of the labeled cells was evaluated in Python (code and data are available at https://doi.org/10.22029/jlupub-18280). We identified and quantified the distribution of biocytin-backfilled ORNs as a control using the same protocol.

2.8 | Statistics

Statistical difference was analyzed using Kruskal–Wallis paired samples test with Bonferroni correction.

3 | RESULTS

3.1 | S100Z expression in the olfactory system of larval *X. laevis*

Immunohistochemical processing of the olfactory system of premetamorphic *X. laevis* with an antibody against S100Z leads to strong labeling in both the MOE and OB (Figure 1). We found S100Z expression in bipolar cells with an apical dendritic knob, throughout the whole MOE, resembling ORNs (Figure 1a). We identified fibers connected to labeled cells as axons that were clearly projecting into the ON and subsequently into glomerular clusters of the OB (Figure 1b). Within the OB, we found no S100Z-positive cell bodies.

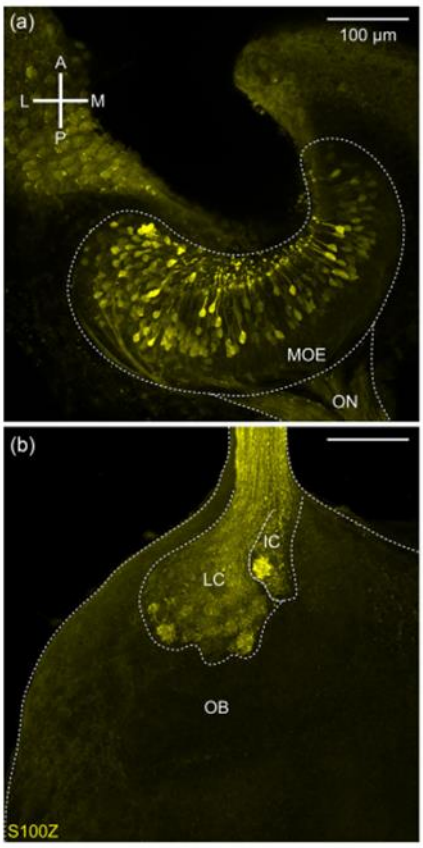

FIGURE 1 S100Z expression in the main olfactory system of larval *Xenopus laevis*. (a) Immunohistochemical staining for S100Z revealed cells with neuron-like morphology, bipolar shape with dendritic knobs, throughout the whole MOE of the peripheral olfactory organ. The axon-like processes of S100Z-positive cells extended into the ON. (b) Axons of S100Z-positive cells projected into glomeruli within the glomerular layer of the OB in premetamorphic tadpoles. No S100Z-positive cell bodies were visible in the different layers of the OB. Structures of the olfactory system and glomerular clusters are outlined with a dotted white line. A, anterior; IC, intermediate cluster; L, lateral; LC, lateral cluster; M, medial; MOE, main olfactory epithelium; OB, olfactory bulb; ON, olfactory nerve; P, posterior.

3.2 | S100Z expression restricted to ORNs

We performed complementary immunohistochemistry in premetamorphic *X. laevis* to confirm the neuronal identity of labeled cells and to check for other cell types that

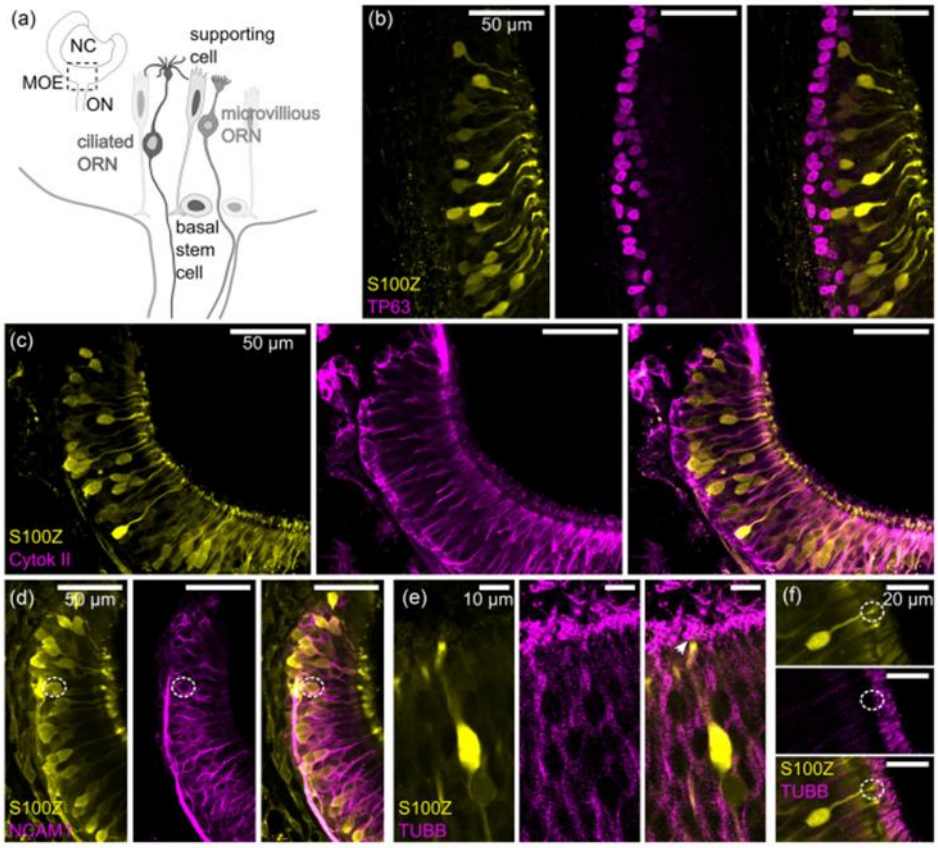

FIGURE 2 S100Z expression exclusively in ORNs. (a) Schematic overview of the peripheral olfactory organ of premetamorphic *X. laevis*. The major cell types of the main olfactory epithelium are highlighted. (b) Stem cell marker TP63 (magenta) was localized in cell nuclei in basal cell layers, highlighting basal stem cells. S100Z-positive cells (yellow) occurred in more intermediate layers of the olfactory epithelium. No co-localization of S100Z and TP63 was found. (c) Supporting cells expressing cytokeratin type II (Cytok II, magenta) did not express S100Z (yellow). (d) Membrane-localized NCAM1 (magenta) is a marker for developing neurons. A subset of S100Z-expressing cells (yellow) was clearly surrounded by NCAM1 immunoreactivity (white dotted circle) and dendrites showed co-localization. (e) Microtubules were labeled with antibodies against beta tubulin (TUBB, magenta). TUBB was found at cellular boundaries and apical appendages, presumably cilia (arrow). S100Z signal only clearly occurred in soma, dendrite, and knob. (f) Individual S100Z-positive neurons show no co-localization of S100Z and TUBB in their dendritic appendages. TUBB expression is expected in cilia, whereby S100Z was located in shorter protrusions from the dendritic knob, potentially indicating microvilli (white dotted circle). MOE, main olfactory epithelium; NC, nasal cavityl; OB, olfactory bulb; ON, olfactory nerve; ORN, olfactory receptor neuron.

potentially express S100Z (Figure 2). Tumor protein 63 (TP63) is expressed in reserve horizontal stem cells in the olfactory epithelium (Schnittke et al., 2015). Antibody labeling against TP63 was localized in cell nuclei in the basal cell layers of the olfactory epithelium, while S100Z-positive cells were located in more intermediate layers (Figure 2b). We found no co-localization of TP63 in S100Z-positive cells.

Supporting cells were labeled with an antibody against Cytok II and revealed their typical morphology with apical cell soma positions and thin processes connecting to the basal lamina of the MOE (Figure 2c). We found no co-localization of labeled supporting cells and S100Z.

An antibody against NCAM1 was used to label immature ORNs within the MOE (Cervino et al., 2017). We found NCAM1 expression in many S100Z-positive cells, and it was

localized to the plasma membrane at the cell soma and in dendritic and axonal processes (Figure 2d).

We applied an antibody against TUBB to check if S100Z-positive neurons possess cilia as dendritic knob appendages. TUBB immunoreactivity was located in the intermediate level of the olfactory epithelium at cell boundaries and in long cilia at the apical interface to the nasal cavity (Figure 2e). In general, the TUBB signal extended more apically than the S100Z signal (arrow). S100Z-immunoreactivity was located in dendrites and the connected knobs of ORNs but was not apparent in TUBB-positive cilia (Figure 2f, white dotted oval). This indicated that S100Z was expressed in microvillars rather than ciliated ORNs.

In summary, we found that S100Z expression occurred exclusively in ORNs within the MOE of premetamorphic *X. laevis* larvae with specific projections into the lateral and intermediate glomerular cluster of the OB.

3.3 | Laterally biased distribution of S100Z-expressing ORNs in the MOE

The fact that projections of S100Z-positive axons were not connecting to the medial OB raises the question how S100Z-expressing ORNs are distributed within the olfactory organ. We manually counted and identified the position of all S100Z-positive ORNs in image stacks of the MOE of premetamorphic animals (n = 11 larvae; Figure 3). For each ORN, we determined the angle from the center of the MOE as a measure of lateral to medial position within the MOE (Figure 3a). The population of S100Z-expressing ORNs showed a bimodal distribution with a strong bias to the lateral side of the MOE (Figure 3b). On average, significantly more S100Z-positive ORNs were found in the lateral half of the olfactory epithelium of each animal than in the medial half (p = .0035, Figure 3c). This was consistently found in every animal analyzed (Figure 3d). We counted and identified biocytin-positive cells (n = 4 larvae) to test if ORNs were generally more frequently found in the lateral MOE. The distribution of the total ORN population is approximately symmetric and centered around the middle of the MOE (Figure 3b). No significant difference between the mean number of biocytin-positive cells was apparent between the lateral and medial MOE (p = .08326). The comparison of biocytin- and S100Z-positive distributions also suggested that the centrally located ORNs had a reduced probability for S100Z expression. On an apical to basal axis, the lateral and medial S100Z-positive ORNs did not differ in distribution (Figure 3e). Nevertheless, we found a tendency that S100Z-expressing ORN somata were located more apically in more ventral layers on the medial half of the MOE (Figure 3f).

3.4 | S100Z expression in ORNs without axon and *pax6*-expressing cells

We wanted to obtain more information about the maturity of S100Z-expressing neurons and labeled ORNs through their axons via transection of the ON using a biocytin backfill in premetamorphic *X. laevis* (Figure 4a–c). All ORNs with a well-developed axon at the transection site were labeled. Growing neurons that have not developed an extended axon yet are excluded from this labeling approach. We found that a biocytin backfill led to the widespread labeling of ORNs in the MOE (Figure 4a). Concurrent labeling with S100Z in a subset of biocytin-filled neurons supports our previous finding of ORN-specific expression of S100Z (Figure 4a). We found partially overlapping subsets of ORNs labeled with biocytin and S100Z (Figure 4a). Furthermore, the biocytin-streptavidin backfill was observable in the axonal projections of ORNs into the AOB and in all glomerular clusters of the OB, namely, the lateral (LC), intermediate (IC), small (SC), and medial clusters (MC; Figure 4b). Only in the LC and IC, we found co-localization of S100Z and biocytin-streptavidin but not in all glomeruli (Figure 4b). Notably, no S100Z signal occurred in the projections to glomeruli of the AOB (Figure 4b). Consistent with this, we also found generally no S100Z expression in the peripheral VNO (Figure 4c). S100Z expression was always restricted to the MOE.

pax6 is one of the main developmental regulators in vertebrates and cellular expression has been well-studied in the OB, pallium, and telencephalon of *Xenopus* (Daume et al., 2022; Moreno et al., 2008; Stoykova & Gruss, 1994). We used an albino *pax6*-GFP transgenic *Xenopus* line to visualize developing neurons within the premetamorphic MOE. *pax6*-dependent GFP expression was distributed throughout the whole MOE (Figure 4d). Many S100Z-expressing cells showed co-localization with *pax6*-GFP signal, but we also found S100Z-positive cells without *pax6* expression (Figure 4d). The axonal projections of *pax6*-positive ORNs projected broadly into all glomerular clusters of the OB (Figure 4e). A subset of *pax6*-positive glomeruli in the LC showed co-localization with S100Z, while another group was devoid of S100Z (Figure 4e). Note that also *pax6*-positive cell somata were found in the mitral and granule cell layers of OB, and that these exhibited no S100Z signal.

Our findings demonstrate that S100Z was expressed in a subgroup of *pax6*-positive ORNs as well as in developing

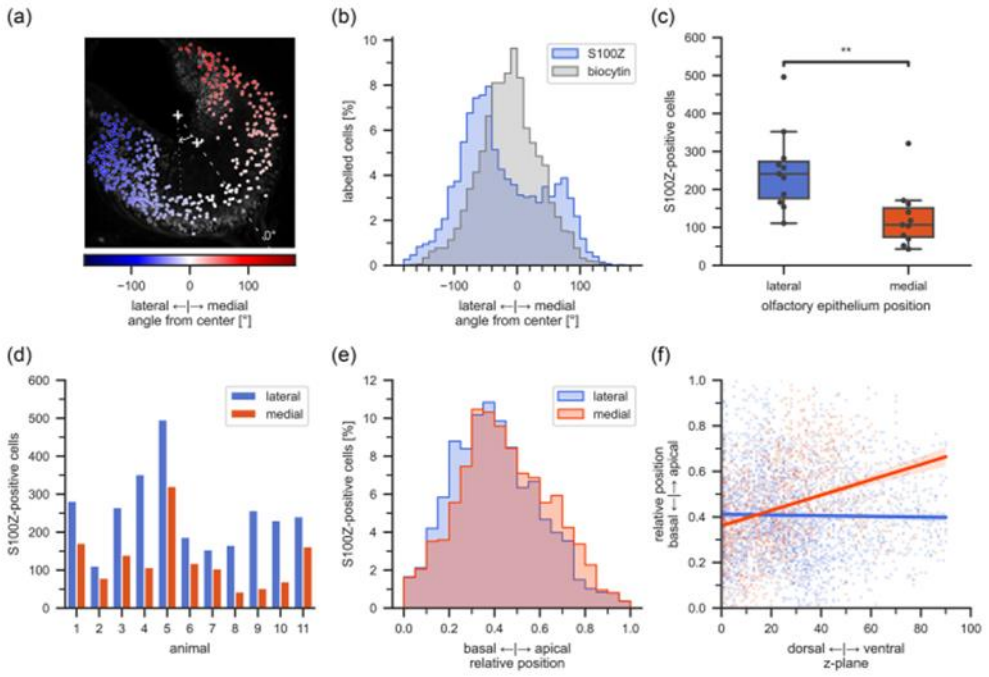

FIGURE 3 Laterally shifted distribution of S100Z-positive cells. (a) Maximum projection of a larval *X. laevis* MOE with an overlay of all S100Z-positive cells. The color gradient from blue (lateral) to red (medial) indicates the angular position within the MOE (zero equals the middle of the MOE). Crosses mark the average coordinates of the manually drawn apical and basal MOE boundaries. Angles were determined between each cell position and the vector that defined the middle of the MOE (dashed line). (b) The bimodal distribution of S100Z-positive cells (blue) was shifted toward a lateral position ($n = 11$ larvae). The general ORN population was labeled via a biocytin backfill and showed a unimodal distribution centered around the middle of the MOE (gray, $n = 4$ larvae). (c) The mean number of S100Z-positive cells in the lateral MOE was significantly higher than in the medial MOE ($n = 11$ larvae). Kruskal–Wallis test. **, $p < .01$. (d) The number of S100Z-positive cells in the lateral MOE was always higher than in the medial MOE in all animals investigated ($n = 11$ larvae). (e) The relative position within the MOE on the apical-basal axis was not different between the lateral and medial S100Z-positive populations, a tendency toward a more basal position on the lateral side notwithstanding. (f) The medial S100Z-positive population featured a correlation between the position on the ventral-dorsal and basal-apical axis. Cells deeper in the medial MOE were shifted to apical positions. MOE, main olfactory epithelium.

ORNs that have not yet made axonal contact with the OB of premetamorphic *X. laevis* larvae.

3.5 | Distinct, partially overlapping localization of S100Z and calretinin

We compared the observed S100Z pattern with another Ca^{2+}-binding protein, calretinin (*calb2*). In premetamorphic *X. laevis*, both calretinin and S100Z occurred in ORNs across the whole MOE (Figure 5a). Here, the two Ca^{2+}-binding proteins showed distinct, but partially overlapping, expression patterns (Figure 5a). In the OB, we found axonal projections of calretinin-positive ORNs in glomeruli of the AOB, LC, and MC and calretinin-expressing cell bodies in more posterior OB layers (Figure 5b).

Within the lateral glomerular cluster, individual glomeruli were either positive for calretinin/S100Z or showed a co-localization of both proteins (Figure 5b). The glomerular organization of the LC was different in each animal investigated (Figure 5c). This was also found for the patterns of calretinin and S100Z occurrence in glomeruli. In all larval animals surveyed, we found roughly similar, but never identical, spatial glomerular distribution patterns of calretinin and S100Z (Figure 5c). The most lateral glomeruli of the LC were mostly only S100Z- or calretinin-positive and rarely positive for both (Figure 5c, asterisk). Glomeruli situated toward the center of the LC were more frequently double positive,

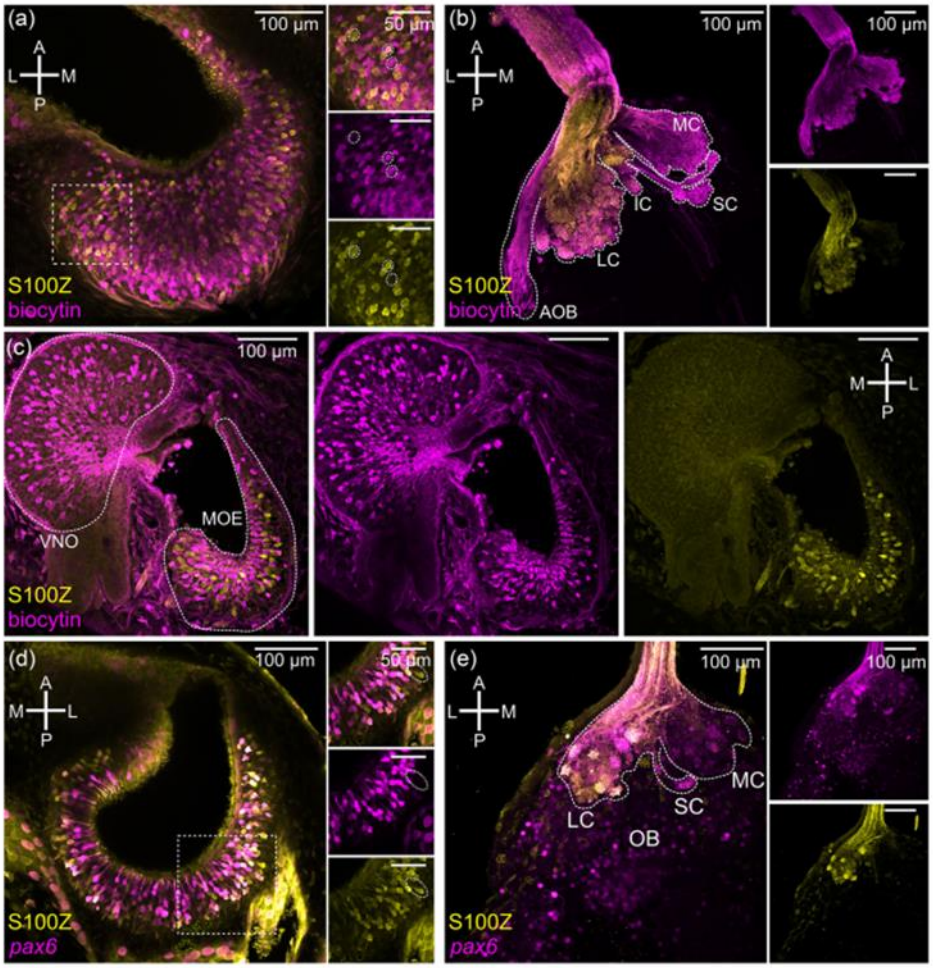

FIGURE 4 Mature and immature receptor neurons express S100Z exclusively in the MOE and not in the VNO of *X. laevis* tadpoles. (a) Biocytin-streptavidin-stained ORNs (magenta) and S100Z-positive ORNs (yellow) were present throughout the whole MOE. Some ORNs showed co-localization with both proteins (highlighted with circles). (b) The axonal projection of biocytin-streptavidin labeled ORNs (magenta) was found in all glomerular clusters within the main OB and AOB of *X. laevis* tadpoles, but axonal projection of S100Z-positive neurons (yellow) was exclusively detected in the LC and IC. (c) Biocytin-streptavidin stained ORNs (magenta) were located in the VNO and MOE of *X. laevis* tadpoles. S100Z-expressing neurons (yellow) occurred in the MOE. (d) Immature *pax6*-positive cells (magenta) and S100Z-positive ORNs (yellow) were present throughout the whole MOE. Although many, not all cells were double positive (e.g., white dotted oval). (e) Axonal projections of *pax6*-positive neurons, indicating an immature status, were detected in the LC and MC within the glomerular layer and different cell types (magenta) within the OB. Some, but not all glomeruli within the LC, showed co-localization for S100Z and *pax6*. A, anterior; AOB, accessory olfactory bulb; IC, intermediate cluster; L, lateral; LC, lateral cluster; M, medial; MC, medial cluster; MOE, main olfactory epithelium; OB, olfactory bulb; ON, olfactory nerve; ORN, olfactory receptor neuron; P, posterior; SC, small cluster; VNO, vomeronasal organ.

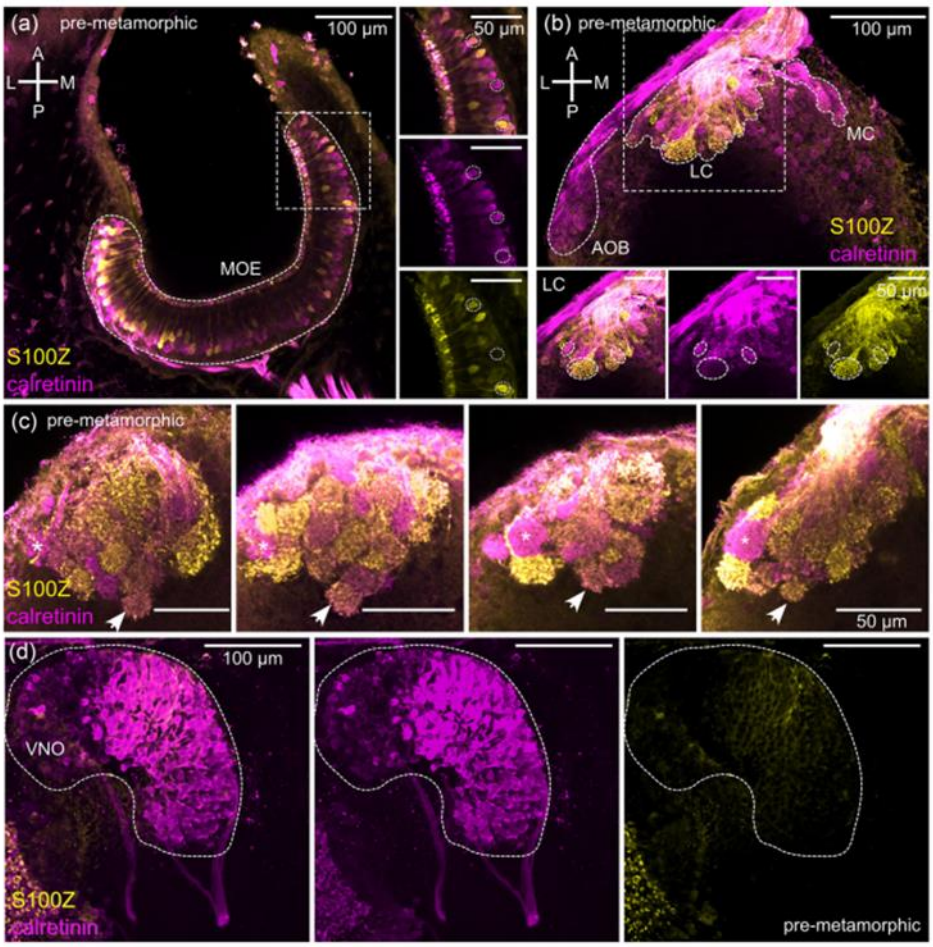

FIGURE 5 Distinct, but partially overlapping expression patterns of calretinin/S100Z. (a) In premetamorphic *X. laevis*, ORNs across the whole MOE expressed calretinin (magenta) and S100Z (yellow). Not all but many cells showed co-localization of the two calcium-binding proteins (e.g., white dotted circles). (b) In premetamorphic animals, the axonal projection of calretinin-expressing neurons (magenta) targeted the AOB, LC, and MC. Within the LC, calretinin- and S100Z-positive (yellow) glomeruli were detected and some were double-positive (white dotted ovals). (c) Expression patterns of calretinin (magenta) and S100Z (yellow) in glomeruli of the lateral cluster in four different premetamorphic animals. The expression patterns were very variable between individuals, but some trends for recurring patterns were apparent. The outer lateral glomeruli within the LC had the tendency to be either S100Z- or calretinin-positive (asterisks), whereas in the medial part of the LC, more glomeruli were S100Z-positive. The most caudal glomerulus in the middle of the LC was often double positive for S100Z/calretinin (arrows). (d) Immunohistochemical staining for calretinin (magenta) labeled neurons throughout the whole VNO in premetamorphic animals, but no S100Z expression (yellow) was found in the VNO. A anterior; AOB, accessory olfactory bulb; L, lateral; LC, lateral cluster; M, medial; MC, medial cluster; MOE, main olfactory epithelium; ORN, olfactory receptor neuron; P, posterior; VNO, vomeronasal organ.

notably a caudally oriented glomerulus was found in many animals (see Figure 5c, arrow). Calretinin expression was also apparent in axons that project to the AOB (Figure 5b). These axons originated from vomeronasal receptor neurons from the VNO that also showed calretinin expression but no S100Z expression (Figure 5d).

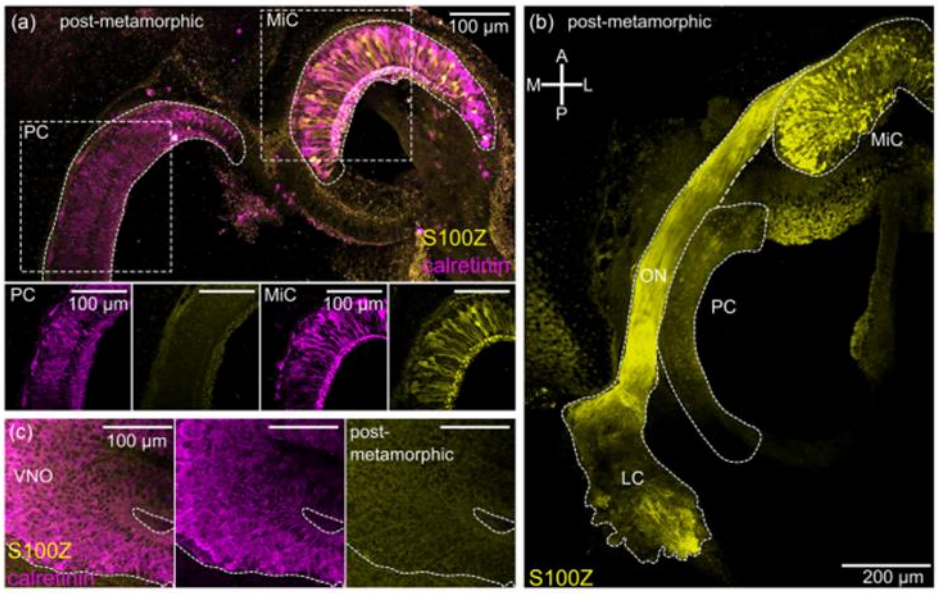

FIGURE 6 S100Z expression restricted to the middle cavity after metamorphosis. (a) In postmetamorphic *X. laevis* calretinin-positive neurons (magenta) were localized in the middle cavity (MiC) and principal cavity (PC). S100Z expression (yellow) occurred only in ORNs of the MiC. (b) In postmetamorphic animals, S100Z-expressing neurons within the olfactory epithelium of the MiC exclusively projected into the lateral glomerular cluster. No expression of S100Z was found in the PC. (c) Immunohistochemical staining for calretinin (magenta) labeled neurons throughout the whole VNO in postmetamorphic animals. No S100Z expression (yellow) was detected in the VNO. A, anterior; L, lateral; LC, lateral cluster; M, medial; MiC, middle cavity; ON, olfactory nerve; ORN, olfactory receptor neuron; P, posterior; PC, principal cavity; VNO, vomeronasal organ.

3.6 | S100Z expression limited to the middle cavity after metamorphosis

During metamorphic remodeling of the olfactory system, the larval MOE is functionally reorganized in the principal cavity , and a new olfactory epithelium forms the middle cavity (for review, see Weiss et al., 2021). The air-filled principal cavity is thought to be specialized for airborne odor detection, whereas the middle cavity is a reproduced larval MOE presumably specialized for waterborne odor detection. After metamorphosis, we found calretinin in ORNs of the middle and principal cavity of the olfactory system, whereas S100Z-expressing neurons were only detectable in the middle cavity (Figure 6a). Comparable to the larval situation, S100Z-expressing ORNs from the middle cavity exclusively projected into the lateral glomerular cluster of the postmetamorphic OB (Figure 6b). Also, no expression of S100Z occurred in the VNO (Figure 6c). Calretinin, on the other hand, could be detected in neurons of the VNO (Figure 6c).

4 | DISCUSSION

4.1 | S100Z expression in the olfactory system

The Ca^{2+}-binding protein family S100 has only been found in vertebrates and is expressed non-ubiquitously (Gonzalez et al., 2020). Although not very well characterized, S100Z has been shown to be expressed in the olfactory system of fish and mammals (Capsoni et al., 2021; Dieris et al., 2021; Hecker et al., 2019; Kraemer et al., 2008). Antibodies against bovine S100A/S100B reveal S100-immunoreactivity in crypt cells of the fish olfactory rosette and are a recognized marker for this neuronal subtype (Bettini et al., 2017; Germanà et al., 2004). Crypt cells express a single *v1r*-related *ora* gene (Oka et al., 2012), and they converge into a single mediodorsal glomerulus that is activated by kin odor after olfactory imprinting (Ahuja et al., 2013; Biechl et al., 2017; Gayoso et al., 2012; Kress et al., 2015). The specificity of these antibodies has been reported to be highly sensitive to sample preparation

prior to immunolabeling, and with this ambiguity also, other microvillous-like olfactory neurons are labeled (Oka et al., 2012). Therefore, the interpretation of earlier reports on S100 expression in non-mammalian species is not straightforward. In fact, it has been shown that zebrafish crypt cells do not even express *s100* genes and that the antibody may recognize a non-S100 protein, whereas in microvillous-like cells, the antibody actually labels S100Z (Ahuja et al., 2013; Oka et al., 2012). The same antibody has been also shown to label ORNs in larval *X. laevis* (Kerschbaum & Hermann, 1992). Using another antibody raised specifically against *H. sapiens* S100Z, we found labeling in a restricted population of ORNs of the main olfactory system of *X. laevis*. We have performed large-scale RNAseq experiments that support our findings (Data unpublished). A binding protein of S100 occurs in olfactory neuron cilia of another anuran, *Rana catesbeiana*, and thus suggests a role in olfactory transduction (Miwa & Kawamura, 2003).

4.2 | Partially overlapping expression of Ca^{2+}-binding proteins

Generally, many members of different Ca^{2+}-binding protein subfamilies are expressed in a restricted pattern and serve as a marker for separate neuronal populations in the vertebrate central nervous system (Braubach et al., 2012; Kress et al., 2015; Morona & González, 2013). In the olfactory system, calretinin expression is restricted to neuronal cell populations (Germanà et al., 2007). In zebrafish, calretinin is found most strongly in ciliated olfactory sensory neurons, which broadly project to the OB (Braubach et al., 2012; Kress et al., 2015; but see Koide et al., 2009). In this study, most ORNs of the *Xenopus* MOE were calretinin-positive (see also Daume et al., 2022).

In fish and amphibians, calretinin is an accepted marker of mature ORNs, but calretinin expression in embryonic mice is restricted to a limited period during neuronal maturation (Wei et al., 2013). A neuroprotective function of calretinin is proposed for epileptic seizures, but the function of calretinin in the olfactory system remains unclear (Capsoni et al., 2021; Qi et al., 2022).

We cannot link calretinin expression to specific neuronal features or identities, and no clear pattern of co-expression with S100Z was found. Furthermore, we did not observe any consistent expression patterns across the glomerular array in different animals. This implies that the mapping of ORN populations expressing these proteins in the *Xenopus* OB is not stereotypical. This inference is backed by functional measurements, which demonstrate that the glomerular odor map to amino acid odorants is neither stereotypically or chemotopically arranged in the *Xenopus* OB (Offner et al., 2023). We observed one particular, caudally oriented glomerulus in the LC, which was S100Z/calretinin-positive in many animals. It will be interesting to investigate if this glomerulus features some stereotypical properties, like location, function or odor sensitivity.

4.3 | S100Z is not associated with the VNO in *Xenopus*

In mammals, *s100z* has previously been associated with the accessory olfactory system, particularly the VNO. Surprisingly, we did not detect any S100Z expression in the VNO of pre- nor postmetamorphic *Xenopus*. In a large-scale screening of mammalian genomes, it was found that a reduction of the vomeronasal system is accompanied by a convergent inactivation of *s100z*, the transduction channel *trpc2*, the aldehyde oxidase *Aox2* involved in odorant degradation, and the uncharacterized *Mslnl* (Hecker et al., 2019). Conversely, the inactivation of these genes predicts a vomeronasal system reduction in semi-aquatic mammals, namely, otters and phocid seals (Hecker et al., 2019).

Ecological factors such as the terrestrial or aquatic environment can influence the evolution of olfactory system adaptations (Burguera et al., 2023; Kishida, 2021; Weiss et al., 2021). The functional prioritization of selected components of the olfactory system is common among vertebrates and can lead to the enhanced or decreased expression of particular families of olfactory receptor genes (Bear et al., 2016; Kishida, 2021; Taniguchi & Taniguchi, 2014). For instance, multiple lineages of ray-finned fish have independently expanded their olfactory receptor gene families, and this expansion is especially evident in nocturnal amphibious fish (Burguera et al., 2023). Such changes can also result in alterations to the occurrence of cellular properties that are associated with either the main or accessory olfactory system. In cartilaginous fish, the v2r/OlfC family of olfactory receptor genes is dominant over the OR family, and only microvillous ORNs are present in the olfactory organ (Syed et al., 2023).

The most extreme adaptation of the olfactory system completely reduces either the main or accessory system in favor of the other. Among secondarily fully aquatic mammals, baleen whales (Mysticeti) possess only a reduced main olfactory organ and lack a VNO (Kishida et al., 2015). No VNO is apparent in birds, so they depend entirely on their sense of smell through the main olfactory system (Taniguchi & Taniguchi, 2014). On the other hand, fully aquatic sea snakes (Hydrophiins) lack a functional main olfactory system and instead rely on a vomeronasal system (Kishida, 2021).

Our study emphasizes that the expression of *s100z* in non-mammalian species cannot be directly linked to the VNO. This makes *s100z* a less reliable predictor for a reduction of the VNO as a whole or the molecular machinery connected to it. It will be interesting to investigate the *s100z*

expression in animals with olfactory system reductions and other non-mammalian vertebrates in general.

4.4 | S100Z expression pattern correlates with microvillous ORNs and *trpc2*

In non-tetrapod groups, without a distinct VNO, the expression of *trpc2* is still linked to the MOE (Bear et al., 2016). In the MOE, the major two neuronal subpopulations are ciliated and microvillous ORNs (Gliem et al., 2013). In the single olfactory sensory epithelium of bony and cartilaginous fishes, *trpc2* is expressed in microvillous ORNs (Sato et al., 2005; Syed et al., 2023). In early diverging tetrapods, like amphibians, the expression pattern is in an intermediate state. In larval *Xenopus*, *trpc2* expression is not restricted to the VNO but also occurs broadly in the MOE (Sansone, Syed, et al., 2014). After metamorphosis, *trpc2* is expressed in the VNO and in the olfactory epithelium of the water-exposed middle cavity but not in the air-exposed principal cavity (Syed et al., 2017). The pattern in the MOE is mirrored by our observed expression pattern of S100Z. This indicates a common cellular identity that expresses S100Z and TRPC2, at least partially overlapping.

We found indications that S100Z-positive ORNs possess no cilia and that further supports that they belong to the microvillous subpopulation. Also, the absence of S100Z-positive cells in the postmetamorphic principal cavity supports this fact. After metamorphic reorganization, no microvillous, but only ciliated ORNs, can be found in the principal cavity (Hansen et al., 1998). It is unclear if S100Z is expressed by the whole population of microvillous ORNs in the MOE.

Microvillous ORNs expressing *trpc2* are thought to share a common molecular identity with a non-cyclic adenosine monophosphate (cAMP)-dependent transduction pathway and expression of early-derived *v2r* family olfactory receptor genes (Gliem et al., 2013; Hansen et al., 2004; Sato et al., 2005; Syed et al., 2013, 2017). Interestingly, microvillous ORNs from the MOE and the VNO of *X. laevis* express distinct subfamilies of *v2r* genes. *Xenopus* larvae show exclusive expression of late diverging *v2r* genes in the VNO, while ancestral *v2r* genes are restricted to the MOE (Syed et al., 2013). During metamorphosis, the MOE gradually loses its larval expression of ancient V2Rs as it transforms into the air nose (principal cavity). In the basal layers of the newly formed water nose (middle cavity), ancient *v2r* gene expression starts to emerge (Syed et al., 2017). This suggests ancestral *v2r* olfactory receptor genes as likely candidates to be expressed by S100Z-positive ORNs. This is an important hypothesis to test in future experiments.

The functional identity of S100Z-expressing ORNs is not known yet, but V2Rs have been connected to the detection of amino acids (DeMaria et al., 2013; Syed et al., 2017). In larval *Xenopus*, amino acid-responsive ORNs with a phospholipase C (PLC)-dependent transduction pathway show a laterally biased distribution (Gliem et al., 2013; Sansone, Hassenklöver, et al., 2014; Sansone, Syed, et al., 2014; Syed et al., 2013). This lateral bias is also present in the glomerular array of the OB (Gliem et al., 2013). Since S100Z expression in the OB is also lateralized, it would be interesting to test whether S100Z-positive glomeruli are sensitive to amino acid odors.

4.5 | Conclusion

The transition to terrestrial habitats of tetrapods is accompanied by the evolutionary tendency to develop distinct olfactory subsystems, for example, the main and vomeronasal olfactory organ with separate brain circuitry. This trend at the anatomical level is also reflected at the molecular level, which eventually forms distinct olfactory sensory neuron subpopulations with differential gene expression patterns. In amphibians, this molecular segregation is in an intermediate state, despite distinct anatomical peripheral olfactory organs. This is also supported by strict S100Z expression in the main olfactory system and no expression in the VNO. This underlines that the molecular identity of amphibian vomeronasal olfactory neurons is not identical to mammals, including the expression of S100Z. Since the function of *s100z* is still unclear, one can only speculate about the consequences. A functional importance in a specific olfactory neuron subpopulation could be hypothesized and it is possible that the association of *s100z* with vomeronasal sensory neurons in the mammalian lineage confers functional benefits.

AUTHOR CONTRIBUTIONS

Melina Kahl: Conceptualization; formal analysis; investigation; writing—original draft; writing—review and editing; visualization. **Thomas Offner**: Conceptualization; formal analysis; writing—review and editing. **Alena Trendel**: Formal analysis. **Lukas Weiss**: Investigation; writing—review and editing. **Ivan Manzini**: Conceptualization; writing—review and editing; supervision; funding acquisition. **Thomas Hassenklöver**: Conceptualization; formal analysis; writing—original draft; writing—review and editing; visualization; supervision.

ACKNOWLEDGMENTS

The authors thank Christina Anding for expert animal care and Anja Schnecko for technical assistance. This work was supported by Deutsche Forschungsgemeinschaft (DFG) grant 4113/4-1.

Open access funding enabled and organized by Projekt DEAL.

CONFLICT OF INTEREST STATEMENT

The authors declare no competing interests.

DATA AVAILABILITY STATEMENT

The data that support the findings of this study are openly available in JLUpub at https://doi.org/10.22029/jlupub-18280.

ORCID

Melina Kahl https://orcid.org/0009-0006-6223-770X
Thomas Offner https://orcid.org/0000-0002-0228-2545
Lukas Weiss https://orcid.org/0000-0003-3078-8006
Ivan Manzini https://orcid.org/0000-0002-3575-9637
Thomas Hassenklöver https://orcid.org/0000-0002-9895-1263

REFERENCES

Ahuja, G., Ivandić, I., Saltürk, M., Oka, Y., Nadler, W., & Korsching, S. I. (2013). Zebrafish crypt neurons project to a single, identified mediodorsal glomerulus. *Scientific Reports*, *3*, 2063. https://doi.org/10.1038/srep02063

Bear, D. M., Lassance, J.-M., Hoekstra, H. E., & Datta, S. R. (2016). The evolving neural and genetic architecture of vertebrate olfaction. *Current Biology*, *26*, R1039–R1049. https://doi.org/10.1016/j.cub.2016.09.011

Berridge, M. J., Bootman, M. D., & Roderick, H. L. (2003). Calcium signalling: Dynamics, homeostasis and remodelling. *Nature Reviews Molecular Cell Biology*, *4*, 517–529. https://doi.org/10.1038/nrm1155

Berridge, M. J., Lipp, P., & Bootman, M. D. (2000). The versatility and universality of calcium signalling. *Nature Reviews Molecular Cell Biology*, *1*, 11–21. https://doi.org/10.1038/35036035

Bettini, S., Milani, L., Lazzari, M., Maurizii, M. G., & Franceschini, V. (2017). Crypt cell markers in the olfactory organ of *Poecilia reticulata*: Analysis and comparison with the fish model *Danio rerio*. *Brain Structure and Function*, *222*, 3063–3074. https://doi.org/10.1007/s00429-017-1386-2

Biechl, D., Tietje, K., Ryu, S., Grothe, B., Gerlach, G., & Wullimann, M. F. (2017). Identification of accessory olfactory system and medial amygdala in the zebrafish. *Scientific Reports*, *7*, 44295. https://doi.org/10.1038/srep44295

Braubach, O. R., Fine, A., & Croll, R. P. (2012). Distribution and functional organization of glomeruli in the olfactory bulbs of zebrafish (*Danio rerio*). *Journal of Comparative Neurology*, *520*, 2317–2339. https://doi.org/10.1002/cne.23075

Burguera, D., Dionigi, F., Kverková, K., Winkler, S., Brown, T., Pippel, M., Zhang, Y., Shafer, M., Nichols, A. L. A., Myers, E., Němec, P., & Musilova, Z. (2023). Expanded olfactory system in ray-finned fishes capable of terrestrial exploration. *BMC Biology*, *21*, 163. https://doi.org/10.1186/s12915-023-01661-8

Capsoni, S., Iseppe, A. F., Casciano, F., & Pignatelli, A. (2021). Unraveling the role of dopaminergic and calretinin interneurons in the olfactory bulb. *Frontiers in Neural Circuits*, *15*, 718221. https://doi.org/10.3389/fncir.2021.718221

Carafoli, E., Santella, L., Branca, D., & Brini, M. (2001). Generation, control, and processing of cellular calcium signals. *Critical Reviews in Biochemistry and Molecular Biology*, *36*, 107–260. https://doi.org/10.1080/20014091074183

Cervino, A. S., Paz, D. A., & Frontera, J. L. (2017). Neuronal degeneration and regeneration induced by axotomy in the olfactory epithelium of *Xenopus laevis*. *Developmental Neurobiology*, *77*, 1308–1320. https://doi.org/10.1002/dneu.22513

Date-Ito, A., Ohara, H., Ichikawa, M., Mori, Y., & Hagino-Yamagishi, K. (2008). *Xenopus* V1R vomeronasal receptor family is expressed in the main olfactory system. *Chemical Senses*, *33*, 339–346. https://doi.org/10.1093/chemse/bjm090

Daume, D., Offner, T., Hassenklöver, T., & Manzini, I. (2022). Patterns of *tubb2b* promoter-driven fluorescence in the forebrain of larval *Xenopus laevis*. *Frontiers in Neuroanatomy*, *16*, 914281. https://doi.org/10.3389/fnana.2022.914281

DeMaria, S., Berke, A. P., Name, E. V., Heravian, A., Ferreira, T., & Ngai, J. (2013). Role of a ubiquitously expressed receptor in the vertebrate olfactory system. *Journal of Neuroscience*, *33*, 15235–15247. https://doi.org/10.1523/jneurosci.2339-13.2013

Dieris, M., Kowatschew, D., & Korsching, S. I. (2021). Olfactory function in the trace amine-associated receptor family (TAARs) evolved twice independently. *Scientific Reports*, *11*, 7807. https://doi.org/10.1038/s41598-021-87236-5

Donato, R. (2003). Intracellular and extracellular roles of S100 proteins. *Microscopy Research and Technique*, *60*, 540–551. https://doi.org/10.1002/jemt.10296

Elíes, J., Yáñez, M., Pereira, T. M. C., Gil-Longo, J., MacDougall, D. A., & Campos-Toimil, M. (2019). An update to calcium binding proteins. In M. Islam (Ed.), *Advances in experimental medicine and biology*. (pp. 183–213). Springer International Publishing. https://doi.org/10.1007/978-3-030-12457-1_8

Gayoso, J., Castro, A., Anadón, R., & Manso, M. J. (2012). Crypt cells of the zebrafish *Danio rerio* mainly project to the dorsomedial glomerular field of the olfactory bulb. *Chemical Senses*, *37*, 357–369. https://doi.org/10.1093/chemse/bjr109

Germanà, A., Montalbano, G., Laurà, R., Ciriaco, E., del Valle, M. E., & Vega, J. A. (2004). S100 protein-like immunoreactivity in the crypt olfactory neurons of the adult zebrafish. *Neuroscience Letters*, *371*, 196–198. https://doi.org/10.1016/j.neulet.2004.08.077

Germanà, A., Paruta, S., Germanà, G. P., Ochoa-Erena, F. J., Montalbano, G., Cobo, J., & Vega, J. A. (2007). Differential distribution of S100 protein and calretinin in mechanosensory and chemosensory cells of adult zebrafish (*Danio rerio*). *Brain Research*, *1162*, 48–55. https://doi.org/10.1016/j.brainres.2007.05.070

Gliem, S., Syed, A. S., Sansone, A., Kludt, E., Tantalaki, E., Hassenklöver, T., Korsching, S. I., & Manzini, I. (2013). Bimodal processing of olfactory information in an amphibian nose: Odor responses segregate into a medial and a lateral stream. *Cellular and Molecular Life Sciences*, *70*, 1965–1984. https://doi.org/10.1007/s00018-012-1226-8

Gonzalez, L. L., Garrie, K., & Turner, M. D. (2020). Role of S100 proteins in health and disease. *Biochimica et Biophysica Acta (BBA)—Molecular Cell Research*, *1867*, 118677. https://doi.org/10.1016/j.bbamcr.2020.118677

Hansen, A., Anderson, K. T., & Finger, T. E. (2004). Differential distribution of olfactory receptor neurons in goldfish: Structural and molecular correlates. *Journal of Comparative Neurology*, *477*, 347–359. https://doi.org/10.1002/cne.20202

Hansen, A., Reiss, J. O., Gentry, C. L., & Burd, G. D. (1998). Ultrastructure of the olfactory organ in the clawed frog, *Xenopus laevis*,

during larval development and metamorphosis. *Journal of Comparative Neurology*, *398*, 273–288. https://doi.org/10.1002/(SICI)1096-9861(19980824)398:2⟨273::AID-CNE8⟩3.0.CO;2-Y

Hecker, N., Lächele, U., Stuckas, H., Giere, P., & Hiller, M. (2019). Convergent vomeronasal system reduction in mammals coincides with convergent losses of calcium signalling and odorant-degrading genes. *Molecular Ecology*, *28*, 3656–3668. https://doi.org/10.1111/mec.15180

Hermann, A., Donato, R., Weiger, T. M., & Chazin, W. J. (2012). S100 calcium binding proteins and ion channels. *Frontiers in Pharmacology*, *3*, 67. https://doi.org/10.3389/fphar.2012.00067

Kerschbaum, H. H., & Hermann, A. (1992). Calcium-binding proteins in chemoreceptors of *Xenopus laevis*. *Tissue & Cell*, *24*, 719–724. https://doi.org/10.1016/0040-8166(92)90043-7

Kishida, T. (2021). Olfaction of aquatic amniotes. *Cell and Tissue Research*, *383*, 353–365. https://doi.org/10.1007/s00441-020-03382-8

Kishida, T., Thewissen, J., Hayakawa, T., Imai, H., & Agata, K. (2015). Aquatic adaptation and the evolution of smell and taste in whales. *Zoological Letters*, *1*, 9. https://doi.org/10.1186/s40851-014-0002-z

Koide, T., Miyasaka, N., Morimoto, K., Asakawa, K., Urasaki, A., Kawakami, K., & Yoshihara, Y. (2009). Olfactory neural circuitry for attraction to amino acids revealed by transposon-mediated gene trap approach in zebrafish. *Proceedings of the National Academy of Sciences*, *106*, 9884–9889. https://doi.org/10.1073/pnas.0900470106

Kraemer, A. M., Saraiva, L. R., & Korsching, S. I. (2008). Structural and functional diversification in the teleost S100 family of calcium-binding proteins. *BMC Evolutionary Biology*, *8*, 48. https://doi.org/10.1186/1471-2148-8-48

Kress, S., Biechl, D., & Wullimann, M. F. (2015). Combinatorial analysis of calcium-binding proteins in larval and adult zebrafish primary olfactory system identifies differential olfactory bulb glomerular projection fields. *Brain Structure and Function*, *220*, 1951–1970. https://doi.org/10.1007/s00429-014-0765-1

Miwa, N., & Kawamura, S. (2003). Frog p26olf, a molecule with two S100-like regions in a single peptide. *Microscopy Research and Technique*, *60*, 593–599. https://doi.org/10.1002/jemt.10301

Mohrhardt, J., Nagel, M., Fleck, D., Ben-Shaul, Y., & Spehr, M. (2018). Signal detection and coding in the accessory olfactory system. *Chemical Senses*, *43*, 667–695. https://doi.org/10.1093/chemse/bjy061

Moreno, N., Rétaux, S., & González, A. (2008). Spatio-temporal expression of Pax6 in *Xenopus* forebrain. *Brain Research*, *1239*, 92–99. https://doi.org/10.1016/j.brainres.2008.08.052

Morona, R., & González, A. (2013). Pattern of calbindin-D28k and calretinin immunoreactivity in the brain of *Xenopus laevis* during embryonic and larval development. *Journal of Comparative Neurology*, *521*, 79–108. https://doi.org/10.1002/cne.23163

Nieuwkoop, P. D., & Faber, J. (Eds.). (1994). *Normal table of Xenopus laevis (Daudin)*. Garland Science.

Offner, T., Weiss, L., Daume, D., Berk, A., Inderthal, T. J., Manzini, I., & Hassenklöver, T. (2023). Functional odor map heterogeneity is based on multifaceted glomerular connectivity in larval Xenopus olfactory bulb. *iScience*, *26*, 107518. https://doi.org/10.1016/j.isci.2023.107518

Oka, Y., Saraiva, L. R., & Korsching, S. I. (2012). Crypt neurons express a single *v1r*-related *ora* gene. *Chemical Senses*, *37*, 219–227. https://doi.org/10.1093/chemse/bjr095

Preibisch, S., Saalfeld, S., & Tomancak, P. (2009). Globally optimal stitching of tiled 3D microscopic image acquisitions. *Bioinformatics*, *25*, 1463–1465. https://doi.org/10.1093/bioinformatics/btp184

Qi, Y., Cheng, H., Wang, Y., & Chen, Z. (2022). Revealing the precise role of calretinin neurons in epilepsy: We are on the way. *Neuroscience Bulletin*, *38*, 209–222. https://doi.org/10.1007/s12264-021-00753-1

Sansone, A., Hassenklöver, T., Syed, A. S., Korsching, S. I., & Manzini, I. (2014). Phospholipase C and diacylglycerol mediate olfactory responses to amino acids in the main olfactory epithelium of an amphibian. *PLoS ONE*, *9*, e87721. https://doi.org/10.1371/journal.pone.0087721

Sansone, A., Syed, A. S., Tantalaki, E., Korsching, S. I., & Manzini, I. (2014). *Trpc2* is expressed in two olfactory subsystems, the main and the vomeronasal system of larval *Xenopus laevis*. *Journal of Experimental Biology*, *217*, 2235–2238. https://doi.org/10.1242/jeb.103465

Santamaria-Kisiel, L., Rintala-Dempsey, A. C., & Shaw, G. S. (2006). Calcium-dependent and -independent interactions of the S100 protein family. *Biochemical Journal*, *396*, 201–214. https://doi.org/10.1042/bj20060195

Sato, Y., Miyasaka, N., & Yoshihara, Y. (2005). Mutually exclusive glomerular innervation by two distinct types of olfactory sensory neurons revealed in transgenic zebrafish. *Journal of Neuroscience*, *25*, 4889–4897. https://doi.org/10.1523/jneurosci.0679-05.2005

Schindelin, J., Arganda-Carreras, I., Frise, E., Kaynig, V., Longair, M., Pietzsch, T., Preibisch, S., Rueden, C., Saalfeld, S., Schmid, B., Tinevez, J. Y., White, D. J., Hartenstein, V., Eliceiri, K., Tomancak, P., & Cardona, A. (2012). Fiji: An open-source platform for biological-image analysis. *Nature Methods*, *9*, 676–682. https://doi.org/10.1038/nmeth.2019

Schnittke, N., Herrick, D. B., Lin, B., Peterson, J., Coleman, J. H., Packard, A. I., Jang, W., & Schwob, J. E. (2015). Transcription factor p63 controls the reserve status but not the stemness of horizontal basal cells in the olfactory epithelium. *Proceedings of the National Academy of Sciences of the United States of America*, *112*(36), E5068–E5077. https://doi.org/10.1073/pnas.1512272112

Schwaller, B. (2020). Cytosolic Ca^{2+} buffers are inherently Ca^{2+} signal modulators. *Cold Spring Harbor perspectives in biology*, *12*, a035543. https://doi.org/10.1101/cshperspect.a035543

Singh, P., & Ali, S. A (2022). Multifunctional role of S100 protein family in the immune system: An update. *Cells*, *11*, 2274. https://doi.org/10.3390/cells11152274

Stoykova, A., & Gruss, P. (1994). Roles of Pax-genes in developing and adult brain as suggested by expression patterns. *Journal of Neuroscience*, *14*, 1395–1412. https://doi.org/10.1523/jneurosci.14-03-01395.1994

Syed, A. S., Sansone, A., Hassenklöver, T., Manzini, I., & Korsching, S. I. (2017). Coordinated shift of olfactory amino acid responses and V2R expression to an amphibian water nose during metamorphosis. *Cellular and Molecular Life Sciences*, *74*, 1711–1719. https://doi.org/10.1007/s00018-016-2437-1

Syed, A. S., Sansone, A., Nadler, W., Manzini, I., & Korsching, S. I. (2013). Ancestral amphibian v2rs are expressed in the main olfactory epithelium. *Proceedings of the National Academy of Sciences*, *110*, 7714–7719. https://doi.org/10.1073/pnas.1302088110

Syed, A. S., Sharma, K., Policarpo, M., Ferrando, S., Casane, D., & Korsching, S. I. (2023). Ancient and nonuniform loss of olfactory

receptor expression renders the shark nose a de facto vomeronasal organ. *Molecular Biology and Evolution*, *40*, msad076. https://doi.org/10.1093/molbev/msad076

Taniguchi, K., & Taniguchi, K. (2014). Phylogenic studies on the olfactory system in vertebrates. *Journal of Veterinary Medical Science*, *76*, 781–788. https://doi.org/10.1292/jvms.13-0650

Wei, H., Lang, M.-F., & Jiang, X. (2013). Calretinin is expressed in the intermediate cells during olfactory receptor neuron development. *Neuroscience Letters*, *542*, 42–46. https://doi.org/10.1016/j.neulet.2013.03.022

Weiss, L., Manzini, I., & Hassenklöver, T. (2021). Olfaction across the water–air interface in anuran amphibians. *Cell and Tissue Research*, *383*, 301–325. https://doi.org/10.1007/s00441-020-03377-5

Yáñez, M., Gil-Longo, J., & Campos-Toimil, M. (2012). Calcium binding proteins. In *Calcium Signaling* (pp. 461–482). Springer Netherlands. https://doi.org/10.1007/978-94-007-2888-2_19

How to cite this article: Kahl, M., Offner, T., Trendel, A., Weiss, L., Manzini, I., & Hassenklöver, T. (2024). S100Z is expressed in a lateral subpopulation of olfactory receptor neurons in the main olfactory system of *Xenopus laevis*. *Developmental Neurobiology*, 1–15. https://doi.org/10.1002/dneu.22935

5.2 2nd Publication: Olfactory nerve transection transiently activates olfactory ensheathing cells in *Xenopus laevis* larvae

European Journal of Neuroscience

WILEY | EJN European Journal of Neuroscience FENS

RESEARCH REPORT OPEN ACCESS

Olfactory Nerve Transection Transiently Activates Olfactory Ensheathing Cells in *Xenopus laevis* Larvae

Melina Kahl[1] | Lukas Weiss[1,2] | Joshua Walter[1] | Thomas Hassenklöver[1] | Ivan Manzini[1]

[1]Institute of Animal Physiology, Department of Animal Physiology and Molecular Biomedicine, Justus-Liebig-University Giessen, Giessen, Germany | [2]Department of Ecology and Evolutionary Biology, Princeton University, Princeton, NJ, USA

Correspondence: Ivan Manzini (ivan.manzini@physzool.bio.uni-giessen.de)

Received: 20 May 2025 | **Revised:** 7 July 2025 | **Accepted:** 12 July 2025

Associate Editor: C Giovanni Galizia

Funding: This work was supported by Deutsche Forschungsgemeinschaft, 4113/4-1.

Keywords: axonal guidance | degeneration | injury | non-neuronal cells | olfactory system | regeneration | ribosomal protein S6

ABSTRACT

Olfactory ensheathing cells (OECs) play a crucial role in supporting the continuous turnover of olfactory receptor neurons by promoting axon growth and targeting. While OECs have been extensively studied in mammals for their potential in treating nerve injuries, little is known about these cells in non-mammalian vertebrates. We identified and characterized the morphology of OECs, fibroblasts, and macrophages in the olfactory system of *Xenopus laevis* larvae. Additionally, we used antibodies against phosphorylated ribosomal protein S6 (p-rpS6) to visualize the activation of non-neuronal cells in the olfactory nerve (ON) after transection. Various non-neuronal cells in the ON, including OECs, fibroblasts, and macrophages, showed a transient increase in the p-rpS6 signal following transection. Our study provides the first description of non-neuronal cells populating the ON of larval *X. laevis*, and it suggests that rpS6 phosphorylation in these cells may be essential after injury and potentially supports regeneration of the ON. These findings contribute to a broader understanding of OECs and their role in nerve regeneration across species.

1 | Introduction

The olfactory system in vertebrates exhibits a remarkable capacity for regeneration, particularly in the replacement of olfactory receptor neurons (ORNs; Astic and Saucier 2001; Schwob 2002; Manzini 2015). When ORNs reach the end of their lifespan or if they are damaged, e.g., by exposure to toxins, infections, or injury, they undergo apoptosis and/or necrosis and are replaced by new neurons (Deckner et al. 1997; Astic and Saucier 2001; Brenneman et al. 2002; Schwob 2002; Manzini 2015; Hawkins et al. 2017; Werner and Nies 2018). New ORNs differentiate from a heterogeneous population of neuronal stem cells located in basal layers of the olfactory epithelium (OE; Schwob 2002; Ekberg et al. 2012; Manzini 2015) and subsequently extend unmyelinated axons to synaptically connect with projection neurons and interneurons of the olfactory bulb (OB) in the anterior telencephalon (Moreno-Flores et al. 2002; Manzini et al. 2022).

The olfactory nerve (ON) is a critical component of the olfactory system, composed of bundles of ORN axons and several populations of non-neuronal cells, including olfactory ensheathing cells (OECs), fibroblasts, and macrophages. OECs constitute a heterogeneous class of molecularly and functionally diverse glial cells that ensheathe bundles of ORN axons along the ON (Doucette 1993; Sonigra et al. 1999; Chuah and West 2002; Pellitteri et al. 2010; Su and He 2010; Higginson

Abbreviations: OB, olfactory bulb; OE, olfactory epithelium; OECs, olfactory ensheathing cells; ON, olfactory nerve; ORNs, olfactory receptor neurons; p-rpS6, phosphorylated ribosomal protein S6.

and Barnett 2011; Ekberg et al. 2012; Ekberg and St John 2014; Manzini et al. 2022). Axon bundles of ORNs are also surrounded by fibroblasts, which form a perineurium-like structure (Li et al. 1998, 2005; Wright et al. 2020). In addition, the ON is populated by a small number of macrophages (Li et al. 1998, 2005; Wright et al. 2020).

The unambiguous identification of OECs is inherently difficult. In mammals, OECs have been shown to express, among others, vimentin, glial fibrillary acidic protein (GFAP), the calcium-binding protein S100β, neural cell adhesion molecules (NCAMs), p75 neurotrophin receptors (p75NTR), neuropeptide Y, and several axon guidance molecules (Barnett and Chang 2004; Pellitteri et al. 2010; Higginson and Barnett 2011; Ekberg et al. 2012; Rawji et al. 2013; Oprych et al. 2017). Among those, particularly vimentin, a major intermediate filament protein (Ivaska et al. 2007), has been a helpful marker of OECs (Franceschini and Barnett 1996; Schwob et al. 1986; Ramón-Cueto and Avila 1998; Au and Roskams 2003; Lazzari et al. 2013). The transcription factor *sox10*, on the other hand, has been shown to label developing OECs in different vertebrate taxa (Barraud et al. 2010, 2013; Forni et al. 2011; Pingault et al. 2013; Oprych et al. 2017; Perera et al. 2020). None of these markers, however, is suitable for identifying all types of OECs. Fibronectin, an essential element of the extracellular matrix, is known to be expressed in fibroblasts (Ibanez et al. 2007) and has been used to mark fibroblasts in the mammalian ON (Li et al. 2008; Oprych et al. 2017). Macrophage-expressed gene 1 (*mpeg1*), which encodes the pore-forming protein perforin-2, is evolutionarily conserved and commonly expressed in macrophages, making it a reliable marker for macrophage identification (Ellett et al. 2011; Bayly-Jones et al. 2020; Ferrero et al. 2020).

Among the non-neuronal cells of the ON, most information is available about OECs. While initially believed to originate from the olfactory placode, OECs are now widely accepted to derive from the neural crest (Chuah and Au 1991; Valverde et al. 1992; Barraud et al. 2010; Forni et al. 2011; Katoh et al. 2011; Nakajima et al. 2013; Denaro et al. 2022). The promotion of continuous growth and the targeted pathfinding of ORN axons and the phagocytosis of axonal debris within the ON are undoubtedly the key functions of OECs (Doucette 1993; Key and St John 2002; Pellitteri et al. 2010; Su and He 2010; Ekberg et al. 2012; Su et al. 2013; Ekberg and St John 2014; Nazareth et al. 2015; Barton et al. 2017; Denaro et al. 2022; Denaro et al. 2022; Manzini et al. 2022; Zhang et al. 2023). Additionally, OECs are involved in regulating the immune response within the ON (Chen et al. 2025).

OECs have been shown to support neural repair in the olfactory system and, after implantation, also in other regions of the nervous system (Su and He 2010; Ekberg et al. 2012; Roet and Verhaagen 2014). Their potential to promote spinal cord regeneration has been well studied (Raisman 2001; Barton et al. 2017; Huang et al. 2024), showing promising but still inconsistent outcomes (Mackay-Sim 2005; Ekberg et al. 2012; Yao et al. 2018). The underlying molecular mechanisms, i.e., the secretion and regeneration-supporting functions of adhesion molecules, extracellular matrix proteins, and growth factors (Bailey et al. 1993; Pellitteri et al. 2010; Barton et al. 2017; Russo et al. 2020), are not yet fully elucidated.

While extensive research has been conducted on OECs in mammals, information about OECs in non-mammalian vertebrates is very limited (e.g., see Quintana-Urzainqui et al. 2014; Docampo-Seara et al. 2022: catshark; Kreutzberg and Gross 1977; Lazzari et al. 2013, 2014: teleosts; Daston et al. 1990; Burd 1991, 1992; Huang et al. 2005; Lazzari et al. 2016: adult and metamorphic amphibians).

Larvae of the African clawed frog *Xenopus laevis* are particularly suitable for studying injury-mediated neuronal regeneration processes and are widely used in regenerative biology (Manzini 2015; Cervino et al. 2017; Hawkins et al. 2017; Hawkins et al. 2024; Terni et al. 2017; Lara et al. 2024). Nevertheless, the morphology and functions of OECs in *Xenopus* remain largely unclear. The present study aims to identify and describe OECs and other non-neuronal cells in the larval *Xenopus* ON using transgenic animal lines, immunohistochemistry, and single-cell electroporations. In addition, we describe activity changes in non-neuronal cells of the ON, including OECs, that occur after injury of the olfactory system.

2 | Materials and Methods

2.1 | Animals

To obtain our results, we used wild-type, albino, and transgenic *sox10*-GFP [Xla.Tg (sox10:GFP)^{Jpsj}] and *mpeg1*-GFP [Xla.Tg (Dre.mpeg1:eGFP;cryga:mCherry)^{Amaya}] (xenopusresource.org) larvae of *X. laevis* (both sexes). The larvae were maintained and raised in the breeding colony at the animal facility of the Institute of Animal Physiology at Justus Liebig University of Giessen. Premetamorphic larvae with well-developed olfactory systems, ranging from developmental stages 48 to 52, were used (staged after Nieuwkoop and Faber 1994). The animals were kept in water tanks (7.5 L) at a temperature of 19°C–22°C (pH 7.8) and fed with algae (Hobby, Mikrozell, Dohse Aquaristik GmbH und Co. KG).

2.2 | ON Transection

As an injury model for neuronal damage in the olfactory system, we unilaterally transected an ON of larval *X. laevis* (also see Hawkins et al. 2017, Hawkins et al. 2024). The larvae were anesthetized in 0.02% MS-222 (ethyl 3-aminobenzoate methanesulfonate; Sigma-Aldrich). The ON was then transected with fine scissors without damaging the surrounding tissue. The wound was then closed with tissue adhesive (Histoacryl L; Braun). After this procedure, the animals were transferred to a beaker with fresh tap water for recovery. At different time intervals after injury, transected animals were again anesthetized in 0.02% MS-222 and killed by severing the brain and spinal cord with a scalpel. Subsequent experiments were performed on excised tissue blocks containing the OE, ONs, and OB.

2.3 | ORN Labeling via Electroporation

To visualize ORN axons in the ON, fluorophore-coupled dextran (Alexa 488 or Alexa 594; 10.000 MW, Molecular Probes, Thermo

Fisher Scientific) was introduced into ORNs via electroporation (for details, see Hassenklöver and Manzini 2014). *X. laevis* larvae were anesthetized in 0.02% MS-222, and dye crystals of dextran were introduced and dissolved into both nasal cavities. Two platinum electrodes were placed, one inside the nasal cavity and the other at the tissue surrounding the nostril. The electrodes were connected to a voltage pulse generator (ELP-01D; npi Electronics), and six pulses (15 V, 25 ms duration at 2 Hz) with alternating polarity were applied (also see Weiss et al. 2018). The procedure was repeated with the other nasal cavity. After electroporation, the animals were transferred to a beaker filled with fresh tap water for recovery. The right ON was transected 3 or 4 days after electroporation (see section above). The animals were sacrificed at different time points after ON transection (1 h, 3 h, 6 h, 12 h, 24 h, 48 h, 72 h, 1 week, 2 weeks, 3 weeks, and 7 weeks) and further processed. To visualize the regenerated ON at later time points after transection, the ONs of the animals were first transected (see section above) and then electroporated 3 days before they were killed and further processed.

2.4 | Whole Mount Preparation and Immunohistochemistry of the Olfactory System

To label different cell types and to visualize changes in the ON and OB after unilateral ON transection, we performed immunolabeling on tissue slices of the olfactory system. Animals were anesthetized (as described above) and killed by severing the brain at its transition to the spinal cord with a scalpel. Tissue blocks with complete olfactory systems containing the OE, ONs, and OB were cut out with fine scissors and fixed in 4% Roti-Histofix (Roth, pH 7) for 1 h at room temperature on a shaker in an Eppendorf tube. Subsequently, the tissue blocks were washed in 0.1 M phosphate buffer saline (PBS), glued onto a vibratome stage (VT 1200S, Leica), and cut horizontally into 300 µm thick slices. Tissue slices were permeabilized with PBST (PBS containing 0.2% Triton X100; Carl Roth), and non-specific binding was blocked with 2% normal goat serum (NGS; MP Biomedicals) for 1 h. Slices were incubated over two nights at 4°C with the following primary antibodies: anti-vimentin (14h7, RRID: AB_528507, monoclonal, derived from mouse, Developmental Studies Hybridoma Bank); anti-fibronectin (MA5-11981, RRID: AB_10982280, monoclonal, derived from mouse, Thermo Fisher Scientific); anti-phospho-S6 ribosomal protein (Ser235/236) (4858S, RRID: AB_916156, monoclonal, derived from rabbit, Cell Signalling Technology); anti-HuC/HuD (HuC/D) (A-21271, RRID: AB_221448, monoclonal, derived from mouse, Thermo Fisher Scientific). Green fluorescent protein (GFP) signals of transgenic animals were enhanced with anti-GFP (ab1218, RRID: AB_298911, monoclonal, derived from mouse; Abcam).

Primary antibodies were diluted in 2% NGS/PBST (anti-vimentin, anti-phospho-S6 ribosomal protein [Ser235/236], anti-HuC/D: 1:250, anti-fibronectin: 1:100, anti-GFP: 1:50) and washed off with PBS after the incubation period. Subsequently, Alexa 488 or 594-conjugated goat anti-mouse or anti-rabbit secondary antibodies (Invitrogen, Thermo Fisher Scientific) were applied at a dilution of 1:250 in 2% NGS/PBS over one night. The secondary antibodies were washed off with PBS. To stain cell nuclei, the tissue samples were incubated for 20 min in 10 µg/mL propidium iodide (Molecular Probes, Thermo Fisher Scientific). After repeated washing with PBS, the slices were transferred into a small petri dish filled with 500 µL PBS and stabilized with a platinum frame stringed with nylon threads.

2.5 | Sparse Cell Electroporation to Label Individual Cells of the ON

To examine and visualize the morphology of individual cells in the ON, cells of the ON were labeled using single-cell electroporation. Tissue blocks, containing the entire olfactory system, were cut out with fine scissors (as described above) and transferred into frog saline ringer (98 mM NaCl, 2 mM KCl, 1 mM $CaCl_2$, 2 mM $MgCl_2$, 5 mM glucose, 5 mM Natrium-pyruvate, 10 mM HEPES; 230 mOsmol/l, pH 7.8). The palatial tissue covering the ventral side of the ON and OB was removed. The samples were transferred, with the ventral surface facing up, into a small petri dish with a recess in the middle, filled with 500 µL frog saline ringer, and stabilized with a platinum frame stringed with nylon threads. The samples were then placed under a microscope with fluorescent illumination.

Electroporation micropipettes were produced from borosilicate glass capillaries (inner diameter 0.86 mm, outer diameter 1.5 mm, length 10 cm, Hilgenberg) with a horizontal micropipette puller (Model P-1000, Sutter Instruments). The micropipettes were filled with 3 µL Alexa 488 or Alexa 594 dextran solution (10 kDa MW, 3 mM in frog saline ringer, Life Technologies, Invitrogen, Thermo Fisher Scientific) and mounted on the head stage of an Axoporator 800 A (Molecular Devices). This head stage includes a silver wire electrode coated with silver chloride. A reference electrode connected to the Axoporator was placed near the tissue block to close the electrical circuit.

After positioning the micropipette in the frog saline ringer (see above), it was directed toward the ONs using a micromanipulator (PatchStar, Scientifica). When the pipette was in contact with a cell of interest, a train of positive square voltage pulses (50 V, 300 µs, 300 Hz for 500 ms) was triggered to transfer the charged dye along an electric field into a single cell (also see Weiss et al. 2018). Samples were fixed in 4% Roti-Histofix (Roth, pH 7) for 1 h at room temperature. The tissue blocks were then washed in 0.1 M PBS, and nuclear staining was performed with propidium iodide (see above).

2.6 | Multiphoton Imaging

The ONs and the OB were observed using an upright multiphoton microscope (A1R-MP, Nikon). Images were acquired with an excitation laser wavelength of 780 nm as virtual stacks with a z-resolution of 1–3 µm. Fluorescence emission was detected with three different detectors (blue 400–492 nm, green 500–550 nm, and red 601–657 nm).

2.7 | Image and Data Processing

The brightness and contrast of the image stacks obtained from scans of the multi-photon microscope were adjusted using the image processing software ImageJ (Schindelin et al. 2012).

When excited by the multiphoton laser, pigments showed strong autofluorescence and were visible as supersaturated image areas. The blue emission detector (400–492 nm) was used to identify autofluorescence. As we never used samples with blue marker fluorophores, no fluorescence was expected in the blue channel. This allowed mathematical subtraction of autofluorescence (blue detector signal) from the other channels. The volume viewer in ImageJ was used to create virtual cross-sections of the ONs. A median filter with a radius of 0.5 pixels was applied to all planes of the image stacks to reduce background noise. After processing, the images were arranged and annotated with Inkscape (inkscape.org).

In the present study, we used immunohistochemistry against phosphorylated ribosomal protein S6 (p-rpS6) as a proxy for cellular responses after ON transection and during regenerative processes (Knight et al. 2012; Biever et al. 2015; Ring et al. 2023). To quantify cellular activity based on p-rpS6 stainings in unilaterally ON-transected animals, ON/OB hemisphere samples of the same animal were acquired with identical multi-photon microscope settings (gain, laser power, and scan parameters). Supersaturated areas in image stacks were mathematically subtracted as described above. Image stacks were individually cropped in the y-direction to exclude cellular p-rpS6 signals from the OB. The cropping range was determined manually, and the final image size was similar on the transected and non-transected sides of the animal. A Gaussian filter ($\sigma = 35$) was applied to all planes to estimate the background signal, which was then subtracted from the image stacks. Then, all image planes were median-filtered with a three-pixel radius. To measure the effect of ON transection on the p-rpS6 signal, we calculated a ratio of the cumulative p-rpS6 signal intensity between transected and non-transected ON of the same animal (transected/non-transected). Data analysis was performed using custom-written scripts in Python 3 in Jupyter Notebook (code available under https://doi.org/10.22029/jlupub-19833).

2.8 | Statistical Analysis

The results are presented as mean ± standard deviation unless otherwise stated. Statistical significance was determined by the Kruskal–Wallis test, followed by Dunn's multiple comparison post hoc test. We compensated for the family-wise error rate using the Bonferroni-Holm method.

3 | Results

3.1 | The ON Is Populated by Ensheathing Cells, Fibroblasts, and Macrophages

The cellular composition of the ON of *X. laevis* is still largely unknown. To visualize OECs, fibroblasts, and macrophages, we performed immunolabeling on tissue slices of the olfactory system of wild-type and transgenic animals.

Using a *sox10*-GFP transgenic *Xenopus* line, we identified a small number of round-shaped cells primarily located near the surface of the ON (Figure 1A–D). The localization, number, and morphology of these cells are not consistent with descriptions of mature OECs. These cells could, however, possibly be developing immature OECs. Immunolabeling against vimentin stained cells in the ON and the nerve layer of the OB. These cells exhibited a fusiform bipolar morphology characterized by thin extensions originating from their centrally located nuclei (Figure 1E). In cross-sections of the ON, we found that the vimentin-positive cells were present throughout the whole nerve (Figure 1F–H). On average, each ON contained 316 ± 33 vimentin-positive cells ($n = 3$ ONs). These cells consistently surrounded unstained areas of the ON, containing ORN-axons (Figure 1G, asterisk; supplementary Figure S1). The localization, number, and morphology of these cells are consistent with earlier descriptions of OECs in different species (Doucette 1993; Sonigra et al. 1999; Chuah and West 2002; Pellitteri et al. 2010; Su and He 2010; Higginson and Barnett 2011; Ekberg et al. 2012). An antibody against fibronectin labeled spindle-like and oval-shaped cells, which were located on the surface of the ON (Figure 1 J-K). These cells encased the ON along its entire length (Figure 1I–L). On average, each ON contained 37 ± 9 fibronectin-positive cells ($n = 3$ ONs). The localization, number, and morphology of these cells are consistent with earlier descriptions of fibroblasts in different species (Li et al. 2008; Oprych et al. 2017). Using a *mpeg1*-GFP transgenic *Xenopus* line, we identified a small number of round to oval-shaped macrophages mainly located on the surface of the ON and in some cases in the nerve layer of the OB (Figure 1M–P). On average, each ON contained 4 ± 1 *mpeg1*-GFP-positive cells ($n = 3$ ONs).

Together, the location within the ON, morphology, and expression pattern of specific markers allowed us to identify at least three distinct cell types: vimentin-positive putative OECs, fibronectin-positive putative fibroblasts, and *mpeg1*-GFP-positive putative macrophages. Among all cells stained with the three adopted markers, ~89% were vimentin-positive, ~10% were fibronectin-positive, and ~1% were *mpeg1*-GFP-positive.

3.2 | Electroporated Cells of the ON Can Be Classified Into Two Main Morphological Types

We performed single-cell electroporations to visualize the morphology of individual non-neuronal cells of the ON. Electroporation of fluorescently-tagged dextran labeled the cytosol, including the various appendages of cells.

We performed single-cell electroporations in 14 larvae of *X. laevis* and stained 74 individual cells within the ON. The 74 labeled cells could be categorized into two main morphological types (Figure 2). In deeper layers of the ON, the cells exhibited a fusiform bipolar morphology featuring two extensions originating from the centrally located nucleus (nucleus not stained in Figure 2A). The length of the cell shown in Figure 2A is approximately 70 µm. Figure 2B shows an orthogonal projection of another ON with an electroporated fusiform bipolar cell. Of the 74 individual stained cells, 49 had fusiform bipolar morphologies similar to those shown in Figure 2A,B. In more superficial layers of the ON, the electroporated cells had a considerably different morphology (Figure 2C,D). These cells (yellow) had a more compact, flat, and sheet-like morphology,

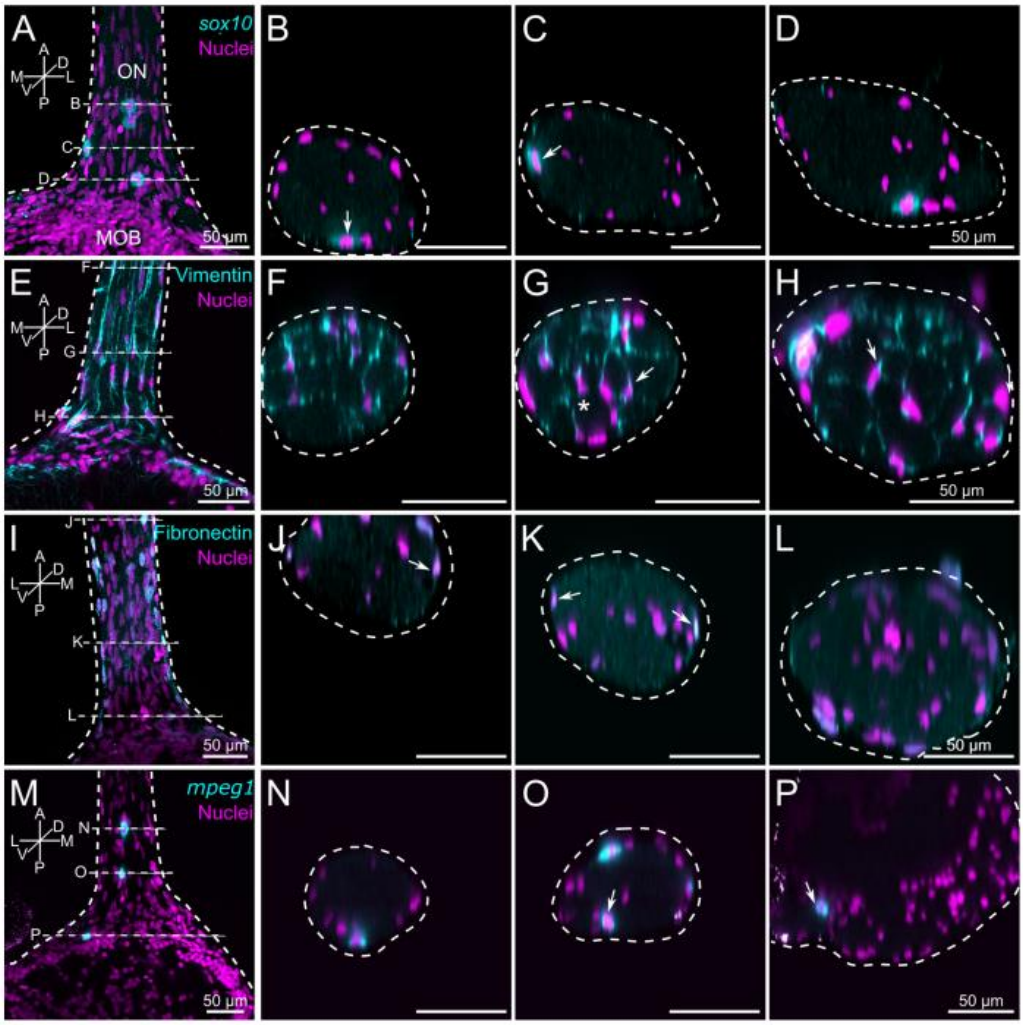

FIGURE 1 | Identification of non-neuronal cells within the olfactory nerve. (A) *sox10*-positive cells (cyan) within the ON. (B–D) Orthogonal projections of the same image stack as in A, visualizing sections at three different locations on the anterior–posterior axis of the ON. (B) anterior; (C) intermediate; and (D) posterior. White arrows point at some *sox10*-positive cells located on the surface of the ON. (E) Vimentin-positive cells (cyan) with a spindle-like bipolar morphology are found throughout the ON and the nerve layer of the OB. (F–H) Orthogonal projections of the same image stack as in E, visualizing sections through the ON. (F) anterior; (G) intermediate; and (H) posterior, close to the OB. White arrows point at some vimentin-positive cells. The asterisk indicates vimentin-positive cells surrounding unstained areas within the ON. (I) Fibronectin-positive cells (cyan) have a long, flat, and oval-shaped morphology and are localized on the surface of the ON. (J-L) Orthogonal projections of the same image stack as in I, visualizing sections through the ON. (J) anterior; (K) intermediate; and (L) posterior, close to the OB. Fibronectin-positive cells encase the whole ON (white arrows). (M) *mpeg1*-positive macrophages (cyan) of different sizes have a round to oval-shaped morphology and are predominantly located on the surface of the ON and within the OB. (N–P) Orthogonal projections of the same image stack as in M, visualizing sections through the ON. (N) anterior; (O) intermediate; and (P) posterior, close to the OB. White arrows point at macrophages. Similar results were obtained in all animals investigated (*sox10*: 4 animals; vimentin: 6 animals; fibronectin: 10 animals; *mpeg1*: 8 animals). Cell nuclei were labeled with propidium iodide (PI, magenta). A, anterior; D, dorsal; L, lateral; M, medial; MOB, main olfactory bulb; ON, olfactory nerve; P, posterior; V, ventral.

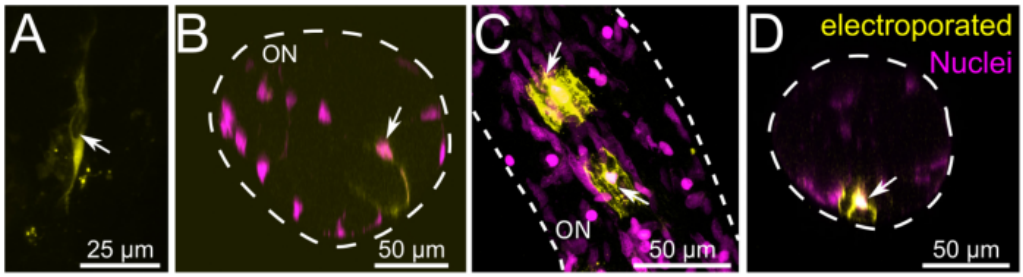

FIGURE 2 | Electroporated non-neuronal cells in the olfactory nerve can be grouped into two main categories. (A) Example of a fusiform bipolar cell situated in deeper layers of the ON with two extensions (yellow) originating from the centrally located nucleus (not stained; arrow). (B) Orthogonal projections of another ON. The arrow indicates the nucleus (magenta) of an electroporated fusiform bipolar cell. The extension of this cell (yellow) forms a circle around an empty area of the ON. (C) Two electroporated cells with a flat, sheet-like morphology located on the surface of the ON (yellow). Arrows label protrusions originating from the centrally located nuclei (magenta). (D) Orthogonal projections of another ON. The arrow indicates an electroporated cell with a flat, sheet-like morphology (yellow). Cell nuclei were labeled with propidium iodide (PI, magenta). ON, olfactory nerve.

with several protrusions originating from the centrally located nuclei (magenta). The length of the cells shown in Figure 2C is approximately 30 µm. Of the 74 individual stained cells, 25 had morphologies like those shown in Figure 2C,D.

In conclusion, non-neuronal cells labeled via single-cell electroporation in the ON can be grouped into two main types: fusiform bipolar and flat, sheet-like.

3.3 | ON Transection Leads to Phosphorylation of rpS6 in Non-Neuronal Cells in the ON

We performed immunolabelings of the olfactory system of larval *X. laevis* with an antibody against p-rpS6 24 h after unilateral nerve transection.

Expression of p-rpS6 was observable in cells of the ON, the ON layer of the OB, the glomerular layer, and the projection neuron layer of the OB (Figure 3A,B). In the OB, labeled cells were present on both the non-transected and transected sides. In the ON, on the other hand, p-rpS6-positive cells were mainly found on the transected side. Phosphorylated rpS6 evoked a strong cytoplasmic staining in cells with fusiform bipolar morphology (Figure 3C). Cell nuclei stained with propidium iodide were localized in the center of these cells (Figure 3C). Cross-sectional rendering of the ON revealed that p-rpS6-positive cells were present throughout the whole width of the ON (Figure 3D). We regularly observed that these cells surrounded empty areas of the ON (Figure 3D, asterisks), which contained axons of ORNs (see supplementary Figure S1).

To distinguish the activated cell types within the ON, we performed immunohistochemistry using previously identified markers (see Figure 1) and an antibody against p-rpS6.

Vimentin-positive cells, most likely OECs (see also Figure 1), in the ON and the nerve layer of the OB also expressed p-rpS6 (Figure 4A). A high number of double-positive cells for both p-rpS6 and vimentin could be observed (Figure 4B, arrows). The double-positive cells had a fusiform bipolar morphology, indicating that most of these cells are OECs (Figure 4B). However, the number of vimentin-positive cells was higher and more widespread than the p-rpS6-positive cells. This observation can, in part, be explained by the fact that the antibody against vimentin, in addition to cells of the ON, also stained a network of fibers spreading through the whole OB in both the non-transected and transected sides (Figure 4A, Supplementary Figure S2). They were previously identified as processes of radial glial cells (see discussion).

Using transgenic *sox10*-GFP *Xenopus* larvae, we identified several *sox10*-positive cells in the ON also expressing p-rpS6 (Figure 5A). The *sox10* and p-rpS6 double-positive cells had a round shape and were mainly localized near the surface of the ON (Figure 5A). Double-staining with antibodies against fibronectin and p-rpS6 double-labeled several elongated cells with a spindle-like morphology located on the surface of the ON, and some cells that were oval-shaped (Figure 5B, arrows). These observations showed that only a few fibronectin-positive fibroblasts were activated after transection and expressed p-rpS6. Using the transgenic *mpeg1 Xenopus* larvae, we also observed that ON macrophages expressed p-rpS6 after nerve transection. The macrophages were located on the surface of the ON and the transition area between the ON and the OB (Figure 5C, arrow).

In addition to the stainings in the ON and the nerve layer of the OB, p-rpS6-positive cells were also observed in the glomerular and mitral cell layers of the OB. The localization of the p-rpS6-positive cells in these layers suggested that these cells are projection neurons and/or periglomerular cells. The neuronal identity of these cells was confirmed by co-labeling with HuC/HuD neuronal protein (HuC/D), known to label neuron-specific ELAV/Hu RNA binding proteins (Wei and Lai 2022), and p-rpS6 (Supplementary Figure S3).

Together, we found a high expression of p-rpS6 in non-neuronal cells of the ON 24 h after nerve transection. Several non-neuronal ON cells, including numerous OECs, fibroblasts, and macrophages, were among the p-rpS6-positive cells. The expression of

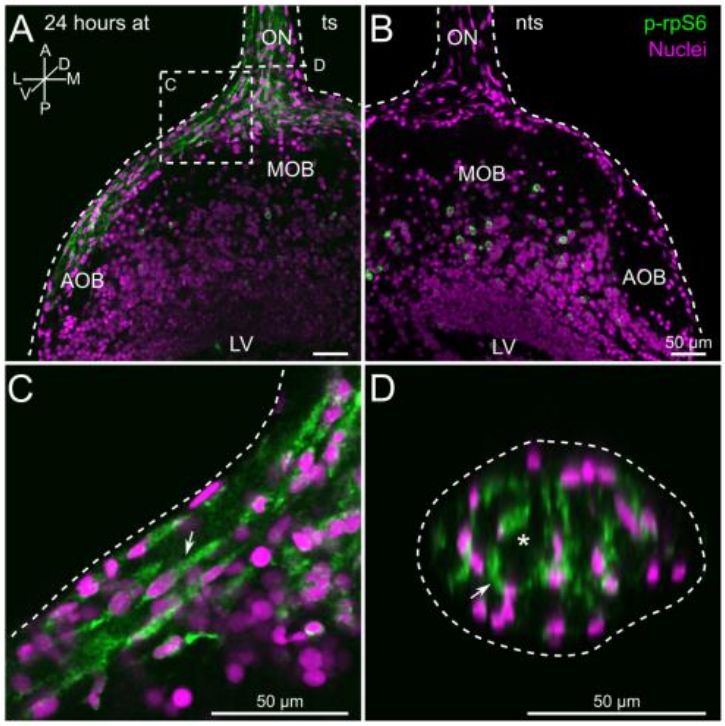

FIGURE 3 | Olfactory nerve transection induces phosphorylation of rpS6 in non-neuronal cells. (A and B) p-rpS6 (green) labeled cells in the ON and OB. In the projection neuron layer of the OB, labeled cells are present on both the non-transected and transected sides. In the nerve layer of the OB and the ON, stained cells are present only on the transected side. (C) Close-up of the encircled area in (A). The p-rpS6-expressing cells in the ON have a fusiform bipolar morphology (white arrow). (D) Cross-section through the nerve shown in A. Stained cells are present across the entire width of the ON (white arrow) and surround circular unstained gaps (white asterisk). Similar results were obtained in all animals investigated ($n=6$). Cell nuclei were labeled with propidium iodide (PI, magenta). A, anterior; AOB, accessory olfactory bulb; at, after transection; D, dorsal; L, lateral; LV, lateral ventricle; M, medial; MOB, main olfactory bulb; nts, non-transected side; ON, olfactory nerve; P, posterior; ts, transected side; V, ventral.

p-rpS6 was strong in transected ONs and the ipsilateral nerve layer of the OB. We conclude that p-rpS6 is an excellent marker for injury-dependent activation of non-neuronal cells in the olfactory system of larval *X. laevis*.

3.4 | Non-Neuronal Cells in the ONs Are Temporarily Activated Within 1–48 h After the Transection of the ON

To investigate the time course of activation of non-neuronal ON cells, we unilaterally transected the ON of *X. laevis* larvae and examined the p-rpS6 signal at different time points after transection. We calculated a ratio of the cumulative p-rpS6 signal between the transected and non-transected sides for each animal.

In non-transected control animals, the p-rpS6 signal was equal in both ONs with a mean signal ratio of 1.0 ± 0.3. We investigated multiple time points, ranging from 1 h to 7 weeks, after ON transection, and the median p-rpS6 signal ratio was statistically not equal across all samples (Figure 6A, Kruskal–Wallis, $p = 2 * 10^{-6}$). ON transection led to a noticeable but not significant increase in p-rpS6 signal on the transected side already after 1 h (Figure 6A–C). This trend was observable with continuously elevated p-rpS6 signal ratios until 24 h after transection. After 24 h, the p-rpS6 signal ratio was significantly increased to 5.2 ± 2.9 ($p < 0.03$). After 48 h, we observed a substantial decrease in the signal to a ratio of 1.4 ± 0.6. This trend continues with highly significant activity differences measured between 24 h and 7 days ($p < 0.001$), 14 days ($p < 0.01$), and 21 days ($p < 0.001$) after transection (Dunn's post hoc test with the Bonferroni–Holm correction).

In addition to the transient elevation of the p-rpS6 signal, we also observed spatial dynamics of the signal localization (Figure 6C). One hour after the ON transection, the p-rpS6 signal was mainly limited to the ON, and nearly no signal was found in the nerve layer of the OB. Six hours after transection, the signal was also visible in the nerve layer of the OB. Twenty-four hours after transection, p-rpS6-positive cells were visible along the entire ON and within the nerve layer of the OB.

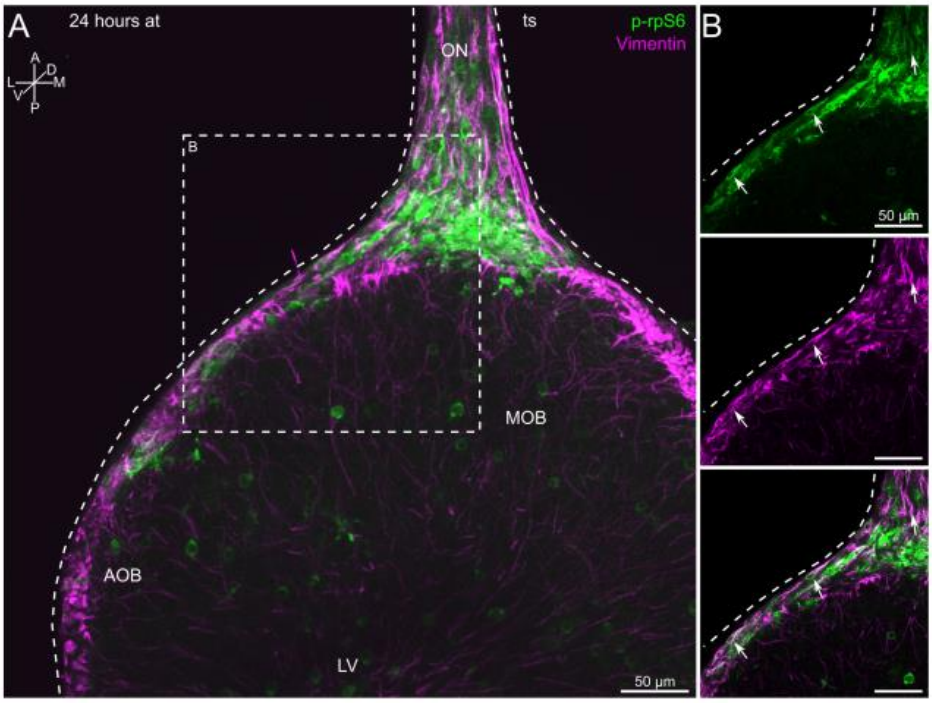

FIGURE 4 | Vimentin and p-rpS6 are co-expressed in cells of transected olfactory nerves. (A) Vimentin (magenta) and p-rpS6 (green) labeled cells populating the transected ON and the nerve layer of the OB. In addition, some ON and OB cells were labeled either by vimentin or p-rpS6. (B) A close-up of the area encircled in A shows the co-localization of vimentin and p-rpS6 in ON cells and their morphology in more detail. The white arrows indicate cells labeled by both markers (upper panel: p-rpS6 channel; middle panel: vimentin channel; lower panel: overlay of both channels). Similar results were obtained in all animals investigated ($n = 9$). Note that the images in A and B result from individually recorded image stacks. A, anterior; AOB, accessory olfactory bulb; at, after transection; D, dorsal; L, lateral; LV, lateral ventricle; M, medial; MOB, main olfactory bulb; ON, olfactory nerve; P, posterior; ts, transected side; V, ventral.

In addition, the connectivity of ORN axons and the morphology of glomeruli in the OB were observed by labeling ORN axons via electroporation. ON transection induced degradation of ORN axons. Over the first week after nerve transection, the OB area innervated by ORN axons gradually decreased on the transected side (Figure 6C; magenta axons). Seven days after nerve transection, most transected axons were already decomposed (Figure 6C; compare with Figure 6B, control side). Twenty-one days after unilateral nerve transection, axons of newly formed ORNs (Figure 6C) had already extensively innervated the OB, and the reinnervation of the OB was widely completed after 49 days (Figure 6C, white axons).

In summary, non-neuronal cells in the transected ON featured a transient increase in p-rpS6, indicating that the activation of these cells was induced by ON transection. This activation begins within 1 h after the transection and reaches its peak after 24 h. Furthermore, we observed that the p-rpS6 signal spreads from the ON to the OB within the first 24 h after transection. Within 7 days after ON transection, the p-rpS6 signal returns to control conditions.

4 | Discussion

In the present study, we characterized several classes of non-neuronal cells populating the ON of larval *X. laevis*. We provide evidence that the ON houses OECs, fibroblasts, and macrophages. Furthermore, by employing the phosphorylation of rpS6 as a proxy for cellular activation, we show that several classes of non-neuronal cells of the ON are transiently activated upon nerve injury. Possible physiological functions of the activation of these non-neuronal cells are discussed.

4.1 | Identification and Localization of Non-Neuronal Cells Within the ON of Larval *X. laevis*

Sox10 is known to be expressed in developing OECs in various vertebrate taxa (Barraud et al. 2010, 2013; Forni et al. 2011; Pingault et al. 2013; Oprych et al. 2017; Perera et al. 2020), and it is used as a marker for cells derived from the neural crest (Alkobtawi et al. 2018; Yang et al. 2020). Based on this

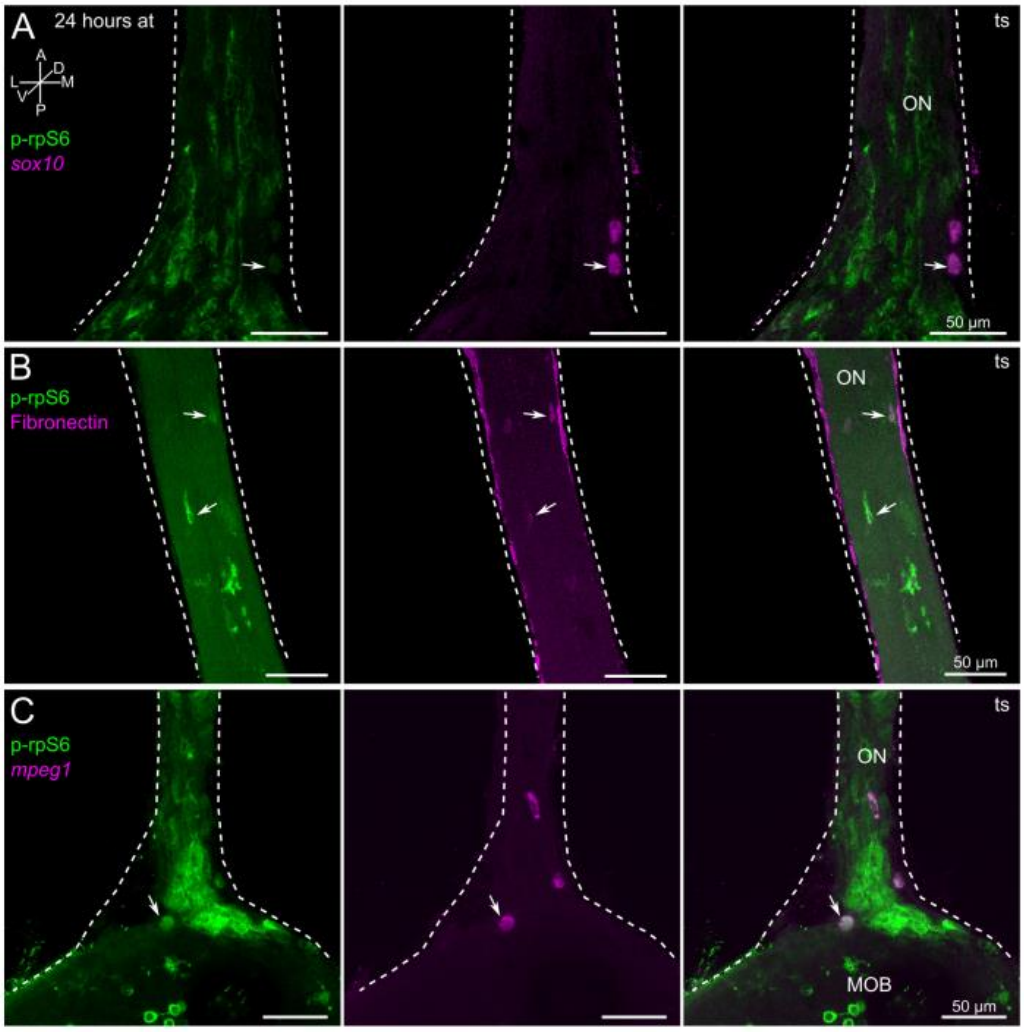

FIGURE 5 | Non-neuronal cells express the activity marker p-rpS6 after olfactory nerve transection. (A) p-rpS6 and *sox10*-GFP are co-localized in cells of transected ONs (arrows). (B) Co-localization of fibronectin and p-rpS6 in flat oval-shaped cells of the transected ON (arrows). (C) p-rpS6-positive macrophages in the transected ON and the transition area between the ON and the OB (arrows). The left-hand column shows the p-rpS6 signal (green), the intermediate column shows the *sox10*, fibronectin, and *mpeg1* signal (magenta), and the right-hand column shows merged images. Similar results were obtained in all animals investigated (*sox10*: 10 animals; fibronectin: 10 animals; *mpeg1*: 7 animals). A, anterior; at, after transection; D, dorsal; L, lateral; M, medial; MOB, main olfactory bulb; ON, olfactory nerve; p, posterior; ts, transected side; V, ventral.

information, we hypothesized that *sox10* could be expressed in OECs of *Xenopus* larvae. Using a *sox10*-GFP *Xenopus* line, we identified a small number of *sox10*-GFP positive cells with a round-shaped morphology located within and on the surface of the ON (see Figures 1 and 5). The morphology, localization, and number of *sox10*-GFP positive cells indicate that these cells are not mature OECs nor other known non-neuronal cells of the ON. We currently do not know the identity of these *sox10*-GFP-positive cells present in the ON of larval *Xenopus*. These cells may be developing, immature precursors on their way to becoming mature OECs.

Next, we employed an antibody against vimentin, a known component of the mammalian OEC intermediate filaments (Franceschini and Barnett 1996). In the ON, vimentin-positive cells exhibited a long, fusiform bipolar morphology and ensheathed bundles of ORN axons throughout the ON. Thereby, vimentin-positive structures resembled filamentous cytoskeletal

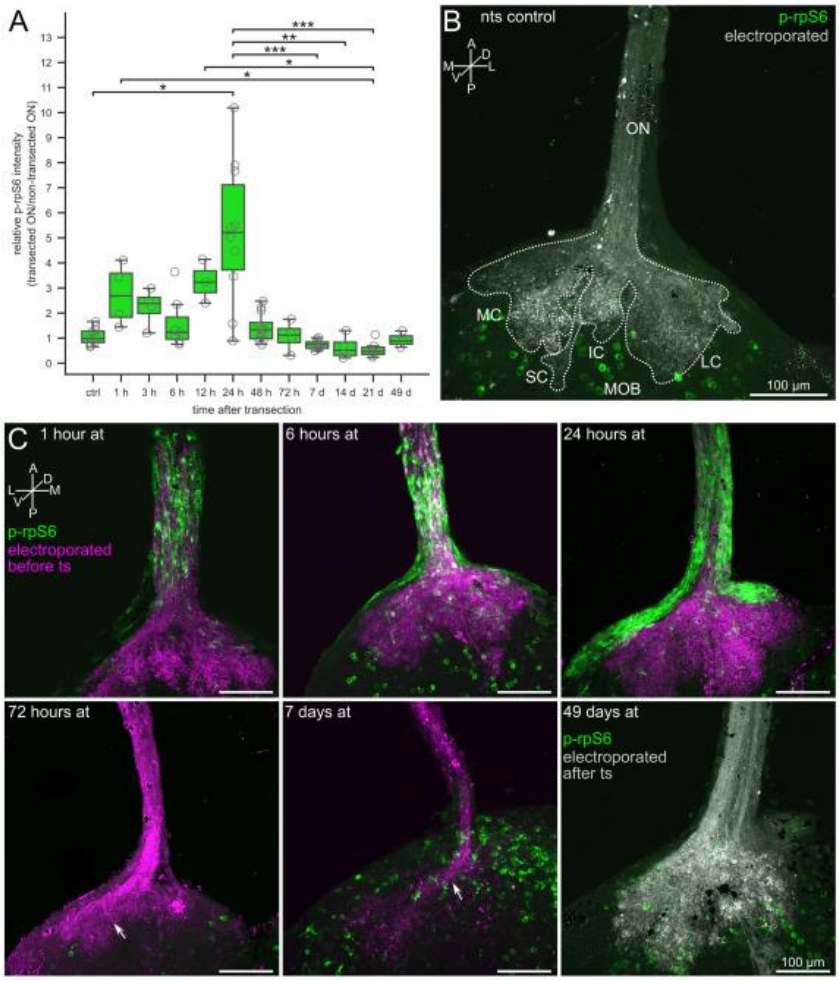

FIGURE 6 | Non-neuronal cells of the olfactory nerve feature transient phosphorylation of rpS6 after olfactory nerve transection. (A) Boxplot of p-rpS6 immunohistochemically labeled cells at different time points after unilateral ON transection. A ratio of cumulative pixel intensities between the transected and non-transected ON of the same animal was calculated to measure changes in activity. Individual data for each animal is marked with grey circles (ctrl, $n = 11$; 1 h, $n = 4$; 3 h, $n = 4$; 6 h, $n = 7$; 12 h, $n = 3$; 24 h, $n = 10$; 48 h, $n = 12$; 72 h, $n = 4$; 7 d, $n = 8$; 14 d, $n = 4$; 21 d, $n = 6$; 49 d, $n = 3$). The black horizontal line indicates the median signal ratio of the animals in the same group. (B) Image of the ON and the OB of a non-transected animal (white, axons of ORNs; green, p-rpS6). The axons of ORNs were stained by nasal electroporation of fluorescent dextrans. The glomerular clusters are outlined with a dotted white line. Several p-rpS6-positive cells (green) were visible in the glomerular and the projection neuron layer of the OB. (C) Transection-induced phosphorylation of rpS6 in non-neuronal cells of the ON and nerve layer of the OB (different time points after transection). Axons of ORNs (magenta) were labeled by nasal electroporation of fluorescent dextrans before ON transection. The transection of the ON induced gradual axonal degradation in the OB. Seven weeks after ON transection, the reinnervation by ORN axons of the OB was reestablished. The axons of regenerated ORNs (white) were labeled by nasal electroporation of dextran 3 days before sample preparation and immunohistochemistry. A, anterior; AOB, accessory olfactory bulb; at, after transection; d, days; D, dorsal; Elp., electroporated; h, hours; IC, intermediate cluster; L, lateral; LC, lateral cluster; LV, lateral ventricle; M, medial; MC, medial cluster; MOB, main olfactory bulb; nts, non-transected side; ON, olfactory nerve; P, posterior; SC, small cluster; V, ventral. Statistical significance was tested using the Kruskal-Wallis test followed by Dunn's post hoc test with Bonferroni-Holm correction (*, $p < 0.05$; **, $p < 0.01$; ***, $p < 0.001$).

elements (see Figure 1). Together, the characteristic vimentin staining is in line with the description of OEC in many vertebrate species (Doucette 1993; Sonigra et al. 1999; Chuah and West 2002; Pellitteri et al. 2010; Su and He 2010; Higginson and Barnett 2011; Ekberg et al. 2012; Manzini et al. 2022). It is thus very likely that most vimentin-positive cells in the ON of

larval *X. laevis* are indeed OECs. As vimentin is also expressed in fibroblasts (Cheng et al. 2016; Tallquist and Molkentin 2017; Sliogeryte and Gavara 2019), we can, however, not exclude that a subgroup of the vimentin-positive cells represents fibroblasts. In addition, vimentin also stained many cells within the OB (see Figure 4 and Supplementary Figure S2). In *Xenopus*, these cells have already been identified as radial glia extending from the surface of the lateral ventricles to the surface of the OB (Nezlin et al. 2003; Huang et al. 2005).

To label fibroblasts, we used an antibody against fibronectin, a glycoprotein known to be expressed in this cell type (Ibanez et al. 2007). We identified several spindle-like and oval-shaped fibronectin-positive cells localized in the superficial layers of the ON (see Figures 1 and 4).

Using an *mpeg1*-GFP transgenic *Xenopus* line, we identified a small number of round to oval-shaped cells located in superficial positions of the ON (see Figures 1 and 4). Given that *mpeg1* is predominantly expressed in macrophage lineages (Ellett et al. 2011; Bayly-Jones et al. 2020; Ferrero et al. 2020), we classified these cells as macrophages.

Together, these findings indicate that the identity and distribution of non-neuronal cells in the ON of larval *X. laevis* are comparable to that found in rodents: OECs surround bundles of ORN axons, fibroblasts form a structure resembling the perineurium, and the number of macrophages on the surface of the ON is relatively low. Our results, however, show that, unlike in rodents, fibroblasts in *Xenopus* do not ensheath nerve fascicles but rather ensheath the whole ON. Also, macrophages are solely located on the surface of the ON and are not present on the surface of individual nerve fascicles. Figure 7 summarizes our findings and renders the cellular composition of the ON in larval *X. laevis*.

4.2 | Distinct Morphologies of Putative Olfactory Ensheathing Cells in the ON of Larval *X. laevis*

Using antibodies against vimentin, p-rpS6, and single-cell electroporations, we identified putative OECs with two morphologies: fusiform bipolar and flat sheet-like. While putative OECs identified with antibodies against vimentin and p-rpS6 had a mainly fusiform bipolar morphology (Figures 1, 3, and 4), single-cell

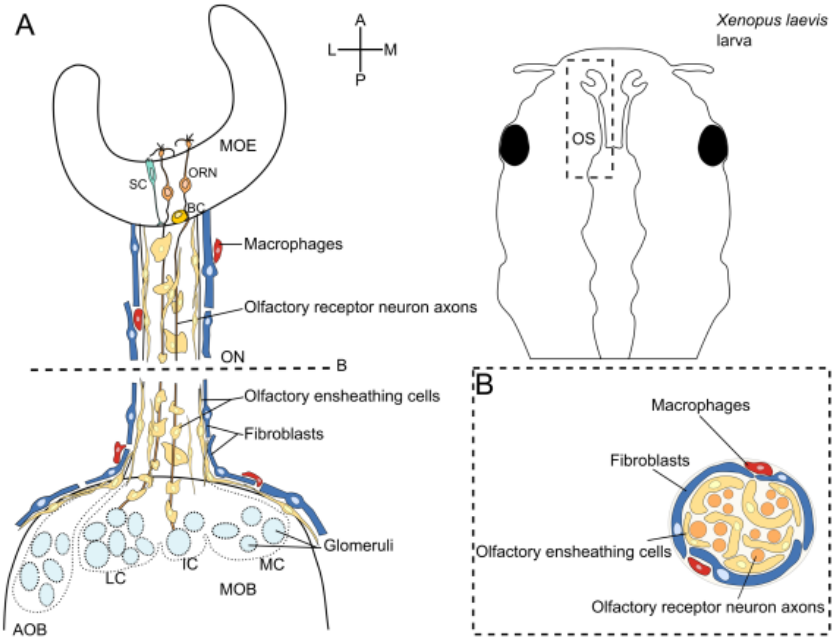

FIGURE 7 | Scheme summarizing the cellular composition of the peripheral olfactory system and olfactory nerve in larval *Xenopus laevis*. (A) The main olfactory epithelium (MOE) contains three main cellular components: olfactory receptor neurons (ORN), non-neuronal supporting cells (SC), and olfactory stem cells/basal cells (BCs). Olfactory receptor neurons extend their axons through the basal lamina of the OE, the olfactory nerve (ON), and enter the olfactory bulb (OB), where they converge into olfactory glomeruli. In the ON, ORN axons are enwrapped by olfactory ensheathing cells (OECs), which ensheathe several axons into fascicles. The ON is surrounded by fibroblasts, which form a perineurium-like structure. A small number of macrophages are located outside this perineurium. The rectangle on the schematic of the larva (right-hand side) indicates the location of the schematic shown on the left-hand side. (B) Illustration of a cross-section through the ON showing the location and arrangement of ORN axons, OECs, fibroblasts, and macrophages. A, anterior; AOB, accessory olfactory bulb; BC, basal cell; IC, intermediate cluster; L, lateral; LC, lateral cluster; M, medial; MC, medial cluster; MOB, main olfactory bulb; MOE, main olfactory epithelium; ON, olfactory nerve; ORN, olfactory receptor neuron; OS, olfactory system; P, posterior; SC, supporting cell.

electroporations revealed cells with an additional morphology, i.e., flat sheet-like. In contrast to fusiform bipolar cells, the flat sheet-like cells were always located in more superficial layers of the ON. Very likely, OECs with different morphologies fulfil different functions. It would, therefore, be very interesting to investigate if there are any shifts in abundance of either type after ON injury. We will tackle this question in future studies.

It has been shown that vertebrate OECs are a heterogeneous cell population varying in size and morphology (e.g., elongated, flattened and branched), capable of switching between these morphologies (Doucette 1993; Sonigra et al. 1999; van den Pol and Santarelli 2003; Barnett and Chang 2004; Huang et al. 2008, 2024; Pellitteri et al. 2010; Ekberg et al. 2012). Based on this information, we assume that the identified flat sheet-like cells in the ON of larval *Xenopus* are a type of OEC. This strongly suggests that the morphology of OECs in larval *Xenopus* is generally similar to that in other vertebrates. Nevertheless, further studies are needed to clarify the morphological diversity of OECs in this larval amphibian.

4.3 | Phosphorylated rpS6 is a Suitable Marker for an Injury-Mediated Activation of Non-Neuronal Cells in the ON

Phosphorylation of rpS6, a component of the 40S ribosomal subunit involved in translation, is broadly used as a readout of the mammalian target of rapamycin complex 1 signaling activation and/or as a neuronal activity marker (Meyuhas 2008, 2015; Biever et al. 2015). The phosphorylation of rpS6 was initially noticed in rat liver regeneration (Gressner and Wool 1976), and later it was found that it is promoted by different pharmacological stimuli and enhanced in a variety of physiological and pathophysiological conditions (Wool et al. 1995; Ruvinsky and Meyuhas 2006; Biever et al. 2015). In mouse hepatocytes, growth factors were the primary mechanism responsible for stimulating rpS6 phosphorylation (Pende et al. 2004). The exact biological role of the phosphorylation of rpS6 is, however, still not determined (Biever et al. 2015).

Here, we aimed to monitor the injury-induced activation of non-neuronal cells in the peripheral olfactory system of larval *X. laevis*. In initial experiments, we observed that 24 h after unilateral ON-transection, many non-neuronal cells were positive for p-rpS6 within the transected ON and the nerve layer of the ipsilateral OB (Figure 3). Thereby, cells of all previously identified subgroups (*sox10*-, vimentin-, fibronectin-, and *mpeg1*-positive cells) were activated (Figures 4 and 5) and probably contribute to reparative processes within the ON.

It is well established that OECs are the primary phagocytic cells in the peripheral olfactory system and serve as the primary immune cells of the ON (Su et al. 2013; Nazareth et al. 2015). They bind, produce, and secrete a variety of proteins, such as cytokines/neurotrophins, which act on surrounding cells (Boruch et al. 2001; Woodhall et al. 2001; Nazareth et al. 2015; Barton et al. 2017; Wright et al. 2020). Among others, through the secretion of anti-inflammatory mediators, OECs can modulate the immune response, potentially reducing inflammation and promoting regeneration by influencing the activity of other immune cells (Denaro et al. 2022; Chen et al. 2025). Also, it has long been known that OECs are involved in the promotion of continuous growth and the targeted pathfinding of ORN-axons within the ON (Doucette 1993; Key and St John 2002; Ekberg et al. 2012; Ekberg and St John 2014; Barton et al. 2017; Denaro et al. 2022).

Fibroblasts have been shown to produce various cytokines and growth factors, which can activate multiple signaling cascades, including the Ras/Raf/MEK/Erk/MAP kinase and phosphatidylinositol-3-kinase (PI3K)/AKT signaling pathways (Meyuhas 2015; Zhang 2017; Plikus et al. 2021). These signaling cascades can lead to the phosphorylation of rpS6 (Meyuhas 2015). Additionally, during tissue development, homeostasis, repair, and disease, fibroblasts secrete extracellular matrix components (Lendahl et al. 2022). These characteristics of fibroblasts may also mediate reparative effects during the regeneration of ON in *X. laevis*.

Macrophages express a diverse array of plasma membrane receptors, enabling them to recognize various endogenous and exogenous ligands (Taylor et al. 2005). Similar to OECs, macrophages are also phagocytic immune cells that have been documented to engulf and degrade apoptotic neuron debris in the CNS (Hume et al. 1983; Napoli and Neumann 2009; Su et al. 2013). However, the ON is almost devoid of macrophages, and ORN axons are not in direct contact with macrophages (Su et al. 2013; Nazareth et al. 2015; Barton et al. 2017; Wright et al. 2020). Our observation that macrophages on the surface of the ON are positive for p-rpS6 suggests that these cells respond to the secretion of signaling molecules from OECs, fibroblasts, and/or other surrounding cells in response to injury.

Together, our results show that after ON-transection, phosphorylation of rpS6, i.e., activation, occurs in subgroups of several non-neuronal cell types of the ON. The activation of these cells is likely involved in modulating the immune response and controlling degenerative and regenerative processes.

4.4 | Time Course of the Injury-Mediated Phosphorylation of rpS6 in Non-Neuronal Cells of the ON

The time course of degeneration and functional regeneration of the olfactory system upon ON-transection in larval *X. laevis* has been thoroughly investigated (Cervino et al. 2017; Hawkins et al. 2017, 2024). After the transection of the ON, all mature ORNs degenerate, and new ORNs are immediately formed from neuronal stem cells of the OE. One week after transection, the first axons of newly formed ORNs reach the OB and start the synaptic reconnection with OB neurons. Seven weeks after ON-transection, all connections are functionally reestablished, and after 7 to 9 weeks, characteristic odorant-induced behavior reappears (Cervino et al. 2017; Hawkins et al. 2017, 2024).

Building on the above findings and our observation that non-neuronal cells in the ON are activated, i.e., p-rpS6-positive, 24 h after ON transection, we set out to analyze the temporal dynamics of this activation. Increased p-rpS6 levels were detectable within 1 h after transection, peaked after 24 h, and sharply declined after 48 h (see Figure 6). One hour after transection, p-rpS6-positive cells were confined to the immediate vicinity of

the injury site. Six hours after transection, their number had increased, and they were located along the entire ON up to the rostral portion of the nerve layer of the OB (Figure 6C). After 24 h, p-rpS6-positive cells were abundantly distributed throughout the ON and across the entire nerve layer of the OB (Figure 6C). Since it is known that non-neuronal cells of the ON can secrete a variety of signaling molecules (Boruch et al. 2001; Woodhall et al. 2001; Meyuhas 2015; Nazareth et al. 2015; Barton et al. 2017; Zhang 2017; Wright et al. 2020; Plikus et al. 2021; Hsueh et al. 2024), the observed widespread activation likely results from the diffusion of signaling molecules released by initially activated cells at the injury site, triggering the activation of neighboring cells.

Alterations in the phosphorylation level of rpS6 were also observed in response to traumatic brain injury in rats as early as 30 min to 24 h after injury (Chen et al. 2007). Given that the mammalian target of rapamycin signaling pathways and the phosphorylation of rpS6 promote cellular and neuronal synaptic growth and repair (Ruvinsky and Meyuhas 2006; Chen et al. 2007), it can be speculated that activation of these pathways may also contribute to the regenerative capacity of the olfactory system after nerve injury. It would, therefore, be exciting to study whether rapamycin-assisted inhibition of the mammalian target of rapamycin-complex 1 inhibition, which would result in a decreased phosphorylation of rpS6 (Biever et al. 2015), influences the immune response and the overall regenerative capacity of the olfactory system.

5 | Conclusion

Using transgenic *Xenopus* lines, single-cell electroporations, and various cell-type-specific markers, we identified several non-neuronal cell types that populate the ON of larval *X. laevis*, including OECs, fibroblasts, and macrophages. Furthermore, we described the spatial localization of these cell types within the ON. Their spatial distribution in *Xenopus* is similar to the distribution of these cell types in the ON of mammalian species. However, unlike in mammals, in *Xenopus*, fibroblasts do not ensheath nerve fascicles but rather ensheath the whole ON. Additionally, unlike in other mammals, macrophages are located on the surface of the ON and are not present within the ON itself. Furthermore, we used the phosphorylation of rpS6 as a proxy for cellular activation after injury. Various non-neuronal cell types within the ON showed an increased p-rpS6 signal as early as 1 h to 24 h after ON transection. Morphology, expression of cell type-specific proteins, location, and injury-induced activity suggest that the described rpS6-expressing cells are a mixture of OECs, fibroblasts, and macrophages. Our results show that upon ON transection, the phosphorylation level of rpS6 transiently increases, suggesting that it may be an essential mechanism supporting regenerative processes.

Together, the present study provides the first description of non-neuronal cells of the ON of larval *X. laevis* and their injury-induced activation. The results of this study provide the basis for further investigations on how the various non-neuronal cell types of the ON support regenerative processes in the olfactory system of larval *X. laevis*.

Author Contributions

Melina Kahl: conceptualization, formal analysis, investigation, methodology, validation, visualization, writing – original draft, writing – review and editing. **Lukas Weiss:** conceptualization, formal analysis, investigation, methodology, validation, visualization, writing – original draft, writing – review and editing. **Joshua Walter:** investigation, methodology, validation, visualization, writing – original draft, writing – review and editing. **Thomas Hassenklöver:** conceptualization, data curation, formal analysis, methodology, supervision, validation, visualization, writing – original draft, writing – review and editing. **Ivan Manzini:** conceptualization, funding acquisition, project administration, supervision, validation, visualization, writing – original draft, writing – review and editing.

Acknowledgments

The authors thank Anja Schnecko for technical assistance. Open Access funding enabled and organized by Projekt DEAL.

Ethics Statement

All animal procedures were performed following the guidelines of laboratory animal research of the Institutional Care and Use Committee of the Justus Liebig University of Gießen (649_M; GI 15/7 Nr. G 89/2017; GI 15/3 Nr. G 15/2018; GI 15/7 Nr. G 2/2019).

Conflicts of Interest

The authors declare no conflicts of interest.

Data Availability Statement

The data supporting the findings of this study are available at https://doi.org/10.22029/jlupub-19833.

Peer Review

The peer review history for this article is available at https://www.webofscience.com/api/gateway/wos/peer-review/10.1111/ejn.70211.

References

Alkobtawi, M., H. Ray, E. H. Barriga, et al. 2018. "Characterization of Pax3 and Sox10 Transgenic Xenopus Laevis Embryos as Tools to Study Neural Crest Development." *Developmental Biology* 444, no. Suppl 1: S202–S208.

Astic, L., and D. Saucier. 2001. "Neuronal Plasticity and Regeneration in the Olfactory System of Mammals: Morphological and Functional Recovery Following Olfactory Bulb Deafferentation." *Cellular and Molecular Life Sciences* 58: 538–545.

Au, E., and A. J. Roskams. 2003. "Olfactory Ensheathing Cells of the lamina Propria in Vivo and in Vitro." *Glia* 41: 224–236.

Bailey, S. B., M. E. Eichler, A. Villadiego, and K. M. Rich. 1993. "The Influence of Fibronectin and Laminin During Schwann Cell Migration and Peripheral Nerve Regeneration Through Silicon Chambers." *Journal of Neurocytology* 22: 176–184.

Barnett, S. C., and L. Chang. 2004. "Olfactory Ensheathing Cells and CNS Repair: Going Solo or in Need of a Friend?" *Trends in Neurosciences* 27: 54–60.

Barraud, P., A. A. Seferiadis, L. D. Tyson, et al. 2010. "Neural Crest Origin of Olfactory Ensheathing Glia." *Proceedings of the National Academy of Sciences of the United States of America* 107: 21040–21045.

Barraud, P., J. A. St John, C. C. Stolt, M. Wegner, and C. V. H. Baker. 2013. "Olfactory Ensheathing Glia Are Required for Embryonic

Olfactory Axon Targeting and the Migration of Gonadotropin-Releasing Hormone Neurons." *Biology Open* 2: 750–759.

Barton, M. J., J. S. John, M. Clarke, A. Wright, and J. Ekberg. 2017. "The Glia Response After Peripheral Nerve Injury: A Comparison Between Schwann Cells and Olfactory Ensheathing Cells and Their Uses for Neural Regenerative Therapies." *International Journal of Molecular Sciences* 18, no. 2: 287.

Bayly-Jones, C., S. S. Pang, B. A. Spicer, J. C. Whisstock, and M. A. Dunstone. 2020. "Ancient but Not Forgotten: New Insights Into MPEG1, a Macrophage Perforin-Like Immune Effector." *Frontiers in Immunology* 11: 581906.

Biever, A., E. Valjent, and E. Puighermanal. 2015. "Ribosomal Protein S6 Phosphorylation in the Nervous System: From Regulation to Function." *Frontiers in Molecular Neuroscience* 8: 75.

Boruch, A. V., J. J. Conners, M. Pipitone, et al. 2001. "Neurotrophic and Migratory Properties of an Olfactory Ensheathing Cell Line." *Glia* 33: 225–229.

Brenneman, K. A., D. F. Meleason, M. Sar, et al. 2002. "Olfactory Mucosal Necrosis in Male CD Rats Following Acute Inhalation Exposure to Hydrogen Sulfide: Reversibility and the Possible Role of Regional Metabolism." *Toxicologic Pathology* 30: 200–208.

Burd, G. D. 1991. "Development of the Olfactory Nerve in the African Clawed Frog, *Xenopus Laevis*: I. Normal Development." *Journal of Comparative Neurology* 304: 123–134.

Burd, G. D. 1992. "Development of the Olfactory Nerve in the Clawed Frog, *Xenopus Laevis*: II. Effects of Hypothyroidism." *Journal of Comparative Neurology* 315: 255–263.

Cervino, A. S., D. A. Paz, and J. L. Frontera. 2017. "Neuronal Degeneration and Regeneration Induced by Axotomy in the Olfactory Epithelium of Xenopus laevis." *Developmental Neurobiology* 77: 1308–1320.

Chen, D., W. Zhang, C. Zuo, Y. Xu, and L. Fu. 2025 "Immune Characteristics of Olfactory Ensheathing Cells and Repair of Nerve Injury." *Frontiers in Immunology* 16: 1571573.

Chen, S., C. M. Atkins, C. L. Liu, O. F. Alonso, W. D. Dietrich, and B. R. Hu. 2007. "Alterations in Mammalian Target of Rapamycin Signaling Pathways After Traumatic Brain Injury." *Journal of Cerebral Blood Flow and Metabolism* 27: 939–949.

Cheng, F., Y. Shen, P. Mohanasundaram, et al. 2016. "Vimentin Coordinates Fibroblast Proliferation and Keratinocyte Differentiation in Wound Healing via TGF-β-Slug Signaling." *Proceedings of the National Academy of Sciences of the United States of America* 113: E4320–E4327.

Chuah, M. I., and C. Au. 1991. "Olfactory Schwann Cells Are Derived From Precursor Cells in the Olfactory Epithelium." *Journal of Neuroscience Research* 29: 172–180.

Chuah, M. I., and A. K. West. 2002. "Cellular and Molecular Biology of Ensheathing Cells." *Microscopy Research and Technique* 58: 216–227.

Daston, M. M., G. D. Adamek, and R. C. Gesteland. 1990. "Ultrastructural Organization of Receptor Cell Axons in Frog Olfactory Nerve." *Brain Research* 537: 69–75.

Deckner, M. L., M. Risling, and J. Frisén. 1997. "Apoptotic Death of Olfactory Sensory Neurons in the Adult Rat." *Experimental Neurology* 143: 132–140.

Denaro, S., S. D'Aprile, C. Alberghina, et al. 2022. "Neurotrophic and Immunomodulatory Effects of Olfactory Ensheathing Cells as a Strategy for Neuroprotection and Regeneration." *Frontiers in Immunology* 13: 1098212.

Docampo-Seara, A., E. Candal, and M. A. Rodríguez. 2022. "Study of the Glial Cytoarchitecture of the Developing Olfactory Bulb of a Shark Using Immunochemical Markers of Radial Glia." *Brain Structure & Function* 227: 1067–1082.

Doucette, R. 1993. "Glial Progenitor Cells of the Nerve Fiber Layer of the Olfactory Bulb: Effect of Astrocyte Growth Media." *Journal of Neuroscience Research* 35: 274–287.

Ekberg, J. A. K., D. Amaya, A. Mackay-Sim, and J. A. St John. 2012. "The Migration of Olfactory Ensheathing Cells During Development and Regeneration." *Neurosignals* 20: 147–158.

Ekberg, J. A. K., and J. A. St John. 2014. "Crucial Roles for Olfactory Ensheathing Cells and Olfactory Mucosal Cells in the Repair of Damaged Neural Tracts." *Anatomical Record (Hoboken)* 297: 121–128.

Ellett, F., L. Pase, J. W. Hayman, A. Andrianopoulos, and G. J. Lieschke. 2011. "mpeg1 Promoter Transgenes Direct Macrophage-Lineage Expression in Zebrafish." *Blood* 117: e49–e56.

Ferrero, G., E. Gomez, S. Lyer, et al. 2020. "The Macrophage-Expressed Gene (Mpeg) 1 Identifies a Subpopulation of B Cells in the Adult Zebrafish." *Journal of Leukocyte Biology* 107: 431–443.

Forni, P. E., C. Taylor-Burds, V. S. Melvin, T. Williams, and S. Wray. 2011. "Neural Crest and Ectodermal Cells Intermix in the Nasal Placode to Give Rise to GnRH-1 Neurons, Sensory Neurons, and Olfactory Ensheathing Cells." *Journal of Neuroscience* 31: 6915–6927.

Franceschini, I. A., and S. C. Barnett. 1996. "Low-Affinity NGF-Receptor and E-N-CAM Expression Define Two Types of Olfactory Nerve Ensheathing Cells That Share a Common Lineage." *Developmental Biology* 173: 327–343.

Gressner, A. M., and I. G. Wool. 1976. "Influence of Glucagon and Cyclic Adenosine 3′:5′-Monophosphate on the Phosphorylation of Rat Liver Ribosomal Protein S6." *Journal of Biological Chemistry* 251: 1500–1504.

Hassenklöver, T., and I. Manzini. 2014. "The Olfactory System as a Model to Study Axonal Growth Patterns and Morphology in Vivo." *Journal of Visualized Experiments* 92: e52143.

Hawkins, S. J., Y. Gärtner, T. Offner, et al. 2024. "The Olfactory Network of Larval *Xenopus Laevis* Regenerates Accurately After Olfactory Nerve Transection." *European Journal of Neuroscience* 60: 3719–3741.

Hawkins, S. J., L. Weiss, T. Offner, K. Dittrich, T. Hassenklöver, and I. Manzini. 2017. "Functional Reintegration of Sensory Neurons and Transitional Dendritic Reduction of Mitral/Tufted Cells During Injury-Induced Recovery of the Larval *Xenopus* Olfactory Circuit." *Frontiers in Cellular Neuroscience* 11: 380.

Higginson, J. R., and S. C. Barnett. 2011. "The Culture of Olfactory Ensheathing Cells (OECs)—A Distinct Glial Cell Type." *Experimental Neurology* 229: 2–9.

Hsueh, Y.-H., K.-P. Chen, W. Buddhakosai, et al. 2024. "Secretome of the Olfactory Ensheathing Cells Influences the Behavior of Neural Stem Cells." *International Journal of Molecular Sciences* 26, no. 1: 281.

Huang, H.-Y., M.-J. Xiong, F.-Q. Pu, J.-X. Liao, F.-Q. Zhu, and W.-J. Zhang. 2024. "Application and Challenges of Olfactory Ensheathing Cells in Clinical Trials of Spinal Cord Injury." *European Journal of Pharmacology* 963: 176238.

Huang, Q., S. Zhao, A. Gaudin, B. Quennedey, and J. Gascuel. 2005. "Glial Fibrillary Acidic Protein and Vimentin Expression in the Frog Olfactory System During Metamorphosis." *Neuroreport* 16: 1439–1442.

Huang, Z., Y. Wang, L. Cao, et al. 2008. "Migratory Properties of Cultured Olfactory Ensheathing Cells by Single-Cell Migration Assay." *Cell Research* 18: 479–490.

Hume, D. A., V. H. Perry, and S. Gordon. 1983. "Immunohistochemical Localization of a Macrophage-Specific Antigen in Developing Mouse Retina: Phagocytosis of Dying Neurons and Differentiation of Microglial Cells to Form a Regular Array in the Plexiform Layers." *Journal of Cell Biology* 97: 253–257.

Ibanez, C., D. Ito, M. Zawadzka, N. D. Jeffery, and R. J. M. Franklin. 2007. "Calponin Is Expressed by Fibroblasts and Meningeal Cells But Not Olfactory Ensheathing Cells in the Adult Peripheral Olfactory System." *Glia* 55: 144–151.

Ivaska, J., H.-M. Pallari, J. Nevo, and J. E. Eriksson. 2007. "Novel Functions of Vimentin in Cell Adhesion, Migration, and Signaling." *Experimental Cell Research* 313: 2050–2062.

Katoh, H., S. Shibata, K. Fukuda, et al. 2011. "The Dual Origin of the Peripheral Olfactory System: Placode and Neural Crest." *Molecular Brain* 4: 34.

Key, B., and J. St John. 2002. "Axon Navigation in the Mammalian Primary Olfactory Pathway: Where to Next?" *Chemical Senses* 27: 245–260.

Knight, Z. A., K. Tan, K. Birsoy, et al. 2012. "Molecular Profiling of Activated Neurons by Phosphorylated Ribosome Capture." *Cell* 151: 1126–1137.

Kreutzberg, G. W., and G. W. Gross. 1977. "General Morphology and Axonal Ultrastructure of the Olfactory Nerve of the Pike, *Esox lucius*." *Cell and Tissue Research* 181: 443–457.

Lara, J., C. Mastela, M. Abd, L. Pitstick, and R. Ventrella. 2024. "Tail Tales: What We Have Learned About Regeneration From Xenopus Laevis Tadpoles." *International Journal of Molecular Sciences* 25, no. 21: 11597.

Lazzari, M., S. Bettini, and V. Franceschini. 2013. "Immunocytochemical Characterization of Olfactory Ensheathing Cells in Fish." *Brain Structure & Function* 218: 539–549.

Lazzari, M., S. Bettini, and V. Franceschini. 2014. "Immunocytochemical Characterisation of Olfactory Ensheathing Cells of Zebrafish." *Journal of Anatomy* 224: 192–206.

Lazzari, M., S. Bettini, and V. Franceschini. 2016. "Immunocytochemical Characterisation of Ensheathing Glia in the Olfactory and Vomeronasal Systems of Ambystoma Mexicanum (Caudata: Ambystomatidae)." *Brain Structure & Function* 221: 955–967.

Lendahl, U., L. Muhl, and C. Betsholtz. 2022. "Identification, Discrimination and Heterogeneity of Fibroblasts." *Nature Communications* 13: 3409.

Li, Y., P. M. Field, and G. Raisman. 1998. "Regeneration of Adult Rat Corticospinal Axons Induced by Transplanted Olfactory Ensheathing Cells." *Journal of Neuroscience* 18: 10514–10524.

Li, Y., P. M. Field, and G. Raisman. 2005. "Olfactory Ensheathing Cells and Olfactory Nerve Fibroblasts Maintain Continuous Open Channels for Regrowth of Olfactory Nerve Fibres." *Glia* 52: 245–251.

Li, Y., D. Li, P. T. Khaw, and G. Raisman. 2008. "Transplanted Olfactory Ensheathing Cells Incorporated Into the Optic Nerve Head Ensheathe Retinal Ganglion Cell Axons: Possible Relevance to Glaucoma." *Neuroscience Letters* 440: 251–254.

Mackay-Sim, A. 2005. "Olfactory Ensheathing Cells and Spinal Cord Repair." *Keio Journal of Medicine* 54: 8–14.

Manzini, I. 2015. "From Neurogenesis to Neuronal Regeneration: The Amphibian Olfactory System as a Model to Visualize Neuronal Development: In Vivo." *Neural Regeneration Research* 10: 872.

Manzini, I., D. Schild, and C. Di Natale. 2022. "Principles of Odor Coding in Vertebrates and Artificial Chemosensory Systems." *Physiological Reviews* 102: 61–154.

Meyuhas, O. 2008. "Physiological Roles of Ribosomal Protein S6: One of Its Kind." *International Review of Cell and Molecular Biology* 268: 1–37.

Meyuhas, O. 2015. "Ribosomal Protein S6 Phosphorylation: Four Decades of Research." In *Int rev Cell mol Biol*, vol. 320, 41–73. Academic Press.

Moreno-Flores, M. T., J. Díaz-Nido, F. Wandosell, and J. Avila. 2002. "Olfactory Ensheathing Glia: Drivers of Axonal Regeneration in the Central Nervous System?" *Journal of Biomedicine & Biotechnology* 2: 37–43.

Nakajima, M., M. Tsuruta, H. Mori, C. Nishikawa, S. Okuyama, and Y. Furukawa. 2013. "A Comparative Study of Axon-Surrounding Cells in the Two Nasal Nerve Tracts From Mouse Olfactory Epithelium and Vomeronasal Organ." *Brain Research* 1503: 16–23.

Napoli, I., and H. Neumann. 2009. "Microglial Clearance Function in Health and Disease." *Neuroscience* 158: 1030–1038.

Nazareth, L., K. E. Lineburg, M. I. Chuah, et al. 2015. "Olfactory Ensheathing Cells Are the Main Phagocytic Cells That Remove Axon Debris During Early Development of the Olfactory System." *Journal of Comparative Neurology* 523: 479–494.

Nezlin, L. P., S. Heermann, D. Schild, and W. Rössler. 2003. "Organization of Glomeruli in the Main Olfactory Bulb of *Xenopus Laevis* Tadpoles." *Journal of Comparative Neurology* 464: 257–268.

Nieuwkoop, P. D., and J. Faber. 1994. *Normal Table of Xenopus Laevis (Daudin): A Systematical and Chronological Survey of the Development From the Fertilized Egg Till the End of Metamorphosis*. New York: Garland Pub.

Oprych, K., D. Cotfas, and D. Choi. 2017. "Common Olfactory Ensheathing Glial Markers in the Developing Human Olfactory System." *Brain Structure & Function* 222: 1877–1895.

Pellitteri, R., M. Spatuzza, S. Stanzani, and D. Zaccheo. 2010. "Biomarkers Expression in Rat Olfactory Ensheathing Cells." *Frontiers in Bioscience (Scholar Edition)* 2: 289–298.

Pende, M., S. H. Um, V. Mieulet, et al. 2004. "S6K1(−/−)/S6K2(−/−) Mice Exhibit Perinatal Lethality and Rapamycin-Sensitive 5′-Terminal Oligopyrimidine mRNA Translation and Reveal a Mitogen-Activated Protein Kinase-Dependent S6 Kinase Pathway." *Molecular and Cellular Biology* 24: 3112–3124.

Perera, S. N., R. M. Williams, R. Lyne, et al. 2020. "Insights Into Olfactory Ensheathing Cell Development From a Laser-Microdissection and Transcriptome-Profiling Approach." *Glia* 68: 2550–2584.

Pingault, V., V. Bodereau, V. Baral, et al. 2013. "Loss-Of-Function Mutations in SOX10 Cause Kallmann Syndrome With Deafness." *American Journal of Human Genetics* 92: 707–724.

Plikus, M. V., X. Wang, S. Sinha, et al. 2021. "Fibroblasts: Origins, Definitions, and Functions in Health and Disease." *Cell* 184: 3852–3872.

Quintana-Urzainqui, I., I. Rodríguez-Moldes, and E. Candal. 2014. "Developmental, Tract-Tracing and Immunohistochemical Study of the Peripheral Olfactory System in a Basal Vertebrate: Insights on Pax6 Neurons Migrating Along the Olfactory Nerve." *Brain Structure & Function* 219: 85–104.

Raisman, G. 2001. "Olfactory Ensheathing Cells - Another Miracle Cure for Spinal Cord Injury?" *Nature Reviews. Neuroscience* 2: 369–375.

Ramón-Cueto, A., and J. Avila. 1998. "Olfactory Ensheathing Glia: Properties and Function." *Brain Research Bulletin* 46: 175–187.

Rawji, K. S., S. X. Zhang, Y.-Y. Tsai, L. J. Smithson, and M. D. Kawaja. 2013. "Olfactory Ensheathing Cells of Hamsters, Rabbits, Monkeys, and Mice Express α-Smooth Muscle Actin." *Brain Research* 1521: 31–50.

Ring, N. A. R., H. Dworak, B. Bachmann, et al. 2023. "The p-rpS6-Zone Delineates Wounding Responses and the Healing Process." *Developmental Cell* 58: 981–992.e6.

Roet, K. C. D., and J. Verhaagen. 2014. "Understanding the Neural Repair-Promoting Properties of Olfactory Ensheathing Cells." *Experimental Neurology* 261: 594–609.

Russo, C., M. Patanè, N. Vicario, et al. 2020. "Olfactory Ensheathing Cells Express Both Ghrelin and Ghrelin Receptor in Vitro: A New Hypothesis in Favor of a Neurotrophic Effect." *Neuropeptides* 79: 101997.

Ruvinsky, I., and O. Meyuhas. 2006. "Ribosomal Protein S6 Phosphorylation: From Protein Synthesis to Cell Size." *Trends in Biochemical Sciences* 31: 342–348.

Schindelin, J., I. Arganda-Carreras, E. Frise, et al. 2012. "Fiji: An Open-Source Platform for Biological-Image Analysis." *Nature Methods* 9: 676–682.

Schwob, J. E. 2002. "Neural Regeneration and the Peripheral Olfactory System." *Anatomical Record* 269: 33–49.

Schwob, J. E., N. B. Farber, and D. I. Gottlieb. 1986. "Neurons of the Olfactory Epithelium in Adult Rats Contain Vimentin." *Journal of Neuroscience* 6: 208–217.

Sliogeryte, K., and N. Gavara. 2019. "Vimentin Plays a Crucial Role in Fibroblast Ageing by Regulating Biophysical Properties and Cell Migration." *Cells* 8, no. 10: 116.

Sonigra, R. J., P. C. Brighton, J. Jacoby, S. Hall, and C. B. Wigley. 1999. "Adult rat Olfactory Nerve Ensheathing Cells Are Effective Promoters of Adult Central Nervous System Neurite Outgrowth in Coculture." *Glia* 25: 256–269.

Su, Z., J. Chen, Y. Qiu, et al. 2013. "Olfactory Ensheathing Cells: The Primary Innate Immunocytes in the Olfactory Pathway to Engulf Apoptotic Olfactory Nerve Debris." *Glia* 61: 490–503.

Su, Z., and C. He. 2010. "Olfactory Ensheathing Cells: Biology in Neural Development and Regeneration." *Progress in Neurobiology* 92: 517–532.

Tallquist, M. D., and J. D. Molkentin. 2017. "Redefining the Identity of Cardiac Fibroblasts." *Nature Reviews Cardiology* 14: 484–491.

Taylor, P. R., L. Martinez-Pomares, M. Stacey, H.-H. Lin, G. D. Brown, and S. Gordon. 2005. "Macrophage Receptors and Immune Recognition." *Annual Review of Immunology* 23: 901–944.

Terni, B., P. Pacciolla, H. Masanas, P. Gorostiza, and A. Llobet. 2017. "Tight Temporal Coupling Between Synaptic Rewiring of Olfactory Glomeruli and the Emergence of Odor-Guided Behavior in *Xenopus* Tadpoles." *Journal of Comparative Neurology* 525: 3769–3783.

Valverde, F., M. Santacana, and M. Heredia. 1992. "Formation of an Olfactory Glomerulus: Morphological Aspects of Development and Organization." *Neuroscience* 49: 255–275.

van den Pol, A. N., and J. G. Santarelli. 2003. "Olfactory Ensheathing Cells: Time Lapse Imaging of Cellular Interactions, Axonal Support, Rapid Morphologic Shifts, and Mitosis." *Journal of Comparative Neurology* 458: 175–194.

Wei, L., and E. C. Lai. 2022. "Regulation of the Alternative Neural Transcriptome by ELAV/Hu RNA Binding Proteins." *Frontiers in Genetics* 13: 848626.

Weiss, L., T. Offner, T. Hassenklöver, and I. Manzini. 2018. "Dye Electroporation and Imaging of Calcium Signaling in Xenopus Nervous System." In *Xenopus*, edited by K. Vleminckx, 217–231. Springer New York.

Werner, S., and E. Nies. 2018. "Olfactory Dysfunction Revisited: A Reappraisal of Work-Related Olfactory Dysfunction Caused by Chemicals." *Journal of Occupational Medicine and Toxicology* 13: 28.

Woodhall, E., A. K. West, and M. I. Chuah. 2001. "Cultured Olfactory Ensheathing Cells Express Nerve Growth Factor, Brain-Derived Neurotrophic Factor, Glia Cell Line-Derived Neurotrophic Factor and Their Receptors." *Brain Research Molecular Brain Research* 88: 203–213.

Wool, I. G., Y. L. Chan, and A. Glück. 1995. "Structure and Evolution of Mammalian Ribosomal Proteins." *Biochemistry and Cell Biology* 73: 933–947.

Wright, A. A., M. Todorovic, M. Murtaza, J. A. St John, and J. A. Ekberg. 2020. "Macrophage Migration Inhibitory Factor and Its Binding Partner HTRA1 Are Expressed by Olfactory Ensheathing Cells." *Molecular and Cellular Neurosciences* 102: 103450.

Yang, L.-N., W.-K. Huang, X.-L. Li, Y.-Z. Bai, and S.-C. Zhang. 2020. "Sox10 Is a Specific Biomarker for Neural Crest Stem Cells in Immunohistochemical Staining in Wistar Rats." *Disease Markers* 2020: 8893703–8893707.

Yao, R., M. Murtaza, J. T. Velasquez, et al. 2018. "Olfactory Ensheathing Cells for Spinal Cord Injury: Sniffing Out the Issues." *Cell Transplantation* 27: 879–889.

Zhang, L.-P., J.-X. Liao, Y.-Y. Liu, H.-L. Luo, and W.-J. Zhang. 2023. "Potential Therapeutic Effect of Olfactory Ensheathing Cells in Neurological Diseases: Neurodegenerative Diseases and Peripheral Nerve Injuries." *Frontiers in Immunology* 14: 1280186.

Zhang, Y. E. 2017. "Non-Smad Signaling Pathways of the TGF-β Family." *Cold Spring Harbor Perspectives in Biology* 9, no. 2: a022129.

Supporting Information

Additional supporting information can be found online in the Supporting Information section. **Supporting Figure S1:** Phosphorylated rpS6-positive olfactory ensheathing cells ensheathe bundles of olfactory receptor neuron axons. **Supporting Figure S2:** Vimentin- and phosphorylated rpS6-positive cells in the non-transected olfactory nerve and olfactory bulb. **Supporting Figure S3:** Co-localization of HuC/D and phosphorylated rpS6 in the olfactory bulb after transection of the olfactory nerve.

6 General discussion

6.1 S100Z expression in the olfactory system of larval and adult *Xenopus laevis*

The distribution of calcium-binding proteins in the olfactory system (OS) of *Xenopus laevis* remains poorly characterized. To address this, a detailed analysis of S100Z expression was conducted. My results revealed that a subpopulation of ORNs in the main OS expresses S100Z. Using immunohistochemistry and distribution analysis of S100Z expressing cells, I found that S100Z-expressing ORNs were located more laterally in the OE and the axons of these cells projected exclusively into the lateral and intermediate glomerular clusters of the main OB. In postmetamorphic frogs, the S100Z expression was restricted to the middle cavity (MC) of the MOE and the axonal projection into the ventro-lateral OB persisted. This pattern aligns with previous findings on ancestral V2R-expressing neurons in *Xenopus laevis* (Gliem *et al.*, 2013; Syed *et al.*, 2013, 2017). Notably, S100Z is exclusive to the main OS in *Xenopus*, whereas in mammals, it is associated with the VNO (Hecker *et al.*, 2019). These findings highlight how OS adaptations are influenced by ecological factors such as terrestrial or aquatic environments (Kishida, 2021; Weiss, Manzini, *et al.*, 2021).

6.1.1 Expression of calcium-binding protein S100 in neurons in the OS

Calcium (Ca^{2+}) is a versatile intracellular secondary messenger that regulates numerous cellular processes (Berridge *et al.*, 2003; Elíes *et al.*, 2020). Since Ca^{2+} overload can be cytotoxic, a homeostatic system maintains ionic balance (Elíes *et al.*, 2020). A wide range of molecular components, including calcium-binding proteins (CBPs), play a key role in Ca^{2+} homeostasis and regulate various signaling pathways (Carafoli *et al.*, 2001; Elíes *et al.*, 2020). A characteristic of many CBPs is an EF-hand calcium-binding motif, which binds Ca^{2+} and regulates target proteins through conformational changes (Chazin, 2011; Zimmer *et al.*, 2013; Gonzalez *et al.*, 2020). With more than 20 currently known members, the S100 proteins build the mayor family of the EF-hand superfamily and are exclusive to vertebrates (Gonzalez *et al.*, 2020). They mediate intra- and extracellular regulatory functions, influencing target cells through paracrine and autocrine signaling (Donato *et al.*, 2013; Donato, 2001; Gonzalez *et al.*, 2020). Following Ca^{2+}-binding, S100 proteins undergo conformational changes that enable interactions with target proteins, including receptors and other S100 members (Van de Graaf *et al.*, 2003; Chazin, 2011; Ozorowski *et al.*, 2013; Wafer *et al.*, 2013; Zimmer *et al.*, 2013). Each S100 family member exhibits a unique expression pattern across different tissues and cell types (Gonzalez *et al.*, 2020), and directly modulates ion channels in neurons, shaping neuronal activity (Hermann *et al.*, 2012).

S100 protein expression has been demonstrated in the OS of various species (Hansen & Finger, 2000; Hansen & Zielinski, 2005; Hecker *et al.*, 2019; Korsching, 2020). In fish, crypt cells within the olfactory rosette are characterized by their distinct morphology and S100

immunoreactivity (Hansen & Finger, 2000; Hansen & Zielinski, 2005; Korsching, 2020). In Zebrafish, crypt cells express a single ORA- (V1R-like) gene and project to a single mediodorsal glomerulus in the OB (Ahuja *et al.*, 2013). Furthermore, some microvillous ORNs were also labelled by using the common S100 antibody to label crypt cells (Germanà *et al.*, 2004; Oka *et al.*, 2012). S100 immunoreactivity has also been detected in sensory cells of amphibians like *Rana catesbeiana* (Miwa & Kawamura, 2003) and *Xenopus laevis* (Kerschbaum & Hermann, 1992), as well as in newly formed ORNs of rats (Sicard *et al.*, 1998) and the OS of rodents in general (Hecker *et al.*, 2019). Prior to my research, our group undertook large-scale RNA sequencing experiments on the OS of *Xenopus laevis* larvae. These experiments revealed an increase in the expression of the calcium-binding protein S100Z, a less well-characterized member of the S100 family. Although its function in the OS remains unclear, existing data suggest an important role in olfactory processes.

6.1.2 A lateral subpopulation of ORNs in *Xenopus laevis* main OS expresses S100Z

In larval zebrafish, *s100z* expression is restricted to the olfactory placode and a subpopulation of cells, most likely neurons (Kraemer *et al.*, 2008). In adults, it is present in ORN-containing regions of the olfactory organ (Dieris *et al.*, 2021). However, studies indicate that S100 antibody specificity in zebrafish is highly sensitive to sample preparation, leading to unintended labeling of microvillous-like cells (Oka *et al.*, 2012). Additionally, the commonly used bovine antibody may misidentify a non-S100 protein in crypt cells, which do not express *s100* genes, while correctly labeling S100Z in microvillous-like cells (Oka *et al.*, 2012; Ahuja *et al.*, 2013). The same antibody has been used to label ORNs in larval *Xenopus laevis* (Kerschbaum & Hermann, 1992), complicating the interpretation of earlier S100 expression studies in non-mammalian species. In mammals, *s100z* is associated with the VNO of the accessory OS (Hecker *et al.*, 2019).

Using a specific antibody raised against *Homo sapiens* S100Z, I identified a restricted population of S100Z expressing ORNs in the main OS of *Xenopus laevis* (Kahl *et al.*, 2024). Their cell bodies were distributed throughout the epithelium, consistent with Kerschbaum *et al.* (1992), who observed S100-immunoreactive material located at various depths in the epithelium of *Xenopus*. However, I found a lateral bias in the distribution of S100Z expressing ORNs in the main OE. Additionally, my findings suggest that their dendritic knobs possess microvilli. In postmetamorphic animals, I observed that S100Z expression was confined to the MC. Following metamorphic reorganization, the PC contains only ciliated ORNs, while the MC contains both ciliated and microvillous (Hansen *et al.*, 1998). It remains unclear whether S100Z is expressed by all microvillous ORNs in the main OE.

Furthermore, I observed that the axons of S100Z expressing ORNs nearly exclusively projected into the lateral glomerular cluster in the OB. *Xenopus laevis* larvae have two

prominent odor processing streams in their OS (Gliem *et al.*, 2013; Hawkins *et al.*, 2024). One stream consists of ciliated ORNs using a cAMP-dependent transduction cascade, which project their axons into the medial glomerular cluster in the OB and respond to odorants like ketones and aldehydes (Gliem *et al.*, 2009; Gliem *et al.*, 2013; Hawkins *et al.*, 2024; Manzini & Schild, 2010). The other stream consists of microvillous ORNs using a cAMP-independent, TRPC2-dependent pathway, projecting to the lateral glomerular cluster and responding to amino acids (Gliem *et al.*, 2013; Hawkins *et al.*, 2024; Lucas *et al.*, 2003; Manzini & Schild, 2010; Sansone *et al.*, 2014; Syed *et al.*, 2017).

In non-tetrapods without an anatomically separated VNO, TRPC2 is restricted to the MOE (Bear *et al.*, 2016). Microvillous ORNs in bony and cartilaginous fish express *trpc2* (Sato *et al.*, 2005; Syed *et al.*, 2023) In *Xenopus* larvae, TRPC2 expression is widespread in the MOE and VNO (Figure 5;Sansone, Syed, *et al.*, 2014). Following metamorphosis, TRPC2 remains only in the water-exposed MC and the VNO, but not in the air-exposed PC (Syed *et al.*, 2017). Interestingly, in *Xenopus laevis* different subfamilies of the V2R receptor genes are expressed by microvillous ORNs in the MOE and VNO. In larval *Xenopus* more ancestral *v2r* genes are restricted to the MOE, while in the VNO exclusive expression of later diverging *v2r* genes was observed (Syed *et al.*, 2013). During metamorphosis, the MOE changes into the PC (air-nose) and gradually stops expressing ancestral V2Rs. Their expression shifts to the basal layers of the developing MC (Syed *et al.*, 2017). Meanwhile, V1Rs are exclusively expressed in the main OS of *Xenopus* (Date-Ito *et al.*, 2008). Given this before mentioned patterns and my observations of S100Z expression, I hypothesize that S100Z is associated with microvillous ORNs expressing ancestral V2Rs and utilizing a cAMP-independent transduction pathway. This could be tested through *in situ* hybridization using probes against *trpc2*, *S100Z*, and selected *V1R* and *V2R* genes.

While V2Rs have been linked to amino acids detection, the function of S100Z-expressing ORNs remains unclear (DeMaria *et al.*, 2013; Syed *et al.*, 2017). In *Xenopus* larvae, amino acid-responsive ORNs using a PLC-dependent, cAMP-independent pathway show a lateral distribution in the OE, which is mirrored in the lateral glomerular clusters of the OB (Gliem *et al.*, 2013; Sansone *et al.*, 2014; Sansone, Syed *et al.*, 2014; Syed *et al.*, 2013). Given the lateralized expression of S100Z in the OB, it would be valuable to investigate whether S100Z-positive glomeruli are sensitive to amino acids.

Immunohistochemical studies of another anuran, *Rana catesbeiana*, revealed that a binding protein of S100 is localized in olfactory neuron cilia in the OE, indicating a role in olfactory transduction (Miwa & Kawamura, 2003). Based on this, I assume that S100Z may also be present in ORN microvilli and play a role in transduction, though its exact function remains unknown. However, CBPs are known to influence excitability of neurons, with some S100

proteins modulating electrical activity and interacting with ion- and ligand-gated channels (Kerschbaum & Hermann, 1992; Hermann *et al.*, 2012). S100 proteins experience a conformational shift after Ca^{2+} binding that permits interaction with target proteins (Van de Graaf *et al.*, 2003; Chazin, 2011; Hermann *et al.*, 2012; Ozorowski *et al.*, 2013; Wafer *et al.*, 2013; Zimmer *et al.*, 2013), including enzymes, cytoskeletal components, transcription factors, scaffolding proteins, unsaturated fatty acids, channels, receptors, signaling molecules, and toll-like receptor ligands (Donato *et al.*, 2013; Donato, 2003; Hermann *et al.*, 2012). Investigating S100Z's role in the OS could provide valuable insights into its function.

6.1.3 Different, partially overlapping distribution for calretinin and S100Z expressing ORNs

In the central nervous system of vertebrates, CBPs are often expressed in distinct neuronal populations and serve as molecular markers (Braubach *et al.*, 2012; Morona & González, 2013). In my research, I also examined calretinin, another CBP than S100Z, known to be expressed in OS neurons (Germanà *et al.*, 2007). While calretinin labels mature ORNs in fish and amphibians, its expression in embryonic mice is transient during neuronal maturation (Koide *et al.*, 2009; Braubach *et al.*, 2012; Wei *et al.*, 2013). Although a neuroprotective role in epileptic seizures has been suggested, its function in the OS remains unclear (Capsoni *et al.*, 2021; Qi *et al.*, 2022). In my study, most ORNs in the main and accessory OS were calretinin-positive and projected in nearly all glomerular clusters in the OB. However, no clear pattern of co-expression with S100Z was found in the OE or OB (Kahl *et al.*, 2024). This aligns with functional measurements showing that the glomerular odour map for amino acid odorants is not chemotopically or stereotypically organized in the *Xenopus* OB (Offner *et al.*, 2023). Thus, no clear pattern of co-expression with S100Z was found and calretinin expression cannot be linked to specific neuronal features or identities yet (also see Daume *et al.*, 2022).

In summary, CBPs may contribute to odorant signal transduction in *Xenopus laevis*. Functional studies on S100Z- and/ or calretinin-expressing cells could clarify its role in the OS. My findings indicate that S100Z serves as a valuable marker for immunohistochemical characterization of a distinct ORN subpopulation in larval and adult *Xenopus laevis*.

6.1.4 The lack of association of S100Z to the VNO of *Xenopus*

In the field of neurobiology, the original idea of the VNO as an exclusive pheromone detector, distinct from the odorant-sensitive main OE, has proven to be oversimplified (Eisthen, 1992, 1997; Weiss, Manzini, *et al.*, 2021). Studies show that the main OE can also detect social olfactory cues, and both the main and accessory OS perform partially overlapping, parallel functions (Mohrhardt *et al.*, 2018; Weiss, Manzini, *et al.*, 2021). Since the anatomically distinct VNO was only observed in terrestrial tetrapods and is absent in many secondarily aquatic tetrapods, it was originally thought to be an adaptation to life on land (Bertmar, 1981; Weiss,

Manzini, *et al.*, 2021). While this could explain the existence of the accessory OS in adult frogs, it does not explain its presence in aquatic larvae of amphibians or an primordial VNO in earlier diverging vertebrates, such as lungfish (Eisthen, 1992; González, 2010; Nakamuta *et al.*, 2012; Chang *et al.*, 2013; Weiss, Manzini, *et al.*, 2021). Indeed, tadpoles possess a functionally tuned MOE to detect waterborne stimuli (Figure 5; Manzini & Schild, 2010) as well as a well-developed VNO (Figure 5; Jungblut *et al.*, 2021; Weiss, Manzini, *et al.*, 2021). Furthermore, adult anurans maintain the VNO after metamorphosis in addition to another water nose, such as the MC in *Xenopus laevis* (Eisthen, 1997; Reiss & Eisthen, 2008; Dittrich *et al.* 2016; Weiss, Manzini *et al.* 2021). The precise functional distinction between the water nose and the adult frogs' water-filled VNO remains unclear (Weiss, Manzini, *et al.*, 2021). Molecular data suggest that the OS of amphibians represents a transitional state between the single olfactory epithelium in fish and the fully segregated mammalian OS. In *Xenopus laevis* V1Rs are exclusively expressed in the main OS, while V2Rs are found in the larval MOE and VNO, as well as in the adult MC and VNO (Date-Ito *et al.*, 2008; Hagino-Yamagishi *et al.*, 2004; Syed *et al.*, 2013, 2017).

The VNO and the AOB, the two main components of the accessory OS, are regressed in aquatic mammals, a number of bats, and primates (Hecker *et al.*, 2019). The CBP S100Z has been linked to the VNO in mammals (Hecker *et al.*, 2019). Unexpectedly I found no expression of S100Z in the pre- or postmetamorphic VNO of *Xenopus laevis* (Kahl *et al.*, 2024). Hecker *et al.* (2019) identified a parallel reduction of the accessory OS in *Catarrhini* (apes), *Cetacea* (whales, dolphins, and porpoises), *Chiroptera* (bats), and manatees (*Trichechus manatus*), coinciding with the convergent inactivation of *s100z*, the transduction channel *trpc2*, the aldehyde oxidase *Aox2* involved in the odorant degradation, and the uncharacterized *MsInl*. In semi-aquatic mammals, such as otters and phocid seals, a reduced accessory OS is expected if these genes are deactivated (Hecker *et al.*, 2019).

OS evolution is influenced by ecological factors, including habitat (Hecker *et al.*, 2019; Kishida, 2021; Weiss, Manzini, *et al.*, 2021; Burguera *et al.*, 2023). Vertebrates frequently prioritize certain OS components over others, which can result in either increased or decreased expression of specific olfactory receptor genes (Taniguchi & Taniguchi, 2014; Bear *et al.*, 2016; Kishida, 2021). During the transition from aquatic to terrestrial life, the number of OR-type genes fluctuated (Niimura, 2009). In mammals, birds, and reptiles, class II OR-type genes increased while class I genes, which primarily detect water-soluble compounds, declined (Saito *et al.*, 2009). In contrast, amphibians, adapted to both environments, retain both OR types (Niimura, 2009). Based on these findings and my results, that S100Z is not associated with the VNO in *Xenopus laevis*, I hypothesize that S100Z expression may represent an adaptive response to the species' habitat.

All in all, my findings indicate that in non-mammalian species, S100Z expression is not directly associated with the VNO, making it an unreliable marker for VNO reduction or the molecular machinery associated with it. Further investigation into S100Z expression across non-mammalian vertebrates, particularly in species with OS reductions, would be interesting (Kahl *et al.*, 2024).

6.2 Organization of the olfactory nerve

Immunohistochemical identification of the cellular composition of the olfactory nerve (ON) of larval *Xenopus laevis* has not yet been thoroughly described and thus a detailed ultrastructural analysis was undertaken. My analysis identified three different non-neuronal cell-types; macrophages, fibroblasts and OECs, consistent with findings in rodents (Li *et al.*, 2005; Wright, 2020). In *Xenopus*, as well as in rodents, ORNs from the OE project their axons into the OB in the forebrain (Nezlin & Schild, 2000; Eisthen & Polese, 2007). Bundled ORN axons of larval *Xenopus laevis* form ON fascicles, which are ensheathed by OECs (Kahl et al. 2025). Unlike in rodents where fibroblasts ensheathe nerve fascicles (Li *et al.*, 2005), fibroblasts in *Xenopus* surround the whole ON (Kahl *et al*., 2005). Also macrophages were found solely on the outside of the ON and were not present on the surface of individual nerve fascicles like in rodents (Li *et al.*, 2005; Wright *et al.* 2020; Kahl *et al.*, 2025). Single-cell electroporation in the ON revealed two different morphologies of putative OECs: bipolar fusiform and flat-sheet like, also consistent with *in vivo* and *in vitro* observations in rodents (Barnett & Chang, 2004). Using transgenic *Xenopus* lines, immunohistochemistry, and multiphoton-microscopy I found transient activation via phosphorylated ribosomal protein S6 235/236 in these non-neuronal cells after ON transection. This demonstrates that the cellular composition of the larval *Xenopus laevis* ON is structurally similar to that of other vertebrates, with non-neuronal cells also influenced by ON injury. Thus, *Xenopus laevis* is a suitable model for studying non-neuronal cell characteristics during vertebrate regeneration.

6.2.1 Identification of olfactory ensheathing cells in *Xenopus laevis* is difficult due to lack of specific markers

Throughout life the OS has a unique neurogenic niche in which ORNs are replaced (Murtaza *et al.*, 2022). Due to the olfactory neuroepithelium's exposure to the external environment there is a continuous turnover of ORNs. Newly generated ORNs are supported and guided by OECs, a unique type of glia cells. In human and mouse brain , glial cells, comprising about half of the central nervous system cells (Von Bartheld *et al.*, 2016; Allen & Lyons, 2018), regulate neurogenesis, axon development, neuronal migration, synapse formation, and circuit function (Allen & Lyons, 2018). OECs are found in the periphery in the lamina propia beneath the olfactory mucosa and encircle the axons of ORNs from the OE to the nerve fibre layer of the OB (Chuah & West, 2002; Graziadei & Graziadei, 1979a,b; Murtaza *et al.*, 2022). They share morphological and molecular characteristics with Schwann cells and astrocytes (Beiersdorfer

et al., 2020; Lakatos *et al.*, 2000; Murtaza *et al.*, 2022; Nazareth *et al.*, 2019), but can be distinguished by their marker protein expression and response to stimuli (Moreno-Flores *et al.*, 2002).

OECs provide structural support and migrate alongside newly forming olfactory axons to facilitate neuronal regeneration (Doucette, 1990; Ekberg *et al.*, 2012; Tennent & Chuah, 1996). They are also considered key innate immune cells of the OS, capable of transitioning from a resting to a phagocytic state to clear axonal debris and bacteria (Murtaza *et al.*, 2022; Nazareth, Lineburg, *et al.*, 2015; Nazareth *et al.*, 2015; Su *et al.*, 2013). Due to the diverse biological functions, OECs are being investigated for nervous system repair, particularly in spinal cord injury, with promising but variable outcomes in humans and animals (Reshamwala *et al.*, 2020; Murtaza *et al.*, 2022). However, the absence of specific OEC markers remains a major challenge in the field (Ekberg *et al.*, 2012; Reshamwala *et al.*, 2020).

OECs express various markers both *in vitro* and *in vivo*, but their overlap with other cell types, such as fibroblasts, complicates clear identification (Au & Roskams, 2003; Oprych *et al.*, 2017; Yao *et al.*, 2018). Rodent studies commonly use p75NTR, GFAP, S100β, vimentin, and nestin for OEC identification, while fibronectin and Thy-1 serve as negative selection markers for fibroblasts (Au & Roskams, 2003; Oprych *et al.*, 2017; Reshamwala *et al.*, 2020). Additional markers like Sox10 have been used in some mammalian studies (Barraud *et al.*, 2010; Ingram *et al.*, 2016; Oprych *et al.*, 2017), but none are OEC-specific (Barnett & Chang, 2004; Pellitteri *et al.*, 2010; Higginson & Barnett, 2011; Lazzari *et al.*, 2014). While research on mammalian OECs has expanded, their cellular characteristics, function, and specific markers remain poorly understood in non-mammalian vertebrates (Lazzari *et al.*, 2016). However, studies in fish and amphibians suggest that conventional mammalian OEC markers can also be applied to these species (Huang *et al.*, 2005; Lazzari *et al.*, 2013, 2014, 2016; Quintana-Urzainqui *et al.*, 2014; Docampo-Seara *et al.*, 2022).

In the course of my work, immunostainings using antibodies against GFAP, S100, p75NTR and the transgenic *Sox10 Xenopus* line did not yield any specific OEC staining in the OS of *Xenopus laevis* larvae. By using a specific *Xenopus*-vimentin antibody I found vimentin expressing cells with different morphologies in the ON and OB of *Xenopus laevis* larvae. The OB's long radial cells were highly specific to radial glia in both location and morphology. Radial glial cells are precursor cells of the central nervous system producing most neurons and glia, either directly or via intermediate progenitors (Allen & Lyons, 2018). In addition radial glia escort extending cells and send processes from the lateral ventricles to the OB (Nezlin *et al.*, 2003; Allen & Lyons, 2018). Using a different vimentin antibody than I did, Huang *et al.* (2005) found that the central regions of the OB in *Xenopus* larvae had the same distribution of vimentin-positive cells. Moreover vimentin-immunopositivity was observed in the glomerular

and ON layer of the goldfish (*Carassius auratus*; Lazzari *et al.*, 2013) and in radial glia in the urodele *Triturus carnifex* (Lazzari *et al.*, 1997). Additionally, to the observed vimentin-expressing radial glia in the OB of *Xenopus*, I found vimentin expressing cells in the ON, which had a long bipolar fusiform morphology and ensheathed bundles of ORN axons throughout the whole ON until reaching the OB (Kahl *et al.,* 2025). Vimentin was mostly expressed in the cells' filamentous and cytoskeletal components. All of the before mentioned observations of vimentin-expressing cells in *Xenopus* larvae's ON are highly specific to OECs, which let me assume that these cells are OECs. I cannot be completely certain that all of the vimentin-positive cells in the ON shown in this work are OECs because of their similarities to other cells, such as the morphology and location of fibroblasts superficially of the ON. Moreover, vimentin is also frequently used as a marker to label cellular activities in cultured mouse cardiac or human and mouse dermal fibroblasts (Cheng *et al.*, 2016; Tallquist & Molkentin, 2017; Sliogeryte & Gavara, 2019). In summary, vimentin does not exclusively identify OECs in *Xenopus laevis* larvae, but can be used to label at least a high number of cells which resemble the typical OEC morphology in the ON.

6.2.2 The cellular composition and spatial distribution of OECs, macrophages and fibroblasts in the ON of *Xenopus laevis* larvae has similarities with findings in rodents

In the ON of rodents OECs create channel-like structures, which offer excellent structural support for extending axons (Li *et al.*, 2005; Nazareth *et al.*, 2019; Wright *et al.*, 2020). Similarly, in *Xenopus*, I found vimentin expressing OECs enwrapping ORN axon bundles and building a channel like structure in both intact and transected ONs. Fibroblasts of rodents ensheathe nerve fascicles (Li *et al.*, 2005), while fibronectin-expressing fibroblasts in *Xenopus laevis* create an outer perineurial-like layer (Kahl *et al.*, 2025). Macrophages are located solely on the surface of the ON in *Xenopus laevis* larvae, while in mice a small number of macrophages are present on the surface of individual nerve fascicles (Wright *et al.*, 2020). Both, OECs and fibroblasts of mice express macrophage migration inhibitory factor, which causes in co-culture a segregation between OECs and macrophage cell line (Wright *et al.*, 2020). The absence of macrophages from ON fascicles is thought to be caused in part by the macrophage migration inhibitory factor (Wright *et al.*, 2020). OECs of rodents are responsible of removing ORN axonal debris during the olfactory systems natural turnover and following injury (Nazareth, Lineburg, *et al.*, 2015, Su *et al.*, 2013) and can phagocytose bacteria (Vincent *et al.*, 2007; Leung *et al.*, 2008; Herbert *et al.*, 2012; Panni *et al.*, 2013). OECs are therefore the main phagocytes of ON fascicles rather than macrophages. They also show the ability to phagocytose significant amounts of axonal debris both *in vivo* and *in vitro*; a function that is probably essential for regeneration (He *et al.*, 2014; Nazareth, Lineburg, *et al.*, 2015; Su *et al.*, 2013; Wright *et al.*, 2020). Whether *Xenopus* OECs perform similar functions during natural

turnover and after injury remains to be determined. Overall, my findings indicate that the cellular composition and organization of the ON in *Xenopus* is similar to those in rodents.

6.2.3 Different morphologies of putative OECs in the ON of *Xenopus laevis* larvae

Vertebrate OECs are a heterogeneous cell population with different morphologies, sizes and antigen profiles, with the capability to switch between the different morphologies (Doucette, 1993; Sonigra *et al.*, 1999; Van Den Pol & Santarelli, 2003; Barnett & Chang, 2004; Huang *et al.*, 2008, 2024; Pellitteri *et al.*, 2010; Ekberg *et al.*, 2012). In mammals, OECs with at least two morphologies, fusiform bipolar and flat sheet-like, have been described (Barnett & Chang, 2004; Huang *et al.*, 2008).Using immunohistochemistry with antibodies against vimentin and single-cell electroporation, I also identified these two different morphologies of putative OECs in larval *Xenopus laevis* (Kahl *et al.*, 2025). The vimentin positive cells had a fusiform bipolar morphology, while the single labelled cells revealed the additional morphology of flat sheet-like putative OECs as well as fusiform bipolar cells. Flat sheet like cells were located in more superficial layer of the ON. The bipolar fusiform cells also in deeper layers (Kahl *et al.*, 2025). The putative OECs in larval *Xenopus laevis* likely have diverse functions, as *in vitro* studies with morphologically different OECs suggested possible different functions that still need to be investigated in more detail (Pixley, 1992; Huang *et al.*, 2008; Ekberg *et al.*, 2012). According to my findings, OEC morphology in *Xenopus laevis* larvae is largely comparable to that of rodents. Nevertheless, more research is required to fully understand the morphological diversity and the different functions of OECs in this species.

6.2.4 ON-transection induces transient phosphorylation of rpS6 235/236 in non-neuronal cells of the ON of *Xenopus laevis* larvae

Head trauma or infections that harm the OS can cause olfactory dysfunction in humans (Doty *et al.*, 1997; Meisami *et al.*, 1998). Mistargeted ORN axons during OB reinnervation may result in odor perception loss after damage (Yee & Costanzo, 1998; Vedin *et al.*, 2004). When the mammalian OE recovers from lesions that are not too severe, there is usually a complete re-colonisation of the OE with ORNs with high accuracy in terms of OE topography of olfactory receptor identity (Schwob *et al.*, 1999; Iwema *et al.*, 2004). But to effectively transmit olfactory information, these newly formed ORNs need to project their axons into the OB and create functional connections in the appropriate glomerulus. During normal development and maintenance of the mammalian OS, ORNs with the same olfactory receptor identity project their axons to particular subsets of glomeruli in the OB (Mombaerts *et al.*, 1996), forming a representative topographical map of receptor identity in the central nervous system (Strotmann *et al.*, 2000; Schaefer *et al.*, 2001; Costanzo & Kobayashi, 2010). Accurate axon targeting is also made possible by an important interaction between ORNs and OECs. Both in their natural location and after injury and transplantation, OECs support neural regeneration through a variety of mechanisms, such as direct interaction with axons and support (Doucette, 1990),

neurotrophic and guidance factor secretion (Barnett & Riddell, 2004; Toft *et al.*, 2013; Barton *et al.*, 2017), phagocytosis of axonal debris (Nazareth, Lineburg, *et al.*, 2015; Su *et al.*, 2013), and efficient migration and integration with other cell types, including microglia and astrocytes (Lakatos *et al.*, 2000, 2003; Vincent *et al.*, 2007; Leung *et al.*, 2008; Panni *et al.*, 2013).

OECs enwrap hundreds of ORN axons along the ON from the OE to the OB, provide axon-growth promoting properties, maintain axon-axon interactions, and support the segregation of ORN bundles to target different regions of the OB (Ramón-Cueto & Valverde, 1995; Schwob, 2002; Barraud *et al.*, 2010; Ekberg *et al.*, 2012). In addition other non-neuronal cell types, such as fibroblasts and macrophages, are present in the ON (Li *et al.*, 2005). Investigating the role of different non-neuronal cells in neurogenesis could improve therapies to cure malfunction of the OS.

As part of my thesis I examined the presence of non-neuronal cells in the ON and their activity after injury. Immunohistochemistry against phosphorylated ribosomal protein S6 235/236 (p-rpS6) was applied to assess the temporal dynamics of this activity. Ribosomal protein S6 is an integral element of the 40S ribosomal subunit and plays a role in translation (Biever *et al.*, 2015). Its phosphorylation serves as a marker for neuronal activity or as an indicator of the mammalian target of rapamycin (mTOR) complex 1 signaling activation (Biever *et al.*, 2015). The mTOR signaling pathway regulates essential cellular processes, including growth, proliferation, protein synthesis, metabolism, and autophagy (Ruvinsky & Meyuhas, 2006; Laplante & Sabatini, 2012). The ribosomal protein S6 contains several phosphorylation sites that are phosphorylated in a sequential fashion, starting with serine 236 and progressing to serine 235, 240, 244, and 247 (Martin-Pérez & Thomas, 1983; Wettenhall *et al.*, 1992; Meyuhas, 2008, 2015). Studies in mice have shown increased rpS6 phosphorylation in response to growth factors, glucose, and amino acids, linking it to protein synthesis, cell growth, and glucose homeostasis (Biever *et al.*, 2015; Meyuhas, 2015; Ring *et al.*, 2023).

In the course of my thesis I transected one ON in *Xenopus* larvae to induce an acute injury. This transection resulted in a transient increase of p-rpS6 expression in non-neuronal cells in the ON already one hour after transection (Kahl *et al.*, 2025). Twenty-four hours after injury, the increase in p-rpS6 positive cells was at its highest and significantly decreased until seven days after transection. Thereafter, no further increase in p-rpS6 was observed up to seven weeks after transection. In consistence with my results, it was shown that rats who had experienced traumatic brain injury also experienced changes in p-rpS6 levels. Chen *et al.* (2007) used western blot analysis to find that p-rpS6 levels in the ipsilateral parietal cortex and hippocampus significantly increased between thirty minutes and twenty-four hours after injury (Chen *et al.*, 2007). Additionally, I observed an increase of p-rpS6 in mitral-tufted cells in the contralateral OB of *Xenopus laevis* larvae twenty-four hours after transection, possibly

influenced by contralateral ORNs projections (Ebbesson *et al.*, 1986; Nezlin & Schild, 2005; Kludt *et al.*, 2015).

Recent studies in mammals show that p-rpS6 occurs in all skin layers and cell types, including keratinocytes, fibroblasts, and endothelial cells, in response to skin injury (Ring *et al.*, 2023). This resulted in the creation of a zone of activation that surrounded the area of the original injury site within minutes and persisted until healing was finished. It was suggested that p-rpS6 is a modulator but not a driver of healing because mice unable to phosphorylate rpS6 exhibited an initial acceleration of wound closure but results in impaired healing (Ring *et al.*, 2023). Given that in my study the expression of p-rpS6 in non-neuronal cells of the ON in *Xenopus* was only temporary and given that macrophages, fibroblasts, and OECs are known to be involved in regenerative processes, rpS6 phosphorylation may also act as a modulator in this process. Furthermore, since rpS6 phosphorylation and the mTOR signaling pathways support the growth and repair of cellular and neuronal synapses (Ruvinsky & Meyuhas, 2006; Chen *et al.*, 2007), these pathways might enhance OS regeneration after nerve damage. Future studies should explore whether rapamycin-induced mTOR-complex 1 inhibition, reducing rpS6 phosphorylation, affects this regenerative capacity (Biever *et al.*, 2015).

As long as there is no damage to the OB or other parts of the central nervous system, ON injuries fully regenerate in one to two months (Holbrook & Leopold, 2006; Barton *et al.*, 2017). However, depending on the species, age, developmental stage, and severity of the injury, recovery from injury can vary in duration, accuracy, and extent (Schwob, 2002; Hawkins *et al.*, 2017, 2024; Schwob *et al.*, 2017). Recently, it was demonstrated that following bilateral ON transection, the OS of *Xenopus laevis* larvae regenerates with high accuracy within seven to nine weeks, resulting in the rehabilitation of odor-guided behavior (Hawkins *et al.*, 2024). In the course of my study, I provoked an acute injury by transecting one ON. This caused gradual axonal degradation in the ON and OB in the larvae, which was also shown by Hawkins *et al.* (2017; 2024). After nerve transection, the axon terminals distal to ON injury remained intact and visible for one to forty-eight hours. Axonal debris were found between forty-eight- and seventy-two-hours following transection. Newly formed ORN axons were identified in the ON and MOB one and two weeks following transection, which is consistent with the findings of Cervino *et al.* (2017) and Hawkins *et al.* (2017). Also, in line with the findings of Hawkins *et al.* (2017; 2024), my study showed morphological regeneration seven weeks following nerve damage in the OS (Kahl *et al.*, 2025). The recovery of the OB network in rodents following ON damage or transection is less precise. Even though the OB is principally reinnervated by ORN axons, the resulting odor map in the OB is not precisely reformed (Costanzo, 2000, 2005; Christensen, 2001; Schwob, 2002; Murai *et al.*, 2016). The distinct ORN regeneration time courses in rodents and amphibians could be the cause of the recovery discrepancies (Hawkins *et al.*, 2024). In rodents, Murai and colleagues found that the OE lost all of its ORNs fourteen

days after the ON injury, and that the reinnervation of the OB was still incomplete forty-two days after injury (Murai *et al.*, 2016). As a result, mitral-tufted cell dendritic connectivity was disrupted, and it took eighty-four days for it to fully recover (Murai *et al.*, 2016). Axons from the ORNs in *Xenopus*, on the other hand, likely reach the OB before a loss of post-synaptic targets takes place because ORNs in the OE already regenerate in one week (Hawkins *et al.*, 2017, 2024).

Rodent studies indicate that OEC behavior depends on the type of nerve injury. After unilateral bulbectomy in mice, Chehrehasa *et al.* (2010) observed that OECs filled the cavity created by the procedure before new axons grew into it. Following OB ablation, it was investigated that the OECs in the accessory OB also proliferate (Chehrehasa *et al.*, 2014). In contrast, OECs did not divide or migrate following ON transection in rats (Li *et al.*, 2005). Instead, they were actively phagocytic, removing axonal debris, and they provided continuous open channels for the regeneration of newly formed axons (Li *et al.*, 2005). In my experiments, after transecting one ON of *Xenopus* larvae, I observed that a mixture of non-neuronal cells, including OECs, responded by expressing p-rpS6. Unfortunately, the exact function of these cells and how they continue to function during the regeneration process is still unclear.

While most knowledge on OEC biology comes from rodent studies, OECs have also been isolated from humans, dogs, pigs, and primates (Imaizumi *et al.*, 2000; Féron *et al.*, 2005; Rubio *et al.*, 2008; Techangamsuwan *et al.*, 2008; Carwardine *et al.*, 2017). Their proliferation and response to growth factors vary fundamentally across species (Wewetzer *et al.*, 2011; Murtaza *et al.*, 2022), suggesting potential differences in their role during regeneration. Further research, including studies in amphibians, is essential to explore their therapeutic potential for OS injuries.

7 Summary

The transition of tetrapods to terrestrial habitats required specific adaptations of the OS to cope with new environmental challenges, including increased exposure to harmful influences. This, among others, necessitated the maintenance of regenerative capacities of the OS. While distinct subpopulations of olfactory cells emerged across species, molecular marker expression varies significantly. One such marker, S100Z, a less well-studied calcium-binding protein, has been associated with specific cell subpopulation in the OE of fish and the VNO of mammals. This raises the question of how S100Z is distributed in the OS of amphibians such as *Xenopus laevis*. In the first part of my thesis, I aimed to investigate the distribution pattern of S100Z in the olfactory system of pre- and postmetamorphic *Xenopus laevis*. Using immunohistochemistry, I characterized a subset of S100Z expressing ORNs within the MOE of premetamorphic, and the MC of postmetamorphic animals. There was no S100Z expression in the accessory OS. Within the premetamorphic larval MOE there was a laterally shifted distribution of S100Z-positive cells. The axons of S100Z expressing cells exclusively projected into the intermediate and lateral glomerular clusters within the OB. The co-localization pattern of S100Z and calretinin appeared variable, with no stereotypical expression. These findings suggest that, unlike in mammals, S100Z expression in *Xenopus laevis* is not associated with the VNO, indicating an intermediate evolutionary state.

An important non-neuronal cell type for regenerative processes in the OS are OECs, which have not been investigated in detail in *Xenopus laevis*, yet. Additionally, a definitive OEC marker is still lacking across species. As an amphibian bridging both aquatic and terrestrial life stages, *Xenopus laevis*, serves as a valuable model to investigate OS adaptations at the cellular and molecular levels. Regarding OECs in the ON of *Xenopus laevis*, I identified and distinguished three non-neuronal cell types: putative OECs, macrophages, and fibroblasts. Vimentin emerged as a promising immunohistochemical marker for OECs in the ON, although it also labelled radial glia in the OB. Single-cell electroporation revealed at least two morphological OEC subtypes: bipolar fusiform and flat-sheet cells. To investigate regenerative responses, I analyzed the expression of the activity marker rpS6 following unilateral ON transection and found a transient increase of p-rpS6 in non-neuronal cells after ON transection.

8 Outlook

The transition from a fully aquatic existence to a terrestrial one necessitated a range of adaptations in the olfactory system, including anatomical, molecular, and functional modifications, crucial for the survival of organisms on land. In the first part of my thesis, I focused on the immunohistochemical expression pattern of S100Z within the OS of pre- and postmetamorphic *Xenopus laevis*, a secondary aquatic amphibian. Although a subgroup of ORNs expressing S100Z was identified, several questions remain unanswered. A comprehensive investigation into the function of S100Z within the OS is necessary. The creation of transgenic animals that express a genetically encoded calcium indicator in S100Z positive neurons could enable a range of new experiments. Ca^{2+}- imaging of the OE and OB would enable the identification of potential ligands for S100Z-positive cells. Additionally, the identification of the odorant receptors utilized by the S100Z-expressing neurons to transmit signals is a critical research focus. *In-situ* hybridization studies would be really promising experiments, since this approach would facilitate the creation of specific probes directed against the target RNA of various olfactory receptor families, in addition to S100Z. This technique may also offer further insights into the presence of cilia or microvilli on dendritic knobs of S100Z-expressing neurons.

The OS maintains lifelong regenerative capacity. Two main cell types are involved in this process: the BCs and the OECs. In the second part of my thesis, I focused identifying different non-neuronal cell-types, including OECs, in the ON of *Xenopus laevis* larvae. Although I found promising molecular markers for different non-neuronal cell types, several questions remain unanswered. A key challenge is the identification of an exclusive OEC marker, crucial for distinguishing the various cell types within the ON. Additionally, a comprehensive study of transgenic macrophage animals is necessary to explore how macrophages respond to injury in the OS of *Xenopus laevis*. A central question is the function and necessity of the phosphorylation of rpS6 after ON transection. Is this phosphorylation an essential component of functional regeneration? Studies using the kinase inhibitor rapamycin may provide promising results. This method might also explain why p-rpS6 was also phosphorylated in MTC within the OB. By improving the knowledge of OEC behavior during regeneration processes these findings might contribute to the development of new therapies for nervous system injuries.

9 References

Ache, B.W. & Young, J.M. (2005) Olfaction: Diverse Species, Conserved Principles. *Neuron*, **48**, 417–430.

Ahuja, G., Ivandić, I., Saltürk, M., Oka, Y., Nadler, W., & Korsching, S.I. (2013) Zebrafish crypt neurons project to a single, identified mediodorsal glomerulus. *Sci. Rep.*, **3**, 2063.

Ahuja, G., Nia, S.B., Zapilko, V., Shiriagin, V., Kowatschew, D., Oka, Y., & Korsching, S.I. (2014) Kappe neurons, a novel population of olfactory sensory neurons. *Sci. Rep.*, **4**, 4037.

Alesci, A., Pergolizzi, S., Lo Cascio, P., Fumia, A., & Lauriano, E.R. (2022) Neuronal regeneration: Vertebrates comparative overview and new perspectives for neurodegenerative diseases. *Acta Zool.*, **103**, 129–140.

Allen, N.J. & Lyons, D.A. (2018) Glia as architects of central nervous system formation and function. *Science (80-.).*, **362**, 181–185.

Altman, J. (1962) Are New Neurons Formed in the Brains of Adult Mammals? *Science (80-.).*, **135**, 1127–1128.

Altner, H. (1962) Untersuchungen über Leistungen und Bau der Nase des südafrikanischen Krallenfrosches *Xenopus laevis* (Daudin, 1803). *Z. Vgl. Physiol.*, **45**, 272–306.

Astic, L. & Saucier, D. (2001) Neuronal plasticity and regeneration in the olfactory system of mammals: morphological and functional recovery following olfactory bulb deafferentation. *Cell. Mol. Life Sci.*, **58**, 538–545.

Au, E. & Roskams, A.J. (2003) Olfactory ensheathing cells of the lamina propria *in vivo* and *in vitro*. *Glia*, **41**, 224–236.

Bakalyar, H.A. & Reed, R.R. (1990) Identification of a Specialized Adenylyl Cyclase That May Mediate Odorant Detection. *Science (80-.).*, **250**, 1403–1406.

Barnett, S.C. & Chang, L. (2004) Olfactory ensheathing cells and CNS repair: going solo or in need of a friend? *Trends Neurosci.*, **27**, 54–60.

Barnett, S.C. & Riddell, J.S. (2004) Olfactory ensheathing cells (OECs) and the treatment of CNS injury: advantages and possible caveats. *J. Anat.*, **204**, 57–67.

Barraud, P., Seferiadis, A.A., Tyson, L.D., Zwart, M.F., Szabo-Rogers, H.L., Ruhrberg, C., Liu, K.J., & Baker, C.V.H. (2010) Neural crest origin of olfactory ensheathing glia. *Proc. Natl. Acad. Sci.*, **107**, 21040–21045.

Barton, M., John, J., Clarke, M., Wright, A., & Ekberg, J. (2017) The Glia Response after Peripheral Nerve Injury: A Comparison between Schwann Cells and Olfactory Ensheathing Cells and Their Uses for Neural Regenerative Therapies. *Int. J. Mol. Sci.*, **18**, 287.

Bear, D.M., Lassance, J.-M., Hoekstra, H.E., & Datta, S.R. (2016) The Evolving Neural and Genetic Architecture of Vertebrate Olfaction. *Curr. Biol.*, **26**, R1039–R1049.

Beiersdorfer, A., Wolburg, H., Grawe, J., Scheller, A., Kirchhoff, F., & Lohr, C. (2020) Sublamina-specific organization of the blood brain barrier in the mouse olfactory nerve layer. *Glia*, **68**, 631–645.

Beites, C.L., Kawauchi, S., Crocker, C.E., & Calof, A.L. (2005) Identification and molecular regulation of neural stem cells in the olfactory epithelium. *Exp. Cell Res.*, **306**, 309–316.

Berridge, M.J., Bootman, M.D., & Roderick, H.L. (2003) Calcium signalling: dynamics, homeostasis and remodelling. *Nat. Rev. Mol. Cell Biol.*, **4**, 517–529.

Berry, M.D. (2004) Mammalian central nervous system trace amines. Pharmacologic amphetamines, physiologic neuromodulators. *J. Neurochem.*, **90**, 257–271.

Bertmar, G. (1981) Evolution of Vomeronasal Organs in Vertebrates. *Evolution (N. Y).*, **35**, 359.

Bettini, S., Lazzari, M., & Franceschini, V. (2019) Molecular Markers in the Study of Non-model Vertebrates: Their Significant Contributions to the Current Knowledge of Tetrapod Glial Cells and Fish Olfactory Neurons. In *Results and Problems in Cell Differentiation*. pp. 355–377.

Biever, A., Valjent, E., & Puighermanal, E. (2015) Ribosomal Protein S6 Phosphorylation in the Nervous System: From Regulation to Function. *Front. Mol. Neurosci.*, **8**, 1–14.

Billig, G.M., Pál, B., Fidzinski, P., & Jentsch, T.J. (2011) Ca2+-activated Cl− currents are dispensable for olfaction. *Nat. Neurosci.*, **14**, 763–769.

Bjarnadóttir, T.K., Fredriksson, R., & Schiöth, H.B. (2005) The gene repertoire and the common evolutionary history of glutamate, pheromone (V2R), taste(1) and other related G protein-coupled receptors. *Gene*, **362**, 70–84.

Bloom, M.L., Johnston, L.B., & Datta, S.R. (2020) Renewal and Differentiation of GCD Necklace Olfactory Sensory Neurons. *Chem. Senses*, **45**, 333–346.

Borowsky, B., Adham, N., Jones, K.A., Raddatz, R., Artymyshyn, R., Ogozalek, K.L., Durkin, M.M., Lakhlani, P.P., Bonini, J.A., Pathirana, S., Boyle, N., Pu, X., Kouranova, E., Lichtblau, H., Ochoa, F.Y., Branchek, T.A., & Gerald, C. (2001) Trace amines: Identification of a family of mammalian G protein-coupled receptors. *Proc. Natl. Acad. Sci.*, **98**, 8966–8971.

Boruch, A. V., Conners, J.J., Pipitone, M., Deadwyler, G., Storer, P.D., Devries, G.H., & Jones, K.J. (2001) Neurotrophic and migratory properties of an olfactory ensheathing cell line. *Glia*, **33**, 225–229.

Brann, J.H. & Firestein, S. (2010) Regeneration of New Neurons Is Preserved in Aged Vomeronasal Epithelia. *J. Neurosci.*, **30**, 15686–15694.

Brann, J.H. & Firestein, S.J. (2014) A lifetime of neurogenesis in the olfactory system. *Front. Neurosci.*, **8**, 1–11.

Braubach, O.R., Fine, A., & Croll, R.P. (2012) Distribution and functional organization of glomeruli in the olfactory bulbs of zebrafish (*Danio rerio*). *J. Comp. Neurol.*, **520**, 2317–2339.

Breer, H., Fleischer, J., & Strotmann, J. (2006) Signaling in the Chemosensory Systems. *Cell. Mol. Life Sci.*, **63**, 1465–1475.

Brennan, P.A. & Zufall, F. (2006) Pheromonal communication in vertebrates. *Nature*, **444**, 308–315.

Buck, L. & Axel, R. (1991) A novel multigene family may encode odorant receptors: A molecular basis for odor recognition. *Cell*, **65**, 175–187.

Burd, G.D. (1991) Development of the olfactory nerve in the African clawed frog, *Xenopus laevis* : I. Normal development. *J. Comp. Neurol.*, **304**, 123–134.

Burguera, D., Dionigi, F., Kverková, K., Winkler, S., Brown, T., Pippel, M., Zhang, Y., Shafer, M., Nichols, A.L.A., Myers, E., Němec, P., & Musilova, Z. (2023) Expanded olfactory system in ray-finned fishes capable of terrestrial exploration. *BMC Biol.*, **21**, 163.

Byrd, C.A. & Burd, G.D. (1991) Development of the olfactory bulb in the clawed frog, *Xenopus laevis* : A morphological and quantitative analysis. *J. Comp. Neurol.*, **314**, 79–90.

Calof, A.L., Bonnin, A., Crocker, C., Kawauchi, S., Murray, R.C., Shou, J., & Wu, H. (2002) Progenitor cells of the olfactory receptor neuron lineage. *Microsc. Res. Tech.*, **58**, 176–188.

Calof, A.L. & Chikaraishi, D.M. (1989) Analysis of neurogenesis in a mammalian neuroepithelium: Proliferation and differentiation of an olfactory neuron precursor in vitro. *Neuron*, **3**, 115–127.

Cao, Y., Oh, B.C., & Stryer, L. (1998) Cloning and localization of two multigene receptor families in goldfish olfactory epithelium. *Proc. Natl. Acad. Sci.*, **95**, 11987–11992.

Capsoni, S., Fogli Iseppe, A., Casciano, F., & Pignatelli, A. (2021) Unraveling the Role of Dopaminergic and Calretinin Interneurons in the Olfactory Bulb. *Front. Neural Circuits*, **15**.

Carafoli, E., Santella, L., Branca, D., & Brini, M. (2001) Generation, Control, and Processing of Cellular Calcium Signals. *Crit. Rev. Biochem. Mol. Biol.*, **36**, 107–260.

Carwardine, D., Prager, J., Neeves, J., Muir, E.M., Uney, J., Granger, N., & Wong, L.-F. (2017) Transplantation of canine olfactory ensheathing cells producing chondroitinase ABC promotes chondroitin sulphate proteoglycan digestion and axonal sprouting following spinal cord injury. *PLoS One*, **12**, e0188967.

Cervino, A.S., Paz, D.A., & Frontera, J.L. (2017) Neuronal degeneration and regeneration induced by axotomy in the olfactory epithelium of *Xenopus laevis*. *Dev. Neurobiol.*, **77**, 1308–1320.

Chamero, P., Leinders-Zufall, T., & Zufall, F. (2012) From genes to social communication: molecular sensing by the vomeronasal organ. *Trends Neurosci.*, **35**, 597–606.

Chang, S., Chung-Davidson, Y.-W., Libants, S. V., Nanlohy, K.G., Kiupel, M., Brown, C.T., & Li, W. (2013) The sea lamprey has a primordial accessory olfactory system. *BMC Evol. Biol.*, **13**, 172.

Chazin, W.J. (2011) Relating Form and Function of EF-Hand Calcium Binding Proteins. *Acc. Chem. Res.*, **44**, 171–179.

Chehrehasa, F., Ekberg, J.A.K., & St John, J.A. (2014) A novel method using intranasal delivery of EdU demonstrates that accessory olfactory ensheathing cells respond to injury by proliferation. *Neurosci. Lett.*, **563**, 90–95.

Chehrehasa, F., Windus, L.C.E., Ekberg, J.A.K., Scott, S.E., Amaya, D., Mackay-Sim, A., & St John, J.A. (2010) Olfactory glia enhance neonatal axon regeneration. *Mol. Cell. Neurosci.*, **45**, 277–288.

Chen, S., Atkins, C.M., Liu, C.L., Alonso, O.F., Dietrich, W.D., & Hu, B.R. (2007) Alterations in Mammalian Target of Rapamycin Signaling Pathways after Traumatic Brain Injury. *J. Cereb. Blood Flow Metab.*, **27**, 939–949.

Cheng, F., Shen, Y., Mohanasundaram, P., Lindström, M., Ivaska, J., Ny, T., & Eriksson, J.E. (2016) Vimentin coordinates fibroblast proliferation and keratinocyte differentiation in wound healing via TGF-β–Slug signaling. *Proc. Natl. Acad. Sci.*, **113**, E4320–E4327.

Cheung, M.C., Jang, W., Schwob, J.E., & Wachowiak, M. (2014) Functional recovery of odor representations in regenerated sensory inputs to the olfactory bulb. *Front. Neural Circuits*, **7**, 1–16.

Christensen, M.D. (2001) Rhinotopy is Disrupted During the Re-innervation of the Olfactory Bulb that Follows Transection of the Olfactory Nerve. *Chem. Senses*, **26**, 359–369.

Chuah, M.I. & West, A.K. (2002) Cellular and molecular biology of ensheathing cells. *Microsc. Res. Tech.*, **58**, 216–227.

Costanzo, R.M. (2000) Rewiring the Olfactory Bulb: Changes in Odor Maps following Recovery from Nerve Transection. *Chem. Senses*, **25**, 199–205.

Costanzo, R.M. (2005) Regeneration and Rewiring the Olfactory Bulb. *Chem. Senses*, **30**, i133–i134.

Costanzo, R.M. & Kobayashi, M. (2010) Age-Related Changes in P2 Odorant Receptor Mapping in the Olfactory Bulb. *Chem. Senses*, **35**, 417–426.

Dalton, R.P. & Lomvardas, S. (2015) Chemosensory Receptor Specificity and Regulation. *Annu. Rev. Neurosci.*, **38**, 331–349.

Date-Ito, A., Ohara, H., Ichikawa, M., Mori, Y., & Hagino-Yamagishi, K. (2008) *Xenopus* V1R Vomeronasal Receptor Family Is Expressed in the Main Olfactory System. *Chem. Senses*, **33**, 339–346.

Daume, D., Offner, T., Hassenklöver, T., & Manzini, I. (2022) Patterns of tubb2b Promoter-Driven Fluorescence in the Forebrain of Larval *Xenopus laevis*. *Front. Neuroanat.*, **16**, 1–13.

DeMaria, S., Berke, A.P., Van Name, E., Heravian, A., Ferreira, T., & Ngai, J. (2013) Role of a Ubiquitously Expressed Receptor in the Vertebrate Olfactory System. *J. Neurosci.*, **33**, 15235–15247.

Dieris, M., Kowatschew, D., & Korsching, S.I. (2021) Olfactory function in the trace amine-associated receptor family (TAARs) evolved twice independently. *Sci. Rep.*, **11**, 7807.

Dittrich, K., Kuttler, J., Hassenklöver, T., & Manzini, I. (2016) Metamorphic remodeling of the olfactory organ of the African clawed frog, *Xenopus laevis*. *J. Comp. Neurol.*, **524**, 986–998.

Docampo-Seara, A., Candal, E., & Rodríguez, M.A. (2022) Study of the glial cytoarchitecture of the developing olfactory bulb of a shark using immunochemical markers of radial glia. *Brain Struct. Funct.*, **227**, 1067–1082.

Donato, R. (2001) S100: a multigenic family of calcium-modulated proteins of the EF-hand type with intracellular and extracellular functional roles. *Int. J. Biochem. Cell Biol.*, **33**, 637–668.

Donato, R. (2003) Intracellular and extracellular roles of S100 proteins. *Microsc. Res. Tech.*, **60**, 540–551.

Donato, R., Cannon, B.R., Sorci, G., Riuzzi, F., Hsu, K., Weber, D.J., & Geczy, C.L. (2013) Functions of S100 proteins. *Curr. Mol. Med.*, **13**, 24–57.

Doty, R.L., Yousem, D.M., Pham, L.T., Kreshak, A.A., Geckle, R., & Lee, W.W. (1997) Olfactory Dysfunction in Patients With Head Trauma. *Arch. Neurol.*, **54**, 1131–1140.

Doucette, R. (1990) Glial influences on axonal growth in the primary olfactory system. *Glia*, **3**, 433–449.

Doucette, R. (1993) Glial progenitor cells of the nerve fiber layer of the olfactory bulb: Effect of astrocyte growth media. *J. Neurosci. Res.*, **35**, 274–287.

Du Plessis, S.S. (1966) Stimulation of Spawning in *Xenopus laevis* by Fowl Manure. *Nature*, **211**, 1092–1092.

Dulac, C. & Axel, R. (1995) A novel family of genes encoding putative pheromone receptors in mammals. *Cell*, **83**, 195–206.

Dulac, C. & Torello, A.T. (2003) Molecular detection of pheromone signals in mammals: from genes to behaviour. *Nat. Rev. Neurosci.*, **4**, 551–562.

Ebbesson, S.O.E., Bazer, G.T., & Jane, J.A. (1986) Some primary olfactory axons project to the contralateral olfactory bulb in *Xenopus laevis*. *Neurosci. Lett.*, **65**, 234–238.

Eisthen, H.L. (1992) Phylogeny of the vomeronasal system and of receptor cell types in the olfactory and vomeronasal epithelia of vertebrates. *Microsc. Res. Tech.*, **23**, 1–21.

Eisthen, H.L. (1997) Evolution of Vertebrate Olfactory Systems. *Brain. Behav. Evol.*, **50**, 222–233.

Eisthen, H.L. (2002) Why Are Olfactory Systems of Different Animals So Similar? *Brain. Behav. Evol.*, **59**, 273–293.

Eisthen, H.L. & Polese, G. (2007) Components of the Vertebrate Olfactory System **390**, 355–406.

Ekberg, J.A.K., Amaya, D., Mackay-Sim, A., & St. John, J.A. (2012) The Migration of Olfactory Ensheathing Cells during Development and Regeneration. *Neurosignals*, **20**, 147–158.

Ekberg, J.A.K. & St john, J.A. (2014) Crucial Roles for Olfactory Ensheathing Cells and Olfactory Mucosal Cells in the Repair of Damaged Neural Tracts. *Anat. Rec.*, **297**, 121–128.

Elíes, J., Yáñez, M., Pereira, T.M.C., Gil-Longo, J., MacDougall, D.A., & Campos-Toimil, M. (2020) An Update to Calcium Binding Proteins. In *Advances in Experimental Medicine and Biology*. pp. 183–213.

Fairless, R. & Barnett, S.C. (2005) Olfactory ensheathing cells: their role in central nervous system repair. *Int. J. Biochem. Cell Biol.*, **37**, 693–699.

Feinstein, P. & Mombaerts, P. (2004) A Contextual Model for Axonal Sorting into Glomeruli in the Mouse Olfactory System. *Cell*, **117**, 817–831.

Féron, F., Perry, C., Cochrane, J., Licina, P., Nowitzke, A., Urquhart, S., Geraghty, T., & Mackay-Sim, A. (2005) Autologous olfactory ensheathing cell transplantation in human spinal cord injury. *Brain*, **128**, 2951–2960.

Firestein, S., Darrow, B., & Shepherd, G.M. (1991) Activation of the sensory current in salamander olfactory receptor neurons depends on a G protein-mediated cAMP second messenger system. *Neuron*, **6**, 825–835.

Fleischer, J. (2021) The Grueneberg ganglion: signal transduction and coding in an olfactory and thermosensory organ involved in the detection of alarm pheromones and predator-secreted kairomones. *Cell Tissue Res.*, **383**, 535–548.

Freitag, J., Krieger, J., Strotmann, J., & Breer, H. (1995) Two classes of olfactory receptors in *Xenopus laevis*. *Neuron*, **15**, 1383–1392.

Germanà, A., Montalbano, G., Laurà, R., Ciriaco, E., del Valle, M.E., & Vega, J.A. (2004) S100 protein-like immunoreactivity in the crypt olfactory neurons of the adult zebrafish. *Neurosci. Lett.*, **371**, 196–198.

Germanà, A., Paruta, S., Germanà, G.P., Ochoa-Erena, F.J., Montalbano, G., Cobo, J., & Vega, J.A. (2007) Differential distribution of S100 protein and calretinin in mechanosensory and chemosensory cells of adult zebrafish (*Danio rerio*). *Brain Res.*, **1162**, 48–55.

Glezer, I. & Malnic, B. (2019) Olfactory receptor function. In *Handbook of Clinical Neurology*, 1st edn. Elsevier B.V., pp. 67–78.

Gliem, S., Schild, D., & Manzini, I. (2009) Highly specific responses to amine odorants of individual olfactory receptor neurons in situ. *Eur. J. Neurosci.*, **29**, 2315–2326.

Gliem, S., Syed, A.S., Sansone, A., Kludt, E., Tantalaki, E., Hassenklöver, T., Korsching, S.I., & Manzini, I. (2013) Bimodal processing of olfactory information in an amphibian nose: odor responses segregate into a medial and a lateral stream. *Cell. Mol. Life Sci.*, **70**, 1965–1984.

Gloriam, D.E.I., Bjarnadóttir, T.K., Yan, Y.-L., Postlethwait, J.H., Schiöth, H.B., & Fredriksson, R. (2005) The repertoire of trace amine G-protein-coupled receptors: large expansion in zebrafish. *Mol. Phylogenet. Evol.*, **35**, 470–482.

González, A. (2010) Lungfishes, like tetrapods, possess a vomeronasal system. *Front. Neuroanat.*, **4**, 1–11.

Gonzalez, L.L., Garrie, K., & Turner, M.D. (2020) Role of S100 proteins in health and disease. *Biochim. Biophys. Acta - Mol. Cell Res.*, **1867**, 118677.

Graziadei, G.A. & Graziadei, P.P. (1979a) Neurogenesis and neuron regeneration in the olfactory system of mammals. II. Degeneration and reconstitution of the olfactory sensory neurons after axotomy. *J. Neurocytol.*, **8**, 197–213.

Graziadei, P. & Bannister, L.H. (1967) Some Observations on the fine structure of the olfactory epithelium in the domestic duck. *Zeitschrift für Zellforsch. und Mikroskopische Anat.*, **80**, 220–228.

Graziadei, P.P.C. & Graziadei, G.A.M. (1979b) Neurogenesis and neuron regeneration in the olfactory system of mammals. I. Morphological aspects of differentiation and structural organization of the olfactory sensory neurons. *J. Neurocytol.*, **8**, 1–18.

Graziadei, P.P.C. & Metcalf, J.F. (1971) Autoradiographic and ultrastructural observations on the frog's olfactory mucosa. *Zeitschrift für Zellforsch. und Mikroskopische Anat.*, **116**, 305–318.

Greer, P.L., Bear, D.M., Lassance, J.-M., Bloom, M.L., Tsukahara, T., Pashkovski, S.L., Masuda, F.K., Nowlan, A.C., Kirchner, R., Hoekstra, H.E., & Datta, S.R. (2016) A Family of non-GPCR Chemosensors Defines an Alternative Logic for Mammalian Olfaction. *Cell*, **165**, 1734–1748.

Haga, S., Hattori, T., Sato, T., Sato, K., Matsuda, S., Kobayakawa, R., Sakano, H., Yoshihara, Y., Kikusui, T., & Touhara, K. (2010) The male mouse pheromone ESP1 enhances female sexual receptive behaviour through a specific vomeronasal receptor. *Nature*, **466**, 118–122.

Hagino-Yamagishi, K., Moriya, K., Kubo, H., Wakabayashi, Y., Isobe, N., Saito, S., Ichikawa, M., & Yazaki, K. (2004) Expression of Vomeronasal Receptor Genes in *Xenopus laevis*. *J. Comp. Neurol.*, **472**, 246–256.

Hagino-Yamagishi, K., Moriya, K., Kubo, H., Wakabayashi, Y., Isobe, N., Saito, S., Ichikawa, M., & Yazaki, K. (2004) Expression of vomeronasal receptor genes in *Xenopus laevis*. *J. Comp. Neurol.*, **472**, 246–256.

Hamdani, E.H. & Døving, K.B. (2007) The functional organization of the fish olfactory system. *Prog. Neurobiol.*, **82**, 80–86.

Hansen, A. (2007) Olfactory and solitary chemosensory cells: two different chemosensory systems in the nasal cavity of the American alligator, Alligator mississippiensis. *BMC Neurosci.*, **8**, 64.

Hansen, A. & Finger, T.E. (2000) Phyletic Distribution of Crypt-Type Olfactory Receptor Neurons in Fishes. *Brain. Behav. Evol.*, **55**, 100–110.

Hansen, A., Reiss, J.O., Gentry, C.L., & Burd, G.D. (1998) Ultrastructure of the olfactory organ in the clawed frog,*Xenopus laevis*, during larval development and metamorphosis. *J. Comp. Neurol.*, **398**, 273–288.

Hansen, A. & Zielinski, B.S. (2005) Diversity in the olfactory epithelium of bony fishes: Development, lamellar arrangement, sensory neuron cell types and transduction components. *J. Neurocytol.*, **34**, 183–208.

Hara, T.J. (1994) Olfaction and gustation in fish: an overview. *Acta Physiol. Scand.*, **152**, 207–217.

Hashiguchi, Y. & Nishida, M. (2007) Evolution of Trace Amine–Associated Receptor (TAAR) Gene Family in Vertebrates: Lineage-Specific Expansions and Degradations of a Second Class of Vertebrate Chemosensory Receptors Expressed in the Olfactory Epithelium. *Mol. Biol. Evol.*, **24**, 2099–2107.

Hassenklöver, T., Kurtanska, S., Bartoszek, I., Junek, S., Schild, D., & Manzini, I. (2008) Nucleotide-induced Ca 2+ signaling in sustentacular supporting cells of the olfactory epithelium. *Glia*, **56**, 1614–1624.

Hawkins, S.J., Gärtner, Y., Offner, T., Weiss, L., Maiello, G., Hassenklöver, T., & Manzini, I. (2024) The olfactory network of larval <scp> *Xenopus laevis* </scp> regenerates accurately after olfactory nerve transection. *Eur. J. Neurosci.*, **60**, 3719–3741.

Hawkins, S.J., Weiss, L., Offner, T., Dittrich, K., Hassenklöver, T., & Manzini, I. (2017) Functional Reintegration of Sensory Neurons and Transitional Dendritic Reduction of Mitral/Tufted Cells during Injury-Induced Recovery of the Larval *Xenopus* Olfactory Circuit. *Front. Cell. Neurosci.*, **11**, 1–17.

He, B.-R., Xie, S.-T., Wu, M.-M., Hao, D.-J., & Yang, H. (2014) Phagocytic Removal of Neuronal Debris by Olfactory Ensheathing Cells Enhances Neuronal Survival and Neurite Outgrowth via p38MAPK Activity. *Mol. Neurobiol.*, **49**, 1501–1512.

Hecker, N., Lächele, U., Stuckas, H., Giere, P., & Hiller, M. (2019) Convergent vomeronasal system reduction in mammals coincides with convergent losses of calcium signalling and odorant-degrading genes. *Mol. Ecol.*, **28**, 3656–3668.

Hegg, C.C. & Lucero, M.T. (2006) Purinergic receptor antagonists inhibit odorant-induced heat shock protein 25 induction in mouse olfactory epithelium. *Glia*, **53**, 182–190.

Herbert, R.P., Harris, J., Chong, K.P., Chapman, J., West, A.K., & Chuah, M.I. (2012) Cytokines and olfactory bulb microglia in response to bacterial challenge in the compromised primary olfactory pathway. *J. Neuroinflammation*, **9**, 109.

Hermann, A., Donato, R., Weiger, T.M., & Chazin, W.J. (2012) S100 Calcium Binding Proteins and Ion Channels. *Front. Pharmacol.*, **3**, 1–10.

Herrada, G. & Dulac, C. (1997) A Novel Family of Putative Pheromone Receptors in Mammals with a Topographically Organized and Sexually Dimorphic Distribution. *Cell*, **90**, 763–773.

Higginson, J.R. & Barnett, S.C. (2011) The culture of olfactory ensheathing cells (OECs)—a distinct glial cell type. *Exp. Neurol.*, **229**, 2–9.

Holbrook, E.H. & Leopold, D.A. (2006) An updated review of clinical olfaction. *Curr. Opin. Otolaryngol. Head Neck Surg.*, **14**, 23–28.

Hoover, K.C. (2010) Smell with inspiration: The evolutionary significance of olfaction. *Am. J. Phys. Anthropol.*, **143**, 63–74.

Huang, H., Xiong, M., Pu, F., Liao, J., Zhu, F., & Zhang, W. (2024) Application and challenges of olfactory ensheathing cells in clinical trials of spinal cord injury. *Eur. J. Pharmacol.*, **963**, 176238.

Huang, Q., Zhao, S., Gaudin, A., Quennedey, B., & Gascuel, J. (2005) Glial fibrillary acidic protein and vimentin expression in the frog olfactory system during metamorphosis. *Neuroreport*, **16**, 1439–1442.

Huang, Z., Wang, Y., Cao, L., Su, Z., Zhu, Y., Chen, Y., Yuan, X., & He, C. (2008) Migratory properties of cultured olfactory ensheathing cells by single-cell migration assay. *Cell Res.*, **18**, 479–490.

Hussain, A., Saraiva, L.R., Ferrero, D.M., Ahuja, G., Krishna, V.S., Liberles, S.D., & Korsching, S.I. (2013) High-affinity olfactory receptor for the death-associated odor cadaverine. *Proc. Natl. Acad. Sci.*, **110**, 19579–19584.

Imaizumi, T., Lankford, K.L., Burton, W. V., Fodor, W.L., & Kocsis, J.D. (2000) Xenotransplantation of transgenic pig olfactory ensheathing cells promotes axonal regeneration in rat spinal cord. *Nat. Biotechnol.*, **18**, 949–953.

Ingram, N.T., Khankan, R.R., & Phelps, P.E. (2016) Olfactory Ensheathing Cells Express α7 Integrin to Mediate Their Migration on Laminin. *PLoS One*, **11**, e0153394.

Iwema, C.L., Fang, H., Kurtz, D.B., Youngentob, S.L., & Schwob, J.E. (2004) Odorant Receptor Expression Patterns Are Restored in Lesion-Recovered Rat Olfactory Epithelium. *J. Neurosci.*, **24**, 356–369.

Johnson, B.A. & Leon, M. (2007) Chemotopic odorant coding in a mammalian olfactory system. *J. Comp. Neurol.*, **503**, 1–34.

Johnstone, K.A., Ciborowski, K.L., Lubieniecki, K.P., Chow, W., Phillips, R.B., Koop, B.F., Jordan, W.C., & Davidson, W.S. (2009) Genomic Organization and Evolution of the Vomeronasal Type 2 Receptor-Like (OlfC) Gene Clusters in Atlantic Salmon, Salmo salar. *Mol. Biol. Evol.*, **26**, 1117–1125.

Jones, D.T. & Reed, R.R. (1989) G olf : an Olfactory Neuron Specific-G Protein Involved in Odorant Signal Transduction. *Science (80-.).*, **244**, 790–795.

Juilfs, D.M., Fülle, H.-J., Zhao, A.Z., Houslay, M.D., Garbers, D.L., & Beavo, J.A. (1997) A subset of olfactory neurons that selectively express cGMP-stimulated phosphodiesterase (PDE2) and guanylyl cyclase-D define a unique olfactory signal transduction pathway. *Proc. Natl. Acad. Sci.*, **94**, 3388–3395.

Jungblut, L.D., Reiss, J.O., & Pozzi, A.G. (2021) Olfactory subsystems in the peripheral olfactory organ of anuran amphibians. *Cell Tissue Res.*, **383**, 289–299.

Kahl, M., Offner, T., Trendel, A., Weiss, L., Manzini, I., & Hassenklöver, T. (2024) S100Z is expressed in a lateral subpopulation of olfactory receptor neurons in the main olfactory system of *Xenopus laevis*. *Dev. Neurobiol.*, **84**, 59–73.

Kahl, M., Weiss, L., Walter, J., Hassenklöver, T., & Manzini, I. (2025). Olfactory nerve transection transiently activates olfactory ensheathing cells in *Xenopus laevis* larvae. Eur. J. Neurosci., **62**, 1-16

Kaplan, M.S. & Hinds, J.W. (1977) Neurogenesis in the Adult Rat: Electron Microscopic Analysis of Light Radioautographs. *Science (80-.).*, **197**, 1092–1094.

Karlson, P. & Lüscher, M. (1959) 'Pheromones': a New Term for a Class of Biologically Active Substances. *Nature*, **183**, 55–56.

Kaupp, U.B. (2010) Olfactory signalling in vertebrates and insects: differences and commonalities. *Nat. Rev. Neurosci.*, **11**, 188–200.

Keller, A. & Vosshall, L.B. (2016) Olfactory perception of chemically diverse molecules. *BMC Neurosci.*, **17**, 55.

Kerschbaum, H.H. & Hermann, A. (1992) Calcium-binding proteins in chemoreceptors of *Xenopus laevis*. *Tissue Cell*, **24**, 719–724.

Key, B. & St John, J. (2002) Axon Navigation in the Mammalian Primary Olfactory Pathway: Where to Next? *Chem. Senses*, **27**, 245–260.

Kimoto, H., Haga, S., Sato, K., & Touhara, K. (2005) Sex-specific peptides from exocrine glands stimulate mouse vomeronasal sensory neurons. *Nature*, **437**, 898–901.

Kishida, T. (2021) Olfaction of aquatic amniotes. *Cell Tissue Res.*, **383**, 353–365.

Kleene, S. & Gesteland, R. (1991) Calcium-activated chloride conductance in frog olfactory cilia. *J. Neurosci.*, **11**, 3624–3629.

Kludt, E., Okom, C., Brinkmann, A., & Schild, D. (2015) Integrating Temperature with Odor Processing in the Olfactory Bulb. *J. Neurosci.*, **35**, 7892–7902.

Koide, T., Miyasaka, N., Morimoto, K., Asakawa, K., Urasaki, A., Kawakami, K., & Yoshihara, Y. (2009) Olfactory neural circuitry for attraction to amino acids revealed by transposon-mediated gene trap approach in zebrafish. *Proc. Natl. Acad. Sci.*, **106**, 9884–9889.

Korsching, S. (2016) Aquatic Olfaction. In *Chemosensory Transduction*. Elsevier, pp. 81–100.

Korsching, S.I. (2020) Taste and Smell in Zebrafish. In *The Senses: A Comprehensive Reference*. Elsevier, pp. 466–492.

Kowatschew, D. & Korsching, S.I. (2022) Lamprey possess both V1R and V2R olfactory receptors, but only V1Rs are expressed in olfactory sensory neurons. *Chem. Senses*, **47**, 1–8.

Kraemer, A.M., Saraiva, L.R., & Korsching, S.I. (2008) Structural and functional diversification in the teleost S100 family of calcium-binding proteins. *BMC Evol. Biol.*, **8**, 48.

Krautwurst, D., Yau, K.-W., & Reed, R.R. (1998) Identification of Ligands for Olfactory Receptors by Functional Expression of a Receptor Library. *Cell*, **95**, 917–926.

Kurahashi, T. & Yau, K.-W. (1993) Co-existence of cationic and chloride components in odorant-induced current of vertebrate olfactory receptor cells. *Nature*, **363**, 71–74.

Lakatos, A., Barnett, S.C., & Franklin, R.J.M. (2003) Olfactory ensheathing cells induce less host astrocyte response and chondroitin sulphate proteoglycan expression than schwann cells following transplantation into adult cns white matter. *Exp. Neurol.*, **184**, 237–246.

Lakatos, A., Franklin, R.J.M., & Barnett, S.C. (2000) Olfactory ensheathing cells and Schwann cells differ in their in vitro interactions with astrocytes. *Glia*, **32**, 214–225.

Laplante, M. & Sabatini, D.M. (2012) mTOR Signaling in Growth Control and Disease. *Cell*, **149**, 274–293.

Lazzari, M., Bettini, S., & Franceschini, V. (2013) Immunocytochemical characterization of olfactory ensheathing cells in fish. *Brain Struct. Funct.*, **218**, 539–549.

Lazzari, M., Bettini, S., & Franceschini, V. (2014) Immunocytochemical characterisation of olfactory ensheathing cells of zebrafish. *J. Anat.*, **224**, 192–206.

Lazzari, M., Bettini, S., & Franceschini, V. (2016) Immunocytochemical characterisation of ensheathing glia in the olfactory and vomeronasal systems of *Ambystoma mexicanum* (Caudata: *Ambystomatidae*). *Brain Struct. Funct.*, **221**, 955–967.

Lazzari, M., Franceschini, V., & Ciani, F. (1997) Glial fibrillary acidic protein and vimentin in radial glia of *Ambystoma mexicanum* and *Triturus carnifex*: an immunocytochemical study. *J. Hirnforsch.*, **38**, 187–194.

Leinders-Zufall, T., Brennan, P., Widmayer, P., S., P.C., Maul-Pavicic, A., Jäger, M., Li, X.-H., Breer, H., Zufall, F., & Boehm, T. (2004) MHC Class I Peptides as Chemosensory Signals in the Vomeronasal Organ. *Science (80-.).*, **306**, 1033–1037.

Leinders-Zufall, T., Cockerham, R.E., Michalakis, S., Biel, M., Garbers, D.L., Reed, R.R., Zufall, F., & Munger, S.D. (2007) Contribution of the receptor guanylyl cyclase GC-D to chemosensory function in the olfactory epithelium. *Proc. Natl. Acad. Sci.*, **104**, 14507–14512.

Leinders-Zufall, T., Lane, A.P., Puche, A.C., Ma, W., Novotny, M. V., Shipley, M.T., & Zufall, F. (2000) Ultrasensitive pheromone detection by mammalian vomeronasal neurons. *Nature*, **405**, 792–796.

Leung, J.Y.K., Chapman, J.A., Harris, J.A., Hale, D., Chung, R.S., West, A.K., & Chuah, M.I. (2008) Olfactory ensheathing cells are attracted to, and can endocytose, bacteria. *Cell. Mol. Life Sci.*, **65**, 2732–2739.

Li, Y., Field, P.M., & Raisman, G. (1998) Regeneration of Adult Rat Corticospinal Axons Induced by Transplanted Olfactory Ensheathing Cells. *J. Neurosci.*, **18**, 10514–10524.

Li, Y., Field, P.M., & Raisman, G. (2005) Olfactory ensheathing cells and olfactory nerve fibroblasts maintain continuous open channels for regrowth of olfactory nerve fibres. *Glia*, **52**, 245–251.

Liao, J., Zhu, F., Liu, Y., Liu, S., Liu, Z., & Zhang, W. (2024) The role of olfactory ensheathing cells in the repair of nerve injury. *Eur. J. Pharmacol.*, **966**, 176346.

Liberles, S.D. & Buck, L.B. (2006) A second class of chemosensory receptors in the olfactory epithelium. *Nature*, **442**, 645–650.

Liberles, S.D., Horowitz, L.F., Kuang, D., Contos, J.J., Wilson, K.L., Siltberg-Liberles, J., Liberles, D.A., & Buck, L.B. (2009) Formyl peptide receptors are candidate chemosensory receptors in the vomeronasal organ. *Proc. Natl. Acad. Sci.*, **106**, 9842–9847.

Lindemann, L., Ebeling, M., Kratochwil, N.A., Bunzow, J.R., Grandy, D.K., & Hoener, M.C. (2005) Trace amine-associated receptors form structurally and functionally distinct subfamilies of novel G protein-coupled receptors. *Genomics*, **85**, 372–385.

Lindemann, L. & Hoener, M.C. (2005) A renaissance in trace amines inspired by a novel GPCR family. *Trends Pharmacol. Sci.*, **26**, 274–281.

Lucas, P., Ukhanov, K., Leinders-Zufall, T., & Zufall, F. (2003) A Diacylglycerol-Gated Cation Channel in Vomeronasal Neuron Dendrites Is Impaired in TRPC2 Mutant Mice. *Neuron*, **40**, 551–561.

Mackay-Sim, A. & Kittel, P. (1991) Cell dynamics in the adult mouse olfactory epithelium: a quantitative autoradiographic study. *J. Neurosci.*, **11**, 979–984.

Malnic, B. (2007) Searching for the Ligands of Odorant Receptors. *Mol. Neurobiol.*, **35**, 175–181.

Malnic, B., Hirono, J., Sato, T., & Buck, L.B. (1999) Combinatorial Receptor Codes for Odors. *Cell*, **96**, 713–723.

Manzini, I. (2015) From neurogenesis to neuronal regeneration: the amphibian olfactory system as a model to visualize neuronal development in vivo. *Neural Regen. Res.*, **10**, 872.

Manzini, I., Frasnelli, J., & Croy, I. (2014) Wie wir riechen und was es für uns bedeutet. *HNO*, **62**, 846–852.

Manzini, I., Heermann, S., Czesnik, D., Brase, C., Schild, D., & Rössler, W. (2007) Presynaptic protein distribution and odour mapping in glomeruli of the olfactory bulb of *Xenopus laevis* tadpoles. *Eur. J. Neurosci.*, **26**, 925–934.

Manzini, I. & Korsching, S. (2011) The peripheral olfactory system of vertebrates: molecular, structural and functional basics of the sense of smell. *e-Neuroforum*, **17**, 68–77.

Manzini, I. & Schild, D. (2010) *Olfactory Coding in Larvae of the African Clawed Frog Xenopus Laevis*, The Neurobiology of Olfaction.

Manzini, I., Schild, D., & Di Natale, C. (2022) Principles of odor coding in vertebrates and artificial chemosensory systems. *Physiol. Rev.*, **102**, 61–154.

Martin-Pérez, J. & Thomas, G. (1983) Ordered phosphorylation of 40S ribosomal protein S6 after serum stimulation of quiescent 3T3 cells. *Proc. Natl. Acad. Sci.*, **80**, 926–930.

Matsunami, H. & Buck, L.B. (1997) A Multigene Family Encoding a Diverse Array of Putative Pheromone Receptors in Mammals. *Cell*, **90**, 775–784.

Measey, J. (2016) Overland movement in African clawed frogs (*Xenopus laevis*): a systematic review. *PeerJ*, **4**, e2474.

Meisami, E., Mikhail, L., Baim, D., & Bhatnagar, K.P. (1998) Human Olfactory Bulb: Aging of Glomeruli and Mitral Cells and a Search for the Accessory Olfactory Bulb a. *Ann. N. Y. Acad. Sci.*, **855**, 708–715.

Meyuhas, O. (2008) Chapter 1 Physiological Roles of Ribosomal Protein S6: One of Its Kind. In *International Review of Cell and Molecular Biology*. pp. 1–37.

Meyuhas, O. (2015) Ribosomal Protein S6 Phosphorylation. In *International Review of Cell and Molecular Biology*. Elsevier Ltd, pp. 41–73.

Miwa, N. & Kawamura, S. (2003) Frog p26olf, a molecule with two S100-like regions in a single peptide. *Microsc. Res. Tech.*, **60**, 593–599.

Miyamichi, K., Serizawa, S., Kimura, H.M., & Sakano, H. (2005) Continuous and Overlapping Expression Domains of Odorant Receptor Genes in the Olfactory Epithelium Determine the Dorsal/Ventral Positioning of Glomeruli in the Olfactory Bulb. *J. Neurosci.*, **25**, 3586–3592.

Mohrhardt, J., Nagel, M., Fleck, D., Ben-Shaul, Y., & Spehr, M. (2018) Signal Detection and Coding in the Accessory Olfactory System. *Chem. Senses*, **43**, 667–695.

Mombaerts, P. (2004) Genes and ligands for odorant, vomeronasal and taste receptors. *Nat. Rev. Neurosci.*, **5**, 263–278.

Mombaerts, P. (2006) Axonal Wiring in the Mouse Olfactory System. *Annu. Rev. Cell Dev. Biol.*, **22**, 713–737.

Mombaerts, P., Wang, F., Dulac, C., Chao, S.K., Nemes, A., Mendelsohn, M., Edmondson, J., & Axel, R. (1996) Visualizing an Olfactory Sensory Map. *Cell*, **87**, 675–686.

Moreno-Flores, M.T., Díaz-Nido, J., Wandosell, F., & Avila, J. (2002) Olfactory Ensheathing Glia: Drivers of Axonal Regeneration in the Central Nervous System? *J. Biomed. Biotechnol.*, **2**, 37–43.

Morona, R. & González, A. (2013) Pattern of calbindin-D28k and calretinin immunoreactivity in the brain of *Xenopus laevis* during embryonic and larval development. *J. Comp. Neurol.*, **521**, 79–108.

Morrison, E.E. & Costanzo, R.M. (1992) Morphology of olfactory epithelium in humans and other vertebrates. *Microsc. Res. Tech.*, **23**, 49–61.

Munger, S.D., Leinders-Zufall, T., McDougall, L.M., Cockerham, R.E., Schmid, A., Wandernoth, P., Wennemuth, G., Biel, M., Zufall, F., & Kelliher, K.R. (2010) An Olfactory Subsystem that Detects Carbon Disulfide and Mediates Food-Related Social Learning. *Curr. Biol.*, **20**, 1438–1444.

Munger, S.D., Leinders-Zufall, T., & Zufall, F. (2009) Subsystem organization of the mammalian sense of smell. *Annu. Rev. Physiol.*, **71**, 115–140.

Murai, A., Iwata, R., Fujimoto, S., Aihara, S., Tsuboi, A., Muroyama, Y., Saito, T., Nishizaki, K., & Imai, T. (2016) Distorted Coarse Axon Targeting and Reduced Dendrite Connectivity Underlie Dysosmia after Olfactory Axon Injury. *eNeuro*, **3**, ENEURO.0242-16.2016.

Murtaza, M., Mohanty, L., Ekberg, J.A.K., & St John, J.A. (2022) Designing Olfactory Ensheathing Cell Transplantation Therapies: Influence of Cell Microenvironment. *Cell Transplant.*, **31**, 9636897221125684.

Nagayama, S., Homma, R., & Imamura, F. (2014) Neuronal organization of olfactory bulb circuits. *Front. Neural Circuits*, **8**, 1–19.

Nakamura, T. & Gold, G.H. (1987) A cyclic nucleotide-gated conductance in olfactory receptor cilia. *Nature*, **325**, 442–444.

Nakamuta, S., Nakamuta, N., & Taniguchi, K. (2011) Distinct axonal projections from two types of olfactory receptor neurons in the middle chamber epithelium of *Xenopus laevis*. *Cell Tissue Res.*, **346**, 27–33.

Nakamuta, S., Nakamuta, N., Taniguchi, K., & Taniguchi, K. (2012) Histological and Ultrastructural Characteristics of the Primordial Vomeronasal Organ in Lungfish. *Anat. Rec.*, **295**, 481–491.

Nara, K., Saraiva, L.R., Ye, X., & Buck, L.B. (2011) A Large-Scale Analysis of Odor Coding in the Olfactory Epithelium. *J. Neurosci.*, **31**, 9179–9191.

Nazareth, L., Chen, M., Shelper, T., Shah, M., Tello Velasquez, J., Walkden, H., Beacham, I., Batzloff, M., Rayfield, A., Todorovic, M., Beagley, K.W., St John, J.A., & Ekberg, J.A.K. (2019) Novel insights into the glia limitans of the olfactory nervous system. *J. Comp. Neurol.*, **527**, 1228–1244.

Nazareth, L., Lineburg, K.E., Chuah, M.I., Tello Velasquez, J., Chehrehasa, F., St John, J.A., & Ekberg, J.A.K. (2015) Olfactory ensheathing cells are the main phagocytic cells that remove axon debris during early development of the olfactory system. *J. Comp. Neurol.*, **523**, 479–494.

Nazareth, L., Tello Velasquez, J., Lineburg, K.E., Chehrehasa, F., St John, J.A., & Ekberg, J.A.K. (2015) Differing phagocytic capacities of accessory and main olfactory ensheathing cells and the implication for olfactory glia transplantation therapies. *Mol. Cell. Neurosci.*, **65**, 92–101.

Nei, M., Niimura, Y., & Nozawa, M. (2008) The evolution of animal chemosensory receptor gene repertoires: roles of chance and necessity. *Nat. Rev. Genet.*, **9**, 951–963.

Nezlin, L.P., Heermann, S., Schild, D., & Rössler, W. (2003) Organization of glomeruli in the main olfactory bulb of *Xenopus laevis* tadpoles. *J. Comp. Neurol.*, **464**, 257–268.

Nezlin, L.P. & Schild, D. (2000) Structure of the olfactory bulb in tadpoles of *Xenopus laevis*. *Cell Tissue Res.*, **302**, 21–29.

Nezlin, L.P. & Schild, D. (2005) Individual olfactory sensory neurons project into more than one glomerulus in *Xenopus laevis* tadpole olfactory bulb. *J. Comp. Neurol.*, **481**, 233–239.

Nieuwkoop, P. D., & Faber, J. (Eds.). (1994). Normal table of *Xenopus laevis* (Daudin). Garland Science.

Niimura, Y. (2009) Evolutionary dynamics of olfactory receptor genes in chordates: interaction between environments and genomic contents. *Hum. Genomics*, **4**, 107–118.

Niimura, Y. & Nei, M. (2007) Extensive Gains and Losses of Olfactory Receptor Genes in Mammalian Evolution. *PLoS One*, **2**, e708.

Offner, T., Weiss, L., Daume, D., Berk, A., Inderthal, T.J., Manzini, I., & Hassenklöver, T. (2023) Functional odor map heterogeneity is based on multifaceted glomerular connectivity in larval *Xenopus olfactory* bulb. *iScience*, **26**, 107518.

Oka, Y., Saraiva, L.R., & Korsching, S.I. (2012) Crypt Neurons Express a Single V1R-Related ora Gene. *Chem. Senses*, **37**, 219–227.

Okano, M. & Takagi, S.F. (1974) Secretion and electrogenesis of the supporting cell in the olfactory epithelium. *J. Physiol.*, **242**, 353–370.

Olivares, J. & Schmachtenberg, O. (2019) An update on anatomy and function of the teleost olfactory system. *PeerJ*, **7**, e7808.

Oprych, K., Cotfas, D., & Choi, D. (2017) Common olfactory ensheathing glial markers in the developing human olfactory system. *Brain Struct. Funct.*, **222**, 1877–1895.

Ozorowski, G., Milton, S., & Luecke, H. (2013) Structure of a C-terminal AHNAK peptide in a 1:2:2 complex with S100A10 and an acetylated N-terminal peptide of annexin A2. *Acta Crystallogr. Sect. D Biol. Crystallogr.*, **69**, 92–104.

Pace, U., Hanski, E., Salomon, Y., & Lancet, D. (1985) Odorant-sensitive adenylate cyclase may mediate olfactory reception. *Nature*, **316**, 255–258.

Panni, P., Ferguson, I.A., Beacham, I., Mackay-Sim, A., Ekberg, J.A.K., & St John, J.A. (2013) Phagocytosis of bacteria by olfactory ensheathing cells and Schwann cells. *Neurosci. Lett.*, **539**, 65–70.

Pellitteri, R., Spatuzza, M., Stanzani, S., & Zaccheo, D. (2010) Biomarkers expression in rat olfactory ensheathing cells. *Front. Biosci. (Schol. Ed).*, **2**, 289–298.

Pfister, P. & Rodriguez, I. (2005) Olfactory expression of a single and highly variable V1r pheromone receptor-like gene in fish species. *Proc. Natl. Acad. Sci.*, **102**, 5489–5494.

Pixley, S.K. (1992) The olfactory nerve contains two populations of glia, identified both in vivo and in vitro. *Glia*, **5**, 269–284.

Qi, Y., Cheng, H., Wang, Y., & Chen, Z. (2022) Revealing the Precise Role of Calretinin Neurons in Epilepsy: We Are on the Way. *Neurosci. Bull.*, **38**, 209–222.

Quintana-Urzainqui, I., Rodríguez-Moldes, I., & Candal, E. (2014) Developmental, tract-tracing and immunohistochemical study of the peripheral olfactory system in a basal vertebrate: insights on Pax6 neurons migrating along the olfactory nerve. *Brain Struct. Funct.*, **219**, 85–104.

Rafols, J.A. & Getchell, T. V. (1983) Morphological relations between the receptor neurons, sustentacular cells and Schwann cells in the olfactory mucosa of the salamander. *Anat. Rec.*, **206**, 87–101.

Raisman, G. (1985) Specialized neuroglial arrangement may explain the capacity of vomeronasal axons to reinnervate central neurons. *Neuroscience*, **14**, 237–254.

Ramón-Cueto, A. & Valverde, F. (1995) Olfactory bulb ensheathing glia: A unique cell type with axonal growth-promoting properties. *Glia*, **14**, 163–173.

Reiss, J.O. & Eisthen, H.L. (2008) Comparative Anatomy and Physiology of Chemical Senses in Amphibians. In *Sensory Evolution on the ThresholdAdaptations in Secondarily Aquatic Vertebrates*. University of California Press, pp. 42–63.

Reshamwala, R., Shah, M., Belt, L., Ekberg, J.A.K., & St John, J.A. (2020) Reliable cell purification and determination of cell purity: crucial aspects of olfactory ensheathing cell transplantation for spinal cord repair. *Neural Regen. Res.*, **15**, 2016–2026.

Ressler, K.J., Sullivan, S.L., & Buck, L.B. (1994) Information coding in the olfactory system: evidence for a stereotyped and highly organized epitope map in the olfactory bulb. *Cell*, **79**, 1245–1255.

Ring, N.A.R., Dworak, H., Bachmann, B., Schädl, B., Valdivieso, K., Rozmaric, T., Heimel, P., Fischer, I., Klinaki, E., Gutasi, A., Schuetzenberger, K., Leinfellner, G., Ferguson, J., Drechsler, S., Mildner, M., Schosserer, M., Slezak, P., Meyuhas, O., Gruber, F., Grillari, J., Redl, H., & Ogrodnik, M. (2023) The p-rpS6-zone delineates wounding responses and the healing process. *Dev. Cell*, **58**, 981-992.e6.

Rivière, S., Challet, L., Fluegge, D., Spehr, M., & Rodriguez, I. (2009) Formyl peptide receptor-like proteins are a novel family of vomeronasal chemosensors. *Nature*, **459**, 574–577.

Rubio, M., Muñoz-Quiles, C., & Ramón-Cueto, A. (2008) Adult olfactory bulbs from primates provide reliable ensheathing glia for cell therapy. *Glia*, **56**, 539–551.

Rünnenburger, K., Breer, H., & Boekhoff, I. (2002) Selective G protein βγ-subunit compositions mediate phospholipase C activation in the vomeronasal organ. *Eur. J. Cell Biol.*, **81**, 539–547.

Ruvinsky, I. & Meyuhas, O. (2006) Ribosomal protein S6 phosphorylation: from protein synthesis to cell size. *Trends Biochem. Sci.*, **31**, 342–348.

Ryba, N.J.P. & Tirindelli, R. (1997) A New Multigene Family of Putative Pheromone Receptors. *Neuron*, **19**, 371–379.

Saito, H., Chi, Q., Zhuang, H., Matsunami, H., & Mainland, J.D. (2009) Odor coding by a Mammalian receptor repertoire. *Sci. Signal.*, **2**, ra9.

Saito, S. & Taniguchi, K. (2000) Expression patterns of glycoconjugates in the three distinctive olfactory pathways of the clawed frog, *Xenopus laevis*. *J. Vet. Med. Sci.*, **62**, 153–159.

Sansone, A., Hassenklöver, T., Syed, A.S., Korsching, S.I., & Manzini, I. (2014) Phospholipase C and Diacylglycerol Mediate Olfactory Responses to Amino Acids in the Main Olfactory Epithelium of an Amphibian. *PLoS One*, **9**, e87721.

Sansone, A., Syed, A.S., Tantalaki, E., Korsching, S.I., & Manzini, I. (2014) Trpc2 is expressed in two olfactory subsystems, the main and the vomeronasal system of larval *Xenopus laevis*. *J. Exp. Biol.*, **217**, 2235–2238.

Saraiva, L.R. & Korsching, S.I. (2007) A novel olfactory receptor gene family in teleost fish. *Genome Res.*, **17**, 1448–1457.

Sato, Y., Miyasaka, N., & Yoshihara, Y. (2005) Mutually Exclusive Glomerular Innervation by Two Distinct Types of Olfactory Sensory Neurons Revealed in Transgenic Zebrafish. *J. Neurosci.*, **25**, 4889–4897.

Schaefer, M.L., Young, D.A., & Restrepo, D. (2001) Olfactory Fingerprints for Major Histocompatibility Complex-Determined Body Odors. *J. Neurosci.*, **21**, 2481–2487.

Schild, D. & Restrepo, D. (1998) Transduction mechanisms in vertebrate olfactory receptor cells. *Physiol. Rev.*, **78**, 429–466.

Schnittke, N., Herrick, D.B., Lin, B., Peterson, J., Coleman, J.H., Packard, A.I., Jang, W., & Schwob, J.E. (2015) Transcription factor p63 controls the reserve status but not the stemness of horizontal basal cells in the olfactory epithelium. *Proc. Natl. Acad. Sci.*, **112**, E5068-77.

Schwob, J.E. (2002) Neural regeneration and the peripheral olfactory system. *Anat. Rec.*, **269**, 33–49.

Schwob, J.E., Jang, W., Holbrook, E.H., Lin, B., Herrick, D.B., Peterson, J.N., & Hewitt Coleman, J. (2017) Stem and progenitor cells of the mammalian olfactory epithelium: Taking poietic license. *J. Comp. Neurol.*, **525**, 1034–1054.

Schwob, J.E., Youngentob, S.L., Ring, G., Iwema, C.L., & Mezza, R.C. (1999) Reinnervation of the rat olfactory bulb after methyl bromide-induced lesion: Timing and extent of reinnervation. *J. Comp. Neurol.*, **412**, 439–457.

Sharma, K., Syed, A.S., Ferrando, S., Mazan, S., & Korsching, S.I. (2019) The chemosensory receptor repertoire of a true shark is dominated by a single olfactory receptor family. *Genome Biol. Evol.*, **11**, 398–405.

Shi, P. & Zhang, J. (2007) Comparative genomic analysis identifies an evolutionary shift of vomeronasal receptor gene repertoires in the vertebrate transition from water to land. *Genome Res.*, **17**, 166–174.

Sicard, G., Féron, F., Andrieu, J.L., Holley, A., & Mackay-Sim, A. (1998) Generation of neurons from a nonneuronal precursor in adult olfactory epithelium in vitro. *Ann. N. Y. Acad. Sci.*, **855**, 223–225.

Silva, L. & Antunes, A. (2017) Vomeronasal Receptors in Vertebrates and the Evolution of Pheromone Detection. *Annu. Rev. Anim. Biosci.*, **5**, 353–370.

Sliogeryte, K. & Gavara, N. (2019) Vimentin Plays a Crucial Role in Fibroblast Ageing by Regulating Biophysical Properties and Cell Migration. *Cells*, **8**, 1164.

Sokpor, G., Abbas, E., Rosenbusch, J., Staiger, J.F., & Tuoc, T. (2018) Transcriptional and Epigenetic Control of Mammalian Olfactory Epithelium Development. *Mol. Neurobiol.*, **55**, 8306–8327.

Sonigra, R.J., Brighton, P.C., Jacoby, J., Hall, S., & Wigley, C.B. (1999) Adult rat olfactory nerve ensheathing cells are effective promoters of adult central nervous system neurite outgrowth in coculture. *Glia*, **25**, 256–269.

Spehr, M. & Munger, S.D. (2009) Olfactory receptors: G protein-coupled receptors and beyond. *J. Neurochem.*, **109**, 1570–1583.

Strotmann, J., Conzelmann, S., Beck, A., Feinstein, P., Breer, H., & Mombaerts, P. (2000) Local Permutations in the Glomerular Array of the Mouse Olfactory Bulb. *J. Neurosci.*, **20**, 6927–6938.

Su, Z., Chen, J., Qiu, Y., Yuan, Y., Zhu, F., Zhu, Y., Liu, X., Pu, Y., & He, C. (2013) Olfactory ensheathing cells: the primary innate immunocytes in the olfactory pathway to engulf apoptotic olfactory nerve debris. *Glia*, **61**, 490–503.

Suzuki, Y., Takeda, M., & Farbman, A.I. (1996) Supporting cells as phagocytes in the olfactory epithelium after bulbectomy. *J. Comp. Neurol.*, **376**, 509–517.

Syed, A.S., Sansone, A., Hassenklöver, T., Manzini, I., & Korsching, S.I. (2017) Coordinated shift of olfactory amino acid responses and V2R expression to an amphibian water nose during metamorphosis. *Cell. Mol. Life Sci.*, **74**, 1711–1719.

Syed, A.S., Sansone, A., Nadler, W., Manzini, I., & Korsching, S.I. (2013) Ancestral amphibian v2r s are expressed in the main olfactory epithelium. *Proc. Natl. Acad. Sci.*, **110**, 7714–7719.

Syed, A.S., Sharma, K., Policarpo, M., Ferrando, S., Casane, D., & Korsching, S.I. (2023) Ancient and Nonuniform Loss of Olfactory Receptor Expression Renders the Shark Nose a De Facto Vomeronasal Organ. *Mol. Biol. Evol.*, **40**, 1–16.

Tallquist, M.D. & Molkentin, J.D. (2017) Redefining the identity of cardiac fibroblasts. *Nat. Rev. Cardiol.*, **14**, 484–491.

Taniguchi, K., Saito, S., Oikawa, T., & Taniguchi, K. (2008) Phylogenic Aspects of the Amphibian Dual Olfactory System. *J. Vet. Med. Sci.*, **70**, 1–9.

Taniguchi, K. & Taniguchi, K. (2014) Phylogenic Studies on the Olfactory System in Vertebrates. *J. Vet. Med. Sci.*, **76**, 781–788.

Techangamsuwan, S., Imbschweiler, I., Kreutzer, R., Kreutzer, M., Baumgärtner, W., & Wewetzer, K. (2008) Similar behaviour and primate-like properties of adult canine Schwann cells and olfactory ensheathing cells in long-term culture. *Brain Res.*, **1240**, 31–38.

Tennent, R. & Chuah, M.. (1996) Ultrastructural study of ensheathing cells in early development of olfactory axons. *Dev. Brain Res.*, **95**, 135–139.

Terni, B., Pacciolla, P., Masanas, H., Gorostiza, P., & Llobet, A. (2017) Tight temporal coupling between synaptic rewiring of olfactory glomeruli and the emergence of odor-guided behavior in *Xenopus* tadpoles. *J. Comp. Neurol.*, **525**, 3769–3783.

Tirindelli, R., Mucignat-Caretta, C., & Ryba, N.J.P. (1998) Molecular aspects of pheromonal communication via the vomeronasal organ of mammals. *Trends Neurosci.*, **21**, 482–486.

Toft, A., Tome, M., Barnett, S.C., & Riddell, J.S. (2013) A comparative study of glial and non-neural cell properties for transplant-mediated repair of the injured spinal cord. *Glia*, **61**, 513–528.

Van de Graaf, S.F.J., Hoenderop, J.G.J., Gkika, D., Lamers, D., Prenen, J., Rescher, U., Gerke, V., Staub, O., Nilius, B., & Bindels, R.J.M. (2003) Functional expression of the epithelial Ca(2+) channels (TRPV5 and TRPV6) requires association of the S100A10-annexin 2 complex. *EMBO J.*, **22**, 1478–1487.

Van Den Pol, A.N. & Santarelli, J.G. (2003) Olfactory ensheathing cells: Time lapse imaging of cellular interactions, axonal support, rapid morphologic shifts, and mitosis. *J. Comp. Neurol.*, **458**, 175–194.

Vassar, R., Chao, S.K., Sitcheran, R., Nuñez, J.M., Vosshall, L.B., & Axel, R. (1994) Topographic organization of sensory projections to the olfactory bulb. *Cell*, **79**, 981–991.

Vedin, V., Slotnick, B., & Berghard, A. (2004) Zonal ablation of the olfactory sensory neuroepithelium of the mouse: effects on odorant detection. *Eur. J. Neurosci.*, **20**, 1858–1864.

Vincent, A.J., Choi-Lundberg, D.L., Harris, J.A., West, A.K., & Chuah, M.I. (2007) Bacteria and PAMPs activate nuclear factor kappaB and Gro production in a subset of olfactory ensheathing cells and astrocytes but not in Schwann cells. *Glia*, **55**, 905–916.

Voigt, J.M., Guengerich, F.P., & Baron, J. (1993) Localization and induction of cytochrome P450 1A1 and aryl hydrocarbon hydroxylase activity in rat nasal mucosa. *J. Histochem. Cytochem.*, **41**, 877–885.

Von Bartheld, C.S., Bahney, J., & Herculano-Houzel, S. (2016) The search for true numbers of neurons and glial cells in the human brain: A review of 150 years of cell counting. *J. Comp. Neurol.*, **524**, 3865–3895.

Wafer, L.N., Tzul, F.O., Pandharipande, P.P., & Makhatadze, G.I. (2013) Novel interactions of the TRTK12 peptide with S100 protein family members: specificity and thermodynamic characterization. *Biochemistry*, **52**, 5844–5856.

Wakabayashi, Y. & Ichikawa, M. (2008) Localization of G protein alpha subunits and morphology of receptor neurons in olfactory and vomeronasal epithelia in Reeve's turtle, *Geoclemys reevesii*. *Zoolog. Sci.*, **25**, 178–187.

Wakisaka, N., Miyasaka, N., Koide, T., Masuda, M., Hiraki-Kajiyama, T., & Yoshihara, Y. (2017) An Adenosine Receptor for Olfaction in Fish. *Curr. Biol.*, **27**, 1437-1447.e4.

Wei, H., Lang, M.-F., & Jiang, X. (2013) Calretinin is expressed in the intermediate cells during olfactory receptor neuron development. *Neurosci. Lett.*, **542**, 42–46.

Weiss, L., Jungblut, L.D., Pozzi, A.G., O'Connell, L.A., Hassenklöver, T., & Manzini, I. (2020) Conservation of Glomerular Organization in the Main Olfactory Bulb of Anuran Larvae. *Front. Neuroanat.*, **14**, 1–8.

Weiss, L., Jungblut, L.D., Pozzi, A.G., Zielinski, B.S., O'Connell, L.A., Hassenklöver, T., & Manzini, I. (2020) Multi-glomerular projection of single olfactory receptor neurons is conserved among amphibians. *J. Comp. Neurol.*, **528**, 2239–2253.

Weiss, L., Manzini, I., & Hassenklöver, T. (2021) Olfaction across the water-air interface in anuran amphibians. *Cell Tissue Res.*, **383**, 301–325.

Weiss, L., Segoviano Arias, P., Offner, T., Hawkins, S.J., Hassenklöver, T., & Manzini, I. (2021) Distinct interhemispheric connectivity at the level of the olfactory bulb emerges during *Xenopus laevis* metamorphosis. *Cell Tissue Res.*, **386**, 491–511.

Weth, F., Nadler, W., & Korsching, S. (1996) Nested expression domains for odorant receptors in zebrafish olfactory epithelium. *Proc. Natl. Acad. Sci.*, **93**, 13321–13326.

Wettenhall, R.E., Erikson, E., & Maller, J.L. (1992) Ordered multisite phosphorylation of *Xenopus* ribosomal protein S6 by S6 kinase II. *J. Biol. Chem.*, **267**, 9021–9027.

Wewetzer, K., Radtke, C., Kocsis, J., & Baumgärtner, W. (2011) Species-specific control of cellular proliferation and the impact of large animal models for the use of olfactory ensheathing cells and Schwann cells in spinal cord repair. *Exp. Neurol.*, **229**, 80–87.

Windus, L.C.E., Chehrehasa, F., Lineburg, K.E., Claxton, C., MacKay-Sim, A., Key, B., & St John, J.A. (2011) Stimulation of olfactory ensheathing cell motility enhances olfactory axon growth. *Cell. Mol. Life Sci.*, **68**, 3233–3247.

Woodhall, E., West, A.K., & Chuah, M.I. (2001) Cultured olfactory ensheathing cells express nerve growth factor, brain-derived neurotrophic factor, glia cell line-derived neurotrophic factor and their receptors. *Mol. Brain Res.*, **88**, 203–213.

Woodley, S. (2015) Chemosignals, hormones, and amphibian reproduction. *Horm. Behav.*, **68**, 3–13.

Woodley, S.K. (2014) *Chemical Signaling in Amphibians*, Neurobiology of Chemical Communication.

Wright, A.A., Todorovic, M., Murtaza, M., St John, J.A., & Ekberg, J.A. (2020) Macrophage migration inhibitory factor and its binding partner HTRA1 are expressed by olfactory ensheathing cells. *Mol. Cell. Neurosci.*, **102**, 103450.

Wyatt, T. (2015) How Animals Communicate Via Pheromones. *Am. Sci.*, **103**, 114.

Xu, Z. & Li, Q. (2020) TAAR Agonists. *Cell. Mol. Neurobiol.*, **40**, 257–272.

Yang, C. & Delay, R.J. (2010) Calcium-activated chloride current amplifies the response to urine in mouse vomeronasal sensory neurons. *J. Gen. Physiol.*, **135**, 3–13.

Yang, L., Jiang, H., Wang, Y., Lei, Y., Chen, J., Sun, N., Lv, W., Wang, C., Near, T.J., & He, S. (2019) Expansion of vomeronasal receptor genes (OlfC) in the evolution of fright reaction in Ostariophysan fishes. *Commun. Biol.*, **2**, 235.

Yao, R., Murtaza, M., Velasquez, J.T., Todorovic, M., Rayfield, A., Ekberg, J., Barton, M., & St John, J. (2018) Olfactory Ensheathing Cells for Spinal Cord Injury: Sniffing Out the Issues. *Cell Transplant.*, **27**, 879–889.

Yee, K.K. & Costanzo, R.M. (1998) Changes in odor quality discrimination following recovery from olfactory nerve transection. *Chem. Senses*, **23**, 513–519.

Zapiec, B. & Mombaerts, P. (2020) The Zonal Organization of Odorant Receptor Gene Choice in the Main Olfactory Epithelium of the Mouse. *Cell Rep.*, **30**, 4220-4234.e5.

Zarzo, M. (2007) The sense of smell: molecular basis of odorant recognition. *Biol. Rev.*, **82**, 455–479.

Zhang, X. & Firestein, S. (2002) The olfactory receptor gene superfamily of the mouse. *Nat. Neurosci.*, **5**, 124–133.

Zimmer, D.B., Eubanks, J.O., Ramakrishnan, D., & Criscitiello, M.F. (2013) Evolution of the S100 family of calcium sensor proteins. *Cell Calcium*, **53**, 170–179.

Zimmerman, A.D. & Munger, S.D. (2021) Olfactory subsystems associated with the necklace glomeruli in rodents. *Cell Tissue Res.*, **383**, 549–557.

10 Used tools

To improve and paraphrase my self-written sentences, I occasionally used the writing tools DeepL (https://www.deepl.com/de/translator) and Scribbr (https://www.scribbr.com/paraphrasing-tool/).

11 Attachments

11.1 Supplementary figures of the 2nd Paper

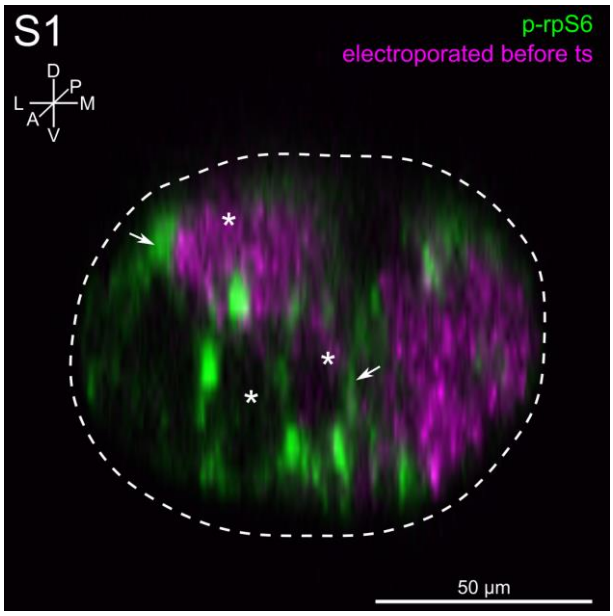

Supplementary figure 1: Phosphorylated rpS6-positive olfactory ensheathing cells ensheathe bundles of olfactory receptor neuron axons. Transversal view of a transected olfactory nerve (encircled by a white dotted line). Olfactory ensheathing cells (green) stained with an antibody against phosphorylated rpS6 enwrap bundles of olfactory receptor neuron axons (magenta) and form tunnel-like structures (white asterisks). Olfactory receptor neuron axons were labeled by nasal electroporation of fluorescent dextrans. Abbreviations: A anterior; D dorsal; L lateral; M medial; P posterior; V ventral.

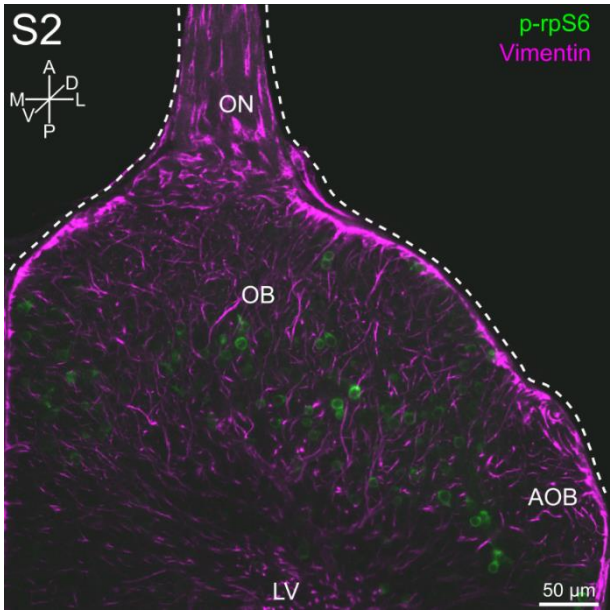

Supplementary figure 2: Vimentin- and phosphorylated rpS6-positive cells in the non-transected olfactory nerve and olfactory bulb. Vimentin (magenta) was detectable in cells of the olfactory nerve and radial glial cells in the olfactory bulb. Phosphorylated rpS6-positive cells (green) were localized in the glomerular-, mitral-, and granule cell layers of the olfactory bulb. Similar results were obtained in all animals investigated (n =9). Abbreviations: A anterior; AOB accessory olfactory bulb; D dorsal; L lateral; LV lateral ventricle; M medial; OB olfactory bulb; ON olfactory nerve; P posterior; V ventral.

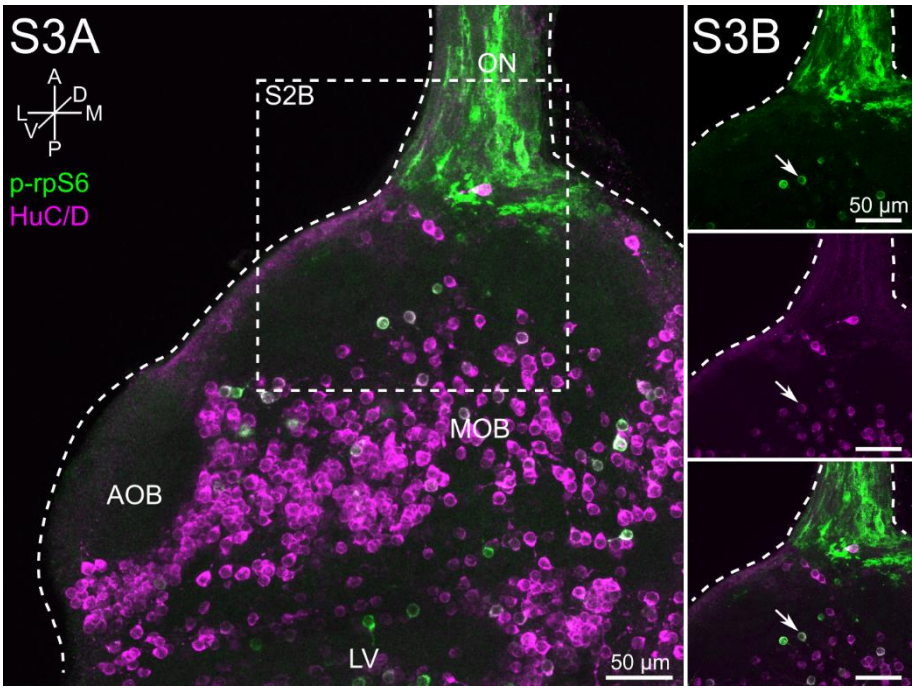

Supplementary figure 3: Co-localization of HuC/D and phosphorylated rpS6 in the olfactory bulb after transection of the olfactory nerve. (S3A) A subgroup of neurons labeled with an antibody against HuC/D (magenta) in the olfactory bulb are also stained with an antibody against phosphorylated rpS6 (green). A strong staining against phosphorylated rpS6 of non-neuronal cells is present in the olfactory nerve. **(S3B)** Close-ups of the area included in the dotted square in S3A. Upper image: green channel; middle image: magenta channel; lower image: both channels merged. The arrows indicate a double-stained neuron (HuC/D and phosphorylated rpS6). Similar results were obtained in all animals investigated (n = 8). Abbreviations: A anterior; AOB accessory olfactory bulb; D dorsal; L lateral; LV lateral ventricle; M medial; MOB main olfactory bulb; ON olfactory nerve; P posterior; V ventral.

12 List of abbreviations

(Abbreviations used for Scientific Background and General Discussion)

ACIII …….. Adenylate-cyclase III

ANO2 ……. Anoctamin-2

AOB ……Accessory olfactory bulb

ATP ……Adenosine-5`-triphosphate

BCs ……Basal cells

Ca2+ ……...Calcium

cAMP ……. Cyclic adenosine monophosphate

CBPs ……. Calcium-binding proteins

CNG ……. Cyclic nucleotide gated

DAG ……..Diacylglycerol

FPRs ……....Formyl peptide receptors

GC-D ……...Guanylyl cyclase

GDP ……Guanosine diphosphate

GPCR ……...G protein-coupled receptors

GTP ……Guanosine-5`-triphosphate

IP3 ……...Inositol-1,4,5-triphosphate

MC ……..Middle cavity

MOB ……Main olfactory bulb

MOE ……...Main olfactory epithelium

MTC ……..Mitral/ tufted cell

mTOR ……Mammalian target of rapamycin

MS4A ...Membrane spanning four-pass proteins

OB ……Olfactory bulb

OE ……...Olfactory epithelium

OECs ……Olfactory ensheathing cells

OlfC ……Olfactory class C GPCRs

ON ……...Olfactory nerve

ORA ……Olfactory receptor class A-related

ORNs ……...Olfactory receptor neurons

OR-type ……Odorant receptors

OS ……Olfactory system

PC ……Principal cavity

PLC ……..Phospholipase C

p-rpS6 ……Phosphorylated ribosomal protein S6 235/236

S100Z ……S100 calcium-binding protein Z

SCs ……Supporting cells

TAARs ……..Trace amine-associated receptors

TRPC2 Transient receptor cation channel type 2

V1Rs ……Vomeronasal type 1 receptors

V2Rs ……Vomeronasal type 2 receptors

VNO ……Vomeronasal organ

13 List of figures

13.1 List of supplementary figures

14 Affidavit

I hereby confirm that my thesis entitled "*Structural development and functional reconstitution in the olfactory system of the clawed frog Xenopus laevis*" is the result of my own work. I declare that I have completed this dissertation single-handedly without the unauthorized help of a second party and only with the assistance acknowledged therein. I have appropriately acknowledged and cited all text passages that are derived verbatim from or are based on the content of published work of others, and all information relating to verbal communications. I consent to the use of an anti-plagiarism software to check my thesis. I have abided by the principles of good scientific conduct laid down in the charter of the Justus Liebig University Giessen „Satzung der Justus-Liebig-Universität Gießen zur Sicherung guter wissenschaftlicher Praxis" in carrying out the investigations described in the dissertation.

Hiermit erkläre ich: Ich habe die vorgelegte Dissertation mit dem Titel „*Strukturelle Entwicklung und funktionelle Wiederherstellung des Geruchssystems des Krallenfroschs Xenopus laevis*" selbstständig und ohne unerlaubte fremde Hilfe und nur mit den Hilfen angefertigt, die ich in der Dissertation angegeben habe. Alle Textstellen, die wörtlich oder sinngemäß aus veröffentlichten Schriften entnommen sind, und alle Angaben, die auf mündlichen Auskünften beruhen, sind als solche kenntlich gemacht. Ich stimme einer evtl. Überprüfung meiner Dissertation durch eine Antiplagiat-Software zu. Bei den von mir durchgeführten und in der Dissertation erwähnten Untersuchungen habe ich die Grundsätze guter wissenschaftlicher Praxis, wie sie in der „Satzung der Justus-Liebig-Universität Gießen zur Sicherung guter wissenschaftlicher Praxis" niedergelegt sind, eingehalten.

_____ _____

Ort, Datum Melina Kahl

15 Acknowledgements

Zu aller erst möchte ich meiner Familie, insbesondere meiner Mama Monika, meinem Papa Gerald und meinem Bruder Marijan, und auch meinen Großeltern Dieter und Erika Kahl-Maly, danken. Ohne euch und eure stetige, liebevolle Unterstützung wäre ich nicht so weit gekommen. Ich danke euch von Herzen! Ich möchte Kai Schneider dafür danken, dass er immer da ist um mich aufzumuntern, wenn das Leben und die Arbeit schwierig sind und dass er meine mürrischen Phasen erträgt und mir zeigt, dass es trotzdem immer etwas zum Lachen gibt. Claire, mein Herz, ich danke dir dafür, dass du so bist wie du bist und mir jeden Tag aufs Neue zeigst, warum es so wichtig ist neugierig zu bleiben. Danke, dass ich deine Mama sein darf!

Meiner lieben Freundin Annalena danke ich ebenfalls dafür, dass sie während dieser herausfordernden Zeit immer für mich da war und mein Gejammer und die Ups and Downs mitgelebt hat. Das gemeinsame Studium und so viele gemeinsame Momente möchte ich nicht mehr missen. Auch bei meinen Freunden Laura-Katharina, Lisa, Johanna und den PEKiP-Mädels möchte ich mich bedanken. Ihr habt immer an mich und mein Können geglaubt und mich immer wieder aufgemuntert, wenn ich an mir gezweifelt habe.

Ein besonderer Dank geht an meine ehemaligen und aktuellen Lablings Thomas Offner, Lukas Weiss, Lukas Jung (ehem. Wichmann), Sara Joy Hawkins, Daniela Daume, Joshua Walter und Any Valencia-Aguilar. Ohne euch wäre dieses Abenteuer nicht möglich gewesen. Indem wir uns gegenseitig unterstützt, genervt und immer wieder aufgemuntert haben, haben wir gemeinsam schwierige Zeiten überstanden. Besonders Joshi möchte ich für die Unterstützung in den letzten beiden Jahren danken in denen wir alleine als Doktoranden ein Team waren! Vielen Dank auch an meine Kolleginnen Anja Schnecko, Katrin Heber und Mirjam Buß. Ich hoffe wir bleiben noch lange in Kontakt und wir schaffen es mal wieder einen extravaganten Abend mit Winetasting, gutem Essen und einer Runde Wizard zu verbringen. Meinen Bachelor-Studenten Alena, Lilly und Joaquin möchte ich ebenfalls danken. Eure Betreuung hat mir regelmäßig einen Anstoß zum Perspektivwechsel gegeben und mir geholfen meine Fähigkeiten als Betreuerin zu verbessern.

Ich möchte Ivan Manzini für seine Unterstützung für diese Arbeit danken. Danke für das Vertrauen in meine Fähigkeiten und die Möglichkeit in deiner Arbeitsgruppe meine Doktorarbeit zu schreiben. Ich möchte Thomas Hassenklöver für seine wissenschaftliche Betreuung, seine Professionalität und seiner stetigen Hilfe bei Auswertungsfragen danken. Ich bin dankbar für all das was du mir beigebracht und erklärt hast.

Danke an mein Thesis-Komitee Prof. Martin Diener, Prof. Reinhard Lakes-Harlan und Prof. Nikola Michael Prpic-Schäper, die mir mit ihren Rückfragen immer wieder Denkanstöße gegeben haben. Ich bin sehr dankbar, dass ich Teil des International Giessen Graduate Centre

for the Life Sciences war. Die lustige Vielfalt an Menschen, die ich kennengelernt habe und die hilfreichen Seminare, die ich besucht habe, haben mich während der Zeit der Promotion sehr unterstützt. Besonders möchte ich mich bei Dr. Christoph Rummel und Dr. Stefanie Rummel bedanken, die mir bei der Vorbereitung und Durchführung von Vorträgen geholfen haben, meine Präsentationsfähigkeiten zu verbessern.